DUST IN THE OUTER LAYERS OF STARS

A Thesis
Submitted For The Degree of
Doctor of Philosophy In The Faculty of Science

KARNATAK UNIVERSITY
DHARWAD

By

M. F. INGALGI

INDIAN INSTITUTE OF ASTROPHYSICS
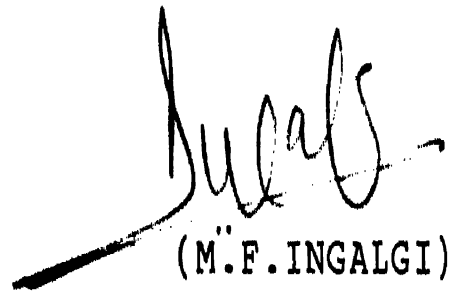BANGALORE 560 034
INDIA

AUGUST 1990

DECLARATION

I hereby declare that the matter embodied in this thesis is the result of the investigations carried out by me at the Indian Institute of Astrophysics, Bangalore, under the guidance of Prof.A.Peraiah. Further I declare that it has not been submitted for the award of any degree, diploma, associateship or fellowship etc., of any University or Institute.

(A.PERAIAH)

RESEARCH GUIDE

(M.F.INGALGI)

CANDIDATE

BANGALORE

AUGUST 1990

Dedicated

To the fond memory of my father

24 October 1988

AKNOWLEDGEMENTS

I take pleasure in expressing my indebtedness to Prof.A.Peraiah, who suggested this problem to me and supervised the work. He always had time for discussion in his busy schedule. The innumerable meetings with him were of immense help in understanding the problem and were thoroughly enjoyable. I am grateful for his encouragement during this work. I deem it a prevelege to thank Prof.J.C.Bhattacharyya, Director, Indian Institute of Astrophysics for providing me with excellent research facilities and the kind enquiries about the work. I also wish to thank the UGC and the Directorate of Collegiate Education Government of Karnataka for providing me an opportunity to take up research work at IIA.

I sincerely thank Prof.B.G.Jyothi Head of the Department of Phyics, Karnataka University, Dharwad and also Prof.N.Umakantha who took keen interest and gave valuable guidance at various stages during this work. Mr.B.A.Varghese was of great help at the computer center and Mr.M.Srinivasa Rao rendered necessary help in the early completion of this work. I take pleasure in thanking both of them. Dr.D.Mohan Rao, Dr.K.E.Rangarajan and Ms.Prasanna Lakshmi made useful suggestions. I sincerely acknowledge their kind gesture. I thank the staff of IIA Library and computer center for all their assistance during this work. Mr.Muthukrishnan did all the drawings and Ms.Pramila Kaverappa has neatly typed the manuscript in a brief time.

Mrs.Revathy and Mr.Krishnamurthy have given a nice appearance to the thesis by their excellent binding skill. I thank the entire staff of IIA for their co-operation and courtesy shown to me during my stay.

I affectionately remember the patience and encourage-ment shown by all my family members.

CONTENTS

CONTENTS

Abstract

We have studied the effects of expansion of dusty matter in spherically symmetric atmospheres, on equivalent widths of the spectral lines form in such media. We have treated a two level atom in non-LTE. Initially the hydrogen Lyman Alpha line has been studied for the purpose of calculating the effects of number density of the neutral atoms on equivalent widths. The temperature variation has been derived from the assumption that the Planck function varies as $1/r^2$ in an atmospheres with pure hydrogen gas. Using this temperature structure and Boltzmann equation, we calculated the number of neutral atoms which formed the hydrogen Lyman Alpha Line.

The dust has been introduced assuming that there is no reemission from the dust and that dust scatters isotropically. This is because the emission of dust will be in the infrared and will not contribute to the emission to the hydrogen Lyman Alpha Line. We have employed the comoving frame method for obtaining the solution of the line transfer equation. The velocities of expansion are measured in terms of mean thermal units and the amounts of gas and dust are measured in terms of the respective optical depths. We have considered two atmospheres: one-without emission and two- with emission in the medium due to thermalization of photons.

In a static medium we obtain symmetric profiles and when the velocity of expansion is introduced we generally obtain P-Cygni type profiles i.e.the absorption being shifted

towards the violet side or emission peak remains at the center gravity of the line. If we introduce dust the emission reduce considerably while dust scatters more photons into the absorpiton core. When there is no dust the absorption core is very wide extending approximately to three Doppler units of either side of the center of the lines. When the optical depth of the dust is large (say five) the width of the absorption core is reduced to only approximately 1.5 Doppler units on either side of the line of the center which means the dust scatters photons into the core of the line and removes photons from the wings. When we introduce velocity of the expansion the lines become a asymmetric the absorption core become narrow.

When thermal emission is introduced there is substantial amounts of emission on the both the sides of the line center with absorption at the center. If we introduce dust then the two peaks of emission wings are reduced substantially, changing the width of the central absorption. If dust is further increased the emission from the wings will vanish completely or the line will have two small emission wings with two unequal heights.

The equivalent widths corresponding to the changes in the amount of dust, expansion velocity, are different in different cases. If the dust optical depth is increased, the equivalent widths in a medium moving with velocity gradients are reduced while the equivalent widths formed in

III

a shell moving with constant velocity increase the emission being considerably reduced. The ratio of heights of the two emission peaks fall as the dust optical depth is increased.

CHAPTER 1

INTRODUCTION

"STARS AND NEBULAE TELL AND SHOW US WHAT THEY PLEASE"

1.1 Study of stellar spectra

By analysing the observed stellar spectra it is possible to learn more about the structure, temperature, chemical composition of stellar atmospheres and other conditions prevailing in the gaseous nebulae. The analysis may also provide information about the structure of the envelope, mode of energy transport through their atmosphere and the dynamics of stellar atmospheres.

Known physical laws that specify the interaction of radiation with stellar material may be applied to derive mathematical models. From these models we try to infer the physical conditions in the atmospheres.

Infrared observations of T-tauri stars, cool super-giants and objects like gaseous nebulae have shown the presence of dust around the ionised core. The mixture of dust and gas present in the stellar atmosphere inter-acts with the radiation resulting in the change of inten-sity. The radiation is absorbed, scattered and re-emitted in other directions at different frequency level.

1.2 Stellar atmosphere

From line shapes (profile) and strengths we can obtain information regarding temperature, electron density, magnetic field, radial and rotational velocities and so on. Under the influence of stellar rotation, spectral lines get broadened. Changes in the shapes of lines will tell us about the dynamics of the gases in the atmospheres.

Due to transparency of stellar gas, the radiation escaping from the surface is the average of the emission from the underlying layers. Greater the temperature of the layer greater will be the emission as well as absorp-tion. The energy absorbed is less than that emitted in case of outer layers because the overlying layers are thin. Though emission is large from the interior layers the absorption also is more by the overlying layers.

A layer can be imagined in such a way that the radiation emitted by layers below it is totally absorbed and the contribution to the emergent radiation is solely

due to the layers above it. Since the radiation emerges from a variety of depths in the stellar atmosphere, it can not be expected to indicate a unique temperature that corresponds to any one layer in the star. The temperature that we derive will be a representative temperature corresponding to some representative depth in the atmosphere.

1.3 What can be learnt from stellar spectra

Study of spectral lines is one of the major interests in astrophysics as it is an established fact that they provide valuable information to infer the physical conditions of the gaseous material present in the stellar bodies.

Stellar atmospheric pressure affects the spectrum of the star. Spectra of two stars with same temperature but different pressures are found to differ. Degree of ionization of atoms depends on the rate at which those atoms can recapture electrons. The process of recapture depends on how closely they are packed together. At higher densities the particles are much closer than at lower densities hence recapture of electrons is easier. This is the reason why the fraction of atoms that are ionised at any instant of time is lower at high pressures than the gas at low pressures.

1.4 Equivalent width of spectral line and curve of growth

Since the profiles of different lines differ in

shape it is convenient to define some measurable quantity that can be used to calculate the total amount of light energy that is subtracted from the spectrum by the line. The most commonly used measure is the "equivalent width". This is the width of a hypothetical line with rectangular profile of zero intensity along its entire width. Equivalent width represents the same subtraction of light from stellar spectrum as is removed by the actual line. It is a substitution for the integrated line strength, and is given by

$$W_\lambda = \int_0^\infty \frac{I_c - I_L}{I_c} \, d\lambda$$

where I_c and I_L are the specific intensities in the continuum and the line centre respectively. It can also be measured in terms of flux from the stellar disc. Equivalent width is a measure of the line strength relative to the background continuum. The integrand of the above equation is known as residual intensity

$$\gamma_{int} = \frac{I_c - I_L}{I_c} = 1 - \frac{I_L}{I_c}$$

and in terms of flux, the residual flux is

$$\gamma_{flux} = 1 - \frac{F_L}{F_c}$$
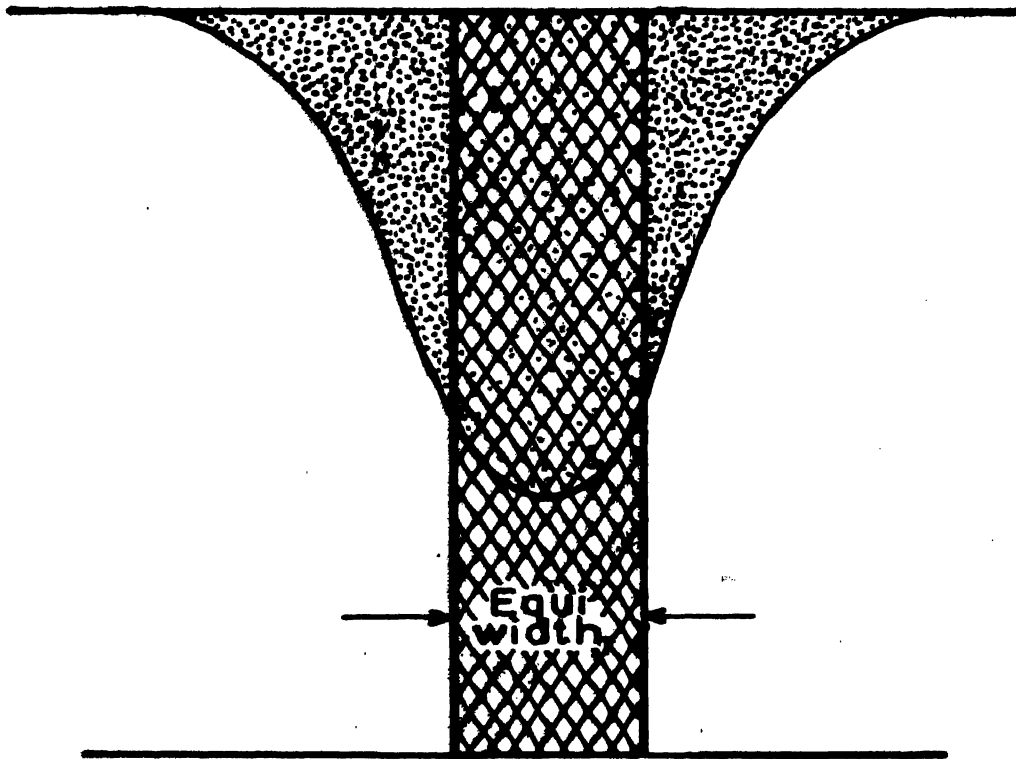
Figure 1.1. Schematic diagram showing equivalent width of a spectral line. The shaded and dotted regions have the same area.

Spectral line profiles of varying equivalent widths are due to varying number of atoms that are present in the stellar photosphere which can produce that line.

Strength of absorption line not only depends on the total abundance of the relevant atomic species but also those in a given ionized and excited state. Temperature and pressures are dependent on the depth of the photosphere. It can be calculated that which fraction of the atoms will be in the relevant excitation state. Since an absorption line arises from atoms at all depths throughout the atmosphere we must consider the contributions from all atoms at various layers to predict the equivalent

width of the line. We have tried to calculate how the equivalent width will vary with total number of atoms present forming the line. . At lower abundances equivalent width is approximately proportional to the total number of atoms present. The line saturates for a larger number

of atoms and for abnormally high number of atoms in the atmosphere broad wings appear on the line due to collisional broadening. In this case the equivalent width increases as the square root of the number of atoms present in the atmosphere. A graph that shows relationship between equivalent width of a line and the number of atoms that produce the line is called a curve of growth.

1.5 Moving atmospheres

It has been established by observations that there exist macroscopic motions in the stellar atmospheres. Wide range of motions even leading to the expansion of the atmosphere as a whole have been evidenced by observational data.

Velocity fields have little effect on radiative transfer in the continuum. However, even a small Doppler frequency shift of a line produces a major change in its absorptivity as seen by a stationary observer. This

strongly influences the line formation. Struve and Elvey in their analysis of the spectra of supergiants have discovered that the Doppler widths inferred from the position of the flat part of the curve of growth were far in excess of the thermal value. They attributed this broadening to non-thermal "turbulent" velocities presumed to have Gaussian distribution. These velocities are very small and act as additional line broadening agents and enhance the line strength.

However the inferred velocities often approach or exceed the speed of sound in the material and it is clear that astrophysical microturbulent velocities are not to be identified with turbulence in the strict fluid-dynamical sense, but rather with unresolved motions. Curves of growth also help in drawing inferences of micro turbulent velocity, but high resolution spectra have shown distinct Doppler shifts and asymmetries that fluctuate in time.

Evidence for velocity patterns on a large scale was provided by Struve's observation that the width of line profiles in certain stars exceeded the Doppler widths obtained from the curve of growth of their spectra. Here one envisions areas on the stellar surface so large to be practically independent of atmospheres moving systematically along the line of sight. Further, periodic Doppler shifts of the lines in some stellar spectra reveal that they are from pulsating stars. Beyond this, objects such as the WR stars, P-Cygni stars and early type super giants

all show characteristic line profiles with blue shifted absorption components and red shifted emission coponents indicative of large scale expansion. It is desirable to know distribution functions describing the amplitudes and scales of the velocity patterns·. A truely consistent theory of stellar atmospheres will require a dynamical theory of the interaction of material velocities, the thermodynamic state of matter and the radiation field. Then only it is possible to fully understand the stellar chromospheres and coronae. An attempt is being made to understand the kinematics of radiative transfer in moving media, i.e. computation of the emergent spectrum using a given velocity field and model atmosphere. The presence of velocity gradient in the expanding medium was relaised by Sobolev which has simplified the problem of radiation transfer in the stellar medium.

Sobolev's method provides an approximate solution in the case of rapid flow with large velocity gradients, where as comoving frame methods provide general solution applicable to lower velocities of few Doppler widths upto very large velocities, as well.

1.6 Transfer equation in fluid frame

For an observer in a stationary frame the opacity and emissivity of the material become angle dependent owing to the effects of Doppler shifts and aberration of light. This results in an inextricable coupling between frequency and angle which presents difficulties in the

calculations of scattering terms with a discrete quadrature term. In view of avoiding difficulties treatment of transfer problem in a frame comoving with the fluid is considered.

In comoving frames opacity and emissivity are isotropic and problems involving partial redistribution effects can be tackled by using standard static redistribution functions. While calculating scattering integrals it may be enough to consider only a small frequency band of width broad enough to contain the profile fully. This bandwidth is independent of the fluid velocity. Dynamical calculations in spherical flow can be handled accurately in a Lagrangian coordinate system.

The effect of high velocities plays an important role in formation of spectral lines in the outer layers of stars. In objects such as Wolf-Rayet stars, P-cygni stars, novae, quasars and planetary nebulae etc. the matter is observed to be moving with very high radial velocities. Earlier, attempts (by Kunasz & Hummer (1974),Peraiah and Wehrse (1978), Wehrse and Peraiah (1979) and others) have been made to solve the problem of transfer of line radiation by moving media. Observer's frame calculations are restricted only to small velocities. For knowing the formation of lines in rapidly moving stellar atmospheres one must study the solution of transfer in the comoving frame.

Chandrasekhar (1945) and Abhyankar (1964) have developed methods for tackling this problem but they were restricted by several assumptions and were valid for plane parallel atmospheres. Mihalas and other workers in this field have made considerable amount of work on comoving frame calculations.

Here we adopt the method developed by Peraiah (1980) to obtain a direct. solution of line transfer in comoving frame of the fluid within the frame work of discrete space theory.

The comoving terms which appear in the transfer equation are

$$(1-\mu^2)\{\frac{V(r)}{r} +\mu^2 \frac{dV(r)}{dr}\} \frac{\partial I(x,\mu,r)}{\partial x} \qquad (1-1)$$

where $I(x,\mu,r)$ is the specific intensity of the ray with frequency $x = \frac{\nu -\nu_o}{\Delta_s}$, Δ_s being some standard frequency interval, ν_o is the central frequency of the line and ν is any frequency point in the line making an angle $\theta = Cos^{-1}\mu$ with the radius vector at a radial point r. $V(r)$ is the velocity of the gas in mean thermal units at point r. Incorporating comoving terms given above in the radiative transfer equation,

For a non-LTE two level atom we write

$$\mu \frac{\partial I(x,\mu,r)}{\partial r} + \frac{1-\mu^2}{r} \frac{\partial I(x,\mu,r)}{\partial \mu} = K(x,r)S_L(r) +$$

$$K_c(r)S_c(r) - [K(x,r)+K_c(r)]I(x,\mu,r)+$$

$$\{(1-\mu^2)\frac{V(r)}{r} +\mu^2 \frac{dV(r)}{dr}\} \frac{\partial I(x,\mu,r)}{\partial x} \qquad (I-2)$$

and for an oppositely directed beam

$$-\mu \frac{\partial I(x,-\mu,r)}{\partial r} - \frac{1-\mu^2}{r} \frac{\partial I(x,-\mu,r)}{\partial \mu} = K(x,r)S_L(r) +$$

$$+K_c(r)S_c(r) - [K(x,r)+K_c(r)]I(x,-\mu,r)+$$

$$\{(1-\mu^2)\frac{V(r)}{r} +\mu^2 \frac{dV(r)}{\partial r}\} \frac{\partial I(x,-\mu,r)}{\partial x} \qquad (1-3)$$

where $K(x,r)$ and $K_c(r)$ are absorption coefficients per unit frequency interval in the line and continuum respectively. $S_L(r)$ and $S_c(r)$ are the line and continuum source fucntions.

The H Lyman α-line has a very large central optical depth and therefore the diffusion of photons into the

line wings assumes greater importance. For an expanding spherical configuration the spectral line formation calculations for complete redistribution and for partial redistribution have shown marked differences. As the effects of redistribution become stronger when the optical depth increases, it becomes necessary to take partial redistribution into account. H Lyman α -line formation for plane parallel, Panagia and Ranieri (1973) and Peraiah and Wehrse (1977) have shown that geometry of the medium does have an appreciable influence on the radiation field of the Lyman α-line. Further it has been established that the expansion leads to considerable changes. Here we have tried to calculate the radiation fields taking partial redistribution, sphericity and also the expansion of the medium into consideration. Calculations are done for atmospheres expanding with constant velocity as well as those with velocities increasing linearly towards the outer surface.

In chapter 4 we have tried the calculations for the line formation in comoving frame with the partial frequency redistribution within the frame work of discrete space theory of transfer of radiation. We have considered radial mass motion of the medium and

photon redistribution from any given point to any other point in the frequency interval $\nu_o \left(\dfrac{1-V_{max}}{c} \right)$ to $\nu_o \left(\dfrac{1+V_{max}}{c} \right)$ where ν_o is the central frequency of the line and V_{max} is the maximum gas velocity. Radiation field obtained in the comoving frame has been translated into the frame of reference of the observer at infinity as these will be useful for direct comparison with the observational facts. In figure 1.2 we have tried to describe this translation.

Radiative transfer equation is solved in the comoving frame by assuming velocity distribution given by

$$V(r) = V_A + \frac{V_B - V_A}{B - A} (r-A) \tag{1-4}$$

where $V(r)$ is the gas velocity at a radial point r and V_A, V_B are the velocities at inner and outermost atmospheric points at distances A and B from the stellar centre. All velocities are measured in mean thermal units. Density in the medium is considered to be varying as $\left(\dfrac{1}{r} \right)$. Frequency and angle dependent source functions S(r) are calculated at every radial point by using the relation

$$S_n = \sum_{i=1}^{I} A_i \sum_{j=1}^{J} S(x_i, \mu_j, \tau_n) C_j \tag{1-5}$$

The optical depth is calculated along the parallel rays as shown in fig.1.2. From above consideration flux received at infinity can be calculated.

Expanding envelope
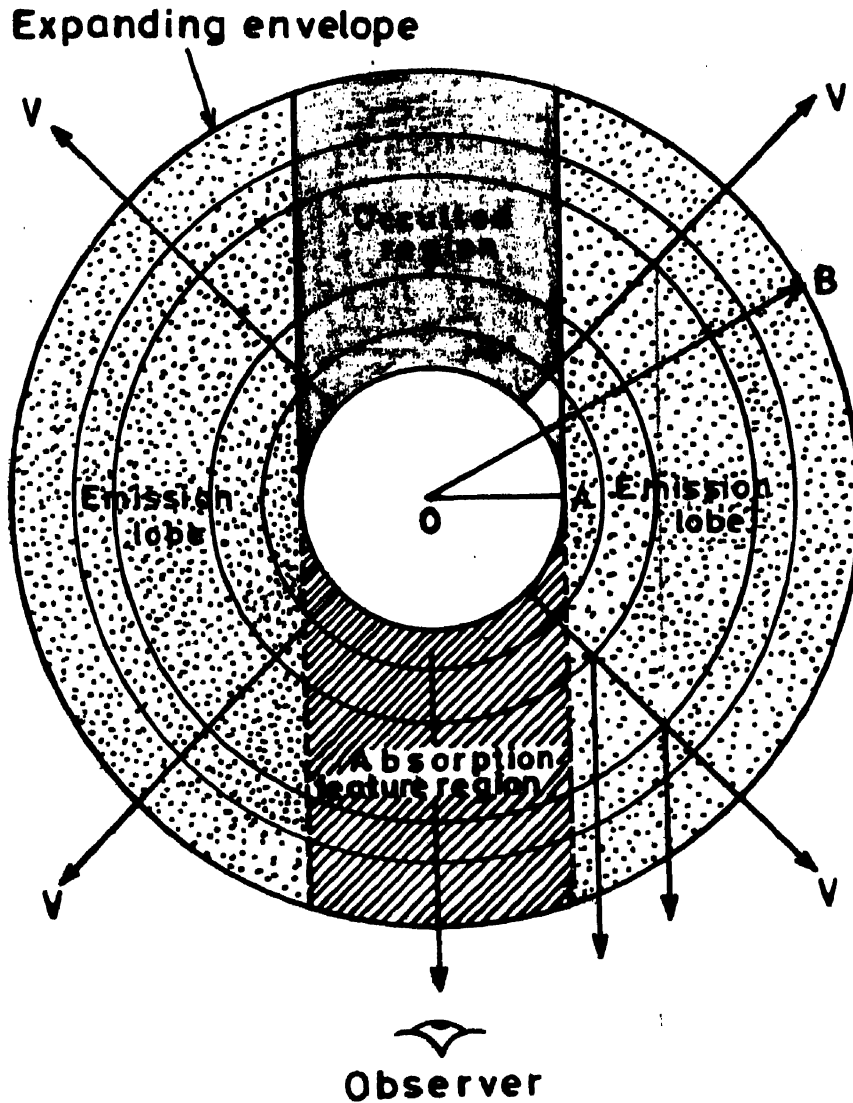
Figure 1.2. Schematic diagram of expanding envelopes surrounding a stellar atmosphere. Material in the occulted region is blocked from view for an external observer by the stellar disc. It also shows how fluxes are calculated by an observer at infinity.

In a purely scattering medium we see absorption lines. When the velocities increase the line centres get shifted towards blue side.

Presence of dust has been evidenced ·by infrared observations of .many stellar objects. We have tried to study the line formation in dusty envelopes. Line formation calculations have been done taking into account the presence of dust, radial expansion, and geometrical extension of envelopes. Effects of dust and velocities of expansion on the equivalent widths of spectral lines are shown at Chapter 5. We have studied the effect of pure scattering by dust and the effect due to absorption has been ignored. Modification: in the profiles for various dust optical depths and velocities has also been shown.

CHAPTER 2

DISCRETE SPACE THEORY OF RADIATIVE TRANSFER EQUATION IN
MONOCHROMATIC RADIATION FIELD.

2.1 Introduction

        Energy generated in the stellar interiors is trans-
mitted on to the atmosphere and leaves the star. Radiative
transfer equation is the basic tool for the study of trans-
mission of radiation through the stellar atmospheres. Since
complex physical processes are going on in the atmosphere
it is difficult to obtain the solution for radiative trans-
fer equation. Different people working in this area have
proposed several methods. As early as 1862,G.G.Stokes
obtained difference equations for reflection by a pile of
identical glass plates. However the method suggested by
Ambartzumian (1943) is better suited for solving the equa-

tion of radiative transfer. This method is based on the principle of invariant imbedding. This method has found extensive use for several workers in this field to calculate the reflection and transmission functions. Chandrasekhar (1960) has used this principle. The invariance principles are consequences of an interaction principle and the star product which are essentially a statement of energy conservation in a finite medium. Redheffer (1962) and Preisendorfer (1965) have developed interaction principle and star product. Grant and Hunt (1969) have added the internal source terms which are useful in stellar atmospheres. This theory was extended to spherical system by Peraiah and Grant (1973). In what follows we shall give the details of the methods which we have used for our calculations.

To obtain solution for the transfer equation following steps are adopted -

1. The atmosphere is divided into a number of 'cells' whose thickness is defined by τ - which is less than or equal to a critical thickness τ_{crit}. This critical thickness of the cell is determined on the basis of physical characteristics of the medium, and is called optical depth.

2. Integration of transfer equation is performed on the 'cell', which is a two dimensional grid bound by $[r_n, r_{n+1}]$ X $[\mu_{j-\frac{1}{2}}, \mu_{j+\frac{1}{2}}]$.

3. We compare these discrete equations with the canonical equations of the interaction principle and obtain the transmission and reflection operators of the shell.

4. Finally we combine all the cells by star algorithm and obtain the radiation field.

2.2 Interaction Principle

Interaction principle is a relation between the incident and emergent radiation fields from a medium of known optical properties.

Consider a cell of optical thickness τ with incident and emergent intensities at its boundaries (n,n+1). Let us assume that the specific intensities U_n^+ and U_{n+1}^- are incident on the cell at these boundaries. Similarly U_n^- and U_{n+1}^+ are the specific intensities emerging from the cell at these boundaries. The symbols + and − represent specific intensities in inward and the opposite directions.
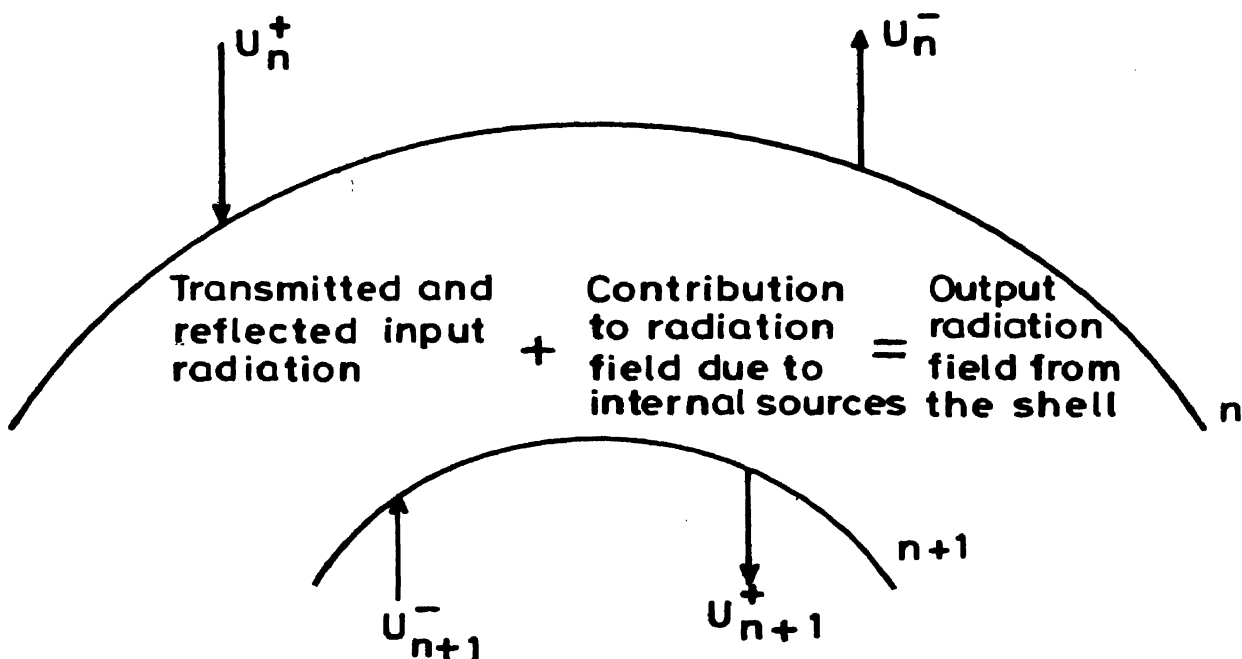
Figure 2.1. Schematic diagram showing the interaction principle.

If $\theta = \cos^{-1}\mu$ is the angle made by a ray with radial vector indicating the direction in which n is increasing, we have

$$U_n^+ \{ U_n(\mu) : 0 < \mu \leq 1 \}$$

and

$$U_n^- \{ U_n(-\mu): 0 < \mu \leq 1 \}$$

U_n^+ — represents the specific intensity of the ray travelling in the direction of μ (inward, increasing 'n') and U_n^- represents the specific intensity of the ray travelling in upward direction. We may select a finite set of values for μ (μ_j: $1 \leq j \leq m$; $0 < \mu_1 < \mu_2 < \mu_3 < \mu_4 \cdots \mu_m \leq 1$) and write U_n^+ and U_n^- as vectors in m-dimensional Euclidean space as

$$U_n^+ = \begin{bmatrix} U_n(\mu_1) \\ U_n(\mu_2) \\ U_n(\mu_3) \\ \cdot \\ \cdot \\ \cdot \\ U_n(\mu_m) \end{bmatrix} \text{ and } U_n^- = \begin{bmatrix} U_n(-\mu_1) \\ U_n(-\mu_2) \\ U_n(-\mu_3) \\ \cdot \\ \cdot \\ \cdot \\ U_n(-\mu_m) \end{bmatrix}$$

Here U_n^+ and U_n^- are the incident and emergent intensity vectors at the nth layer. Similarly U_{n+1}^- and U_{n+1}^+ are the corresponding intensity vectors at the $(n+1)^{th}$ layer.

The emergent radiation field will have dependence on the incident radiation and also has the contributions from the internal sources present in the layer. Let $\Sigma^{+}(n+1,n)$ and $\Sigma^{-}(n,n+1)$ be the contributions to the emergent intensity vectors U_{n+1}^{+} and U_{n}^{-} respectively.

If we define $t(n+1,n)$ and $t(n,n+1)$ as linear operators of diffuse transmission and $r(n,n+1)$ and $r(n+1,n)$ as linear operators of diffuse reflection, the emergent field intensity vectors can be expressed interms of the reflected and transmitted input intensities together with contributions from internal sources as

$$U_{n+1}^{+} = t(n+1,n)\ U_{n}^{+} + r(n,n+1)U_{n+1}^{-} + \Sigma^{+}\ (n+1,n)$$

$$U_{n}^{-} = r(n+1,n)U_{n}^{+} + t(n,n+1)U_{n+1}^{-} + \Sigma^{-}(n,n+1) \qquad (2-1)$$

This pair of equations can well be written in a concise way as

$$
\begin{bmatrix} U_{n+1}^{+} \\ \\ U_{n}^{-} \end{bmatrix}
= S_{(n,n+1)}
\begin{bmatrix} U_{n}^{+} \\ \\ U_{n+1}^{-} \end{bmatrix}
+ \Sigma\ (n,n+1) \qquad (2-2)
$$

$$
\text{where } S_{(n,n+1)} =
\begin{bmatrix} t(n+1,n) & r(n,n+1) \\ r(n+1,n) & t(n,n+1) \end{bmatrix}
\qquad (2-3)
$$

The above equation is called the 'principle of interaction'. Redheffer has developed a theory based on this principle of interaction without the source terms. Introduction of internal source terms was due to Grant and Hunt (1969a). Interaction principle mentioned above is of general form. Reflection and transmission operators include the properties of the medium and the geometry as well. It can be applied to plane parallel case and can also be used to spherical symmetry case. Effects of inhomogeneities of the medium can also be introduced into these operators without much difficulty.

The problem is treated in two stages, i.e. determination of the fluxes emerging from the layers and the determination of flux at any internal layer.

2.3 Star Product

Consider another layer with boundaries $(n+1, n+2)$ adjacent to the $(n, n+1)$ layer. Extending the interaction principle to this layer we an write

$$\begin{bmatrix} U^+_{n+2} \\ U^-_{n+1} \end{bmatrix} = S_{(n+1, n+2)} \begin{bmatrix} U^+_{n+1} \\ U^-_{n+2} \end{bmatrix} + \Sigma\ (n+1, n+2) \qquad (2-4)$$

where

$$S_{(n+1,n+2)} = \begin{bmatrix} t(n+2,n+1) & r(n+1,n+2) \\ r(n+2,n+1) & t(n+1,n+2) \end{bmatrix} \quad .$$

If we combine the two layers with boundaries $(n,n+1)$ and $(n+1,n+2)$ interaction principle for the combined shell can be written by eliminating U^+_{n+1} and U^-_{n+1} from equations (2-2) and (2-4) as

$$\begin{bmatrix} U^+_{n+2} \\ U^-_n \end{bmatrix} = S_{(n,n+2)} \begin{bmatrix} U^+_n \\ U^-_{n+2} \end{bmatrix} + \Sigma(n,n+2) \qquad (2-5)$$

The relation between $S(n,n+1)$, $S(n+1,n+2)$ and $S(n,n+2)$ is given by

$$S(n,n+2) = S(n,n+1) * S(n+1,n+2) \qquad (2-6)$$

this was called 'star product' of two S-matrices by Redheffer (1962).

The reflection and transmission operators, r and t, for this combined 'shell' bound by boundaries $(n,n+2)$ are given by

$$t(n+2,n) = t(n+2,n+1) [I-r(n,n+1)r(n+2,n+1)]^{-1} t(n+1,n)$$

$$t(n,n+2) = t(n,n+1) [I-r(n+2,n+1)r(n,n+1)]^{-1} t(n+1,n+2)$$

$$r(n+2,n) = r(n+1,n)+t(n,n+1)r(n+2,n+1)$$

$$[I-r(n,n+1)r(n+2,n+1)]^{-1}t(n+1,n)$$

$$r(n,n+2) = r(n+1,n+2)+t(n+2,n+1)r(n,n+1)$$

$$[I-r(n+2,n+1)r(n,n+1)]^{-1}t(n+1,n+2)$$

$$(2-7)$$

and

$$\Sigma(n,n+2) = \Lambda(n,n+1;n+2)\Sigma(n,n+1)+ \Lambda'(n;n+1,n+2)$$

$$\Sigma(n+1,n+2) \qquad (2-8)$$

where I- is the identity matrix.

And

$$\Lambda(n,n+1;n+2)=\begin{bmatrix} t(n+2,n+1)[I-r(n,n+1)r(n+2,n+1)]^{-1} & 0 \\ t(n,n+1)r(n+2,n+1)[I-r(n,n+1)r(n+2,n+1)]^{-1} & I \end{bmatrix}$$

$$\Lambda'(n;n+1,n+2)=\begin{bmatrix} I & t(n+2,n+1)r(n,n+1)[I-r(n+2,n+1)r(n,n+1)]^{-1} \\ 0 & t(n,n+1)[I-r(n+2,n+1)r(n,n+1)]^{-1} \end{bmatrix}$$

$$(2-9)$$

also

$$\Sigma(n,n+1) \quad = \quad \begin{bmatrix} \Sigma(n+1,n+2) \\ \\ \Sigma^{-1}(n,n+1) \end{bmatrix}$$ (2-10)

In a similar way

$\Sigma(n+1,n+2)$ may also be defined.

The star product exists whenever either of the inverse operators

$[I-r(n,n+1)r(n+2,n+1)]^{-1}$ or

$[I-r(n+2,n+1)r(n,n+1)]^{-1}$ exists.

Here it may be noted that the existence of either operators implies that of the other. Grant and Hunt (1969) have elaborated the physical significance of these operators.

Each shell has been stratified by pair of planes (n,n+1). It may be conveniently thought of such a shell independent of any system of coordinates. If we use S (α) to denote the S operator for a cell designated by α, then we may write

$S(\alpha*\beta) = S(\alpha) * S(\beta)$ (2-11)

where $\alpha * \beta$ denotes the region obtained by putting the two shells α and β together. If and only if the shells are homogeneous and plane parallel then we have

$$\alpha * \beta = \beta * \alpha \qquad (2-12)$$

otherwise in general, star multiplication is non-commutative. If we have three layers α, β and γ taken in order, it is easy to verify that the result is independent of the order in which the operators are combined.
i.e

$$S[\alpha * (\beta * \gamma)] = S[(\alpha * \beta) * \gamma] = S[\alpha * \beta * \gamma]$$

thus the star-multiplication is associative. If we have to add several shells then

$$S[(\alpha * (\beta * \gamma) * \ldots)] = S[(\alpha * \beta) * \gamma * \ldots] \qquad (2-13)$$

The entire slab of the medium bound by (a,b) is stratified into several layers or shells with varying radii

$$b = x_1 < x_2 < x_3 < \ldots \ldots x_{n+1} = a \text{ see figure 2.2.}$$

Restricting to discrete space theory $S(x_i, x_{i+1})$ can be found to desired accuracy from physical parameters at some point (x_i, x_{i+1}).
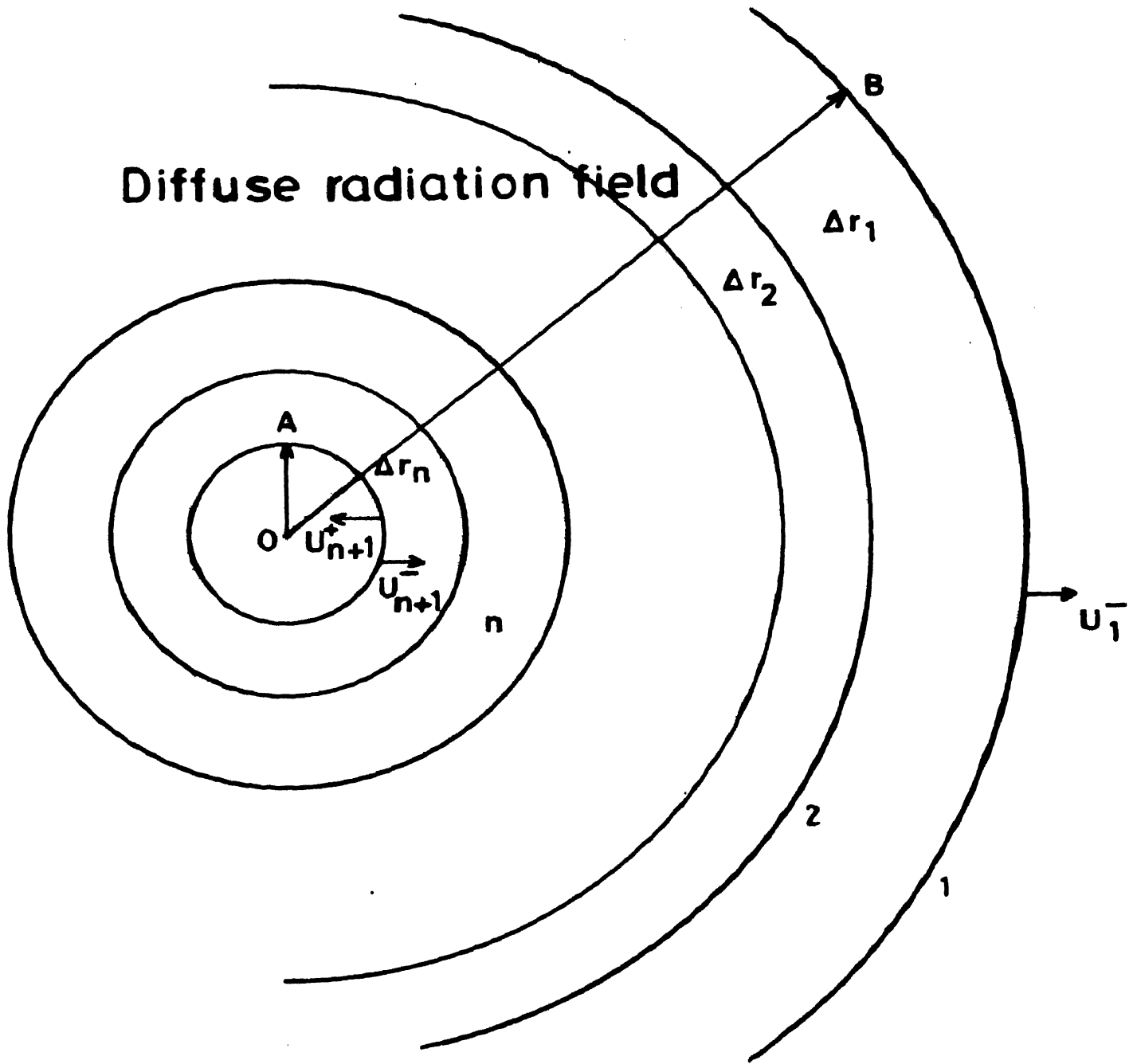
Figure 2.2. Schematic diagram showing the diffuse radiation field in a spherically symmetric atmosphere.

For any pair of values i and j with $i < j$ we can write

$$S(x_i, x_j) = S(x_i, x_{i+1}) * S(x_{i+1}, x_{i+2}) * \ldots$$

$$S(x_{j-1}, x_j)$$

In similar way we can write $\Sigma(x_i, x_j)$ as the linear functional for the sources.

By adding a layer at a time complete exteranl response can be built up. Particularly a fast method of generating S-operators for a medium which is homogeneous and very thick has been used and is known as 'doubling method' [Van-de Hulst (1965). It has been shown that

$$S(2^p d) = S(2^{p-1} d) * S(2^{p-1} d) \qquad (2-14)$$

where $(p = 1,2,3\ldots)$

this shows that we can generate the S-matrix for a layer of thickness $2^p d$ in p-cycles starting with $S(d)$ rather than in 2^p cycles of adding the $S(d)$'s one by one. For $P = 10$, say, only a fraction $10/2^{10} \simeq 10^{-2}$ of the effort required to add 2^{10} layers of thickness d is needed.

2.4. Calculation of radiation field at internal points

For calculating radiation field at any internal point, non-negativity of the transmission and reflection operators is presumed. The necessary pre-condition for this to be satisfied is that the optical thickness of the shell is less than a certain value called the 'criti-

cal size' ($\tau = \tau_{crit}$). If the optical thickness of any shell is larger than this critical value then the shell is divided into subshells in such a way that the thickness of no sub-shell will be greater than τ_{crit}. Star product algorithm is made use of to calculate the combined response from the subshells whose total thickness is T. In other words the entire medium is to be divided into a larger number of shells having optical thickness less than a critical value to cal-culate the radiation field at any point in the stellar atmos-phere.

We have divided the medium into N-number of shells. Interaction principle can be written down for each shell and the whole system of equations are solved (Peraiah 1980).

In the above figure we try to show the atmosphere with a diffuse radiation. To calculate the internal radia-tion field, the atmosphere is divided into N-shells with A and B as the inner and outer radii between 1st shell, (the outermost) and the Nth shell, the solutions U_{n+1}^{+} and U_n^{-} can be obtained from the relations

$$U_{n+1}^{+} = r(1,n+1)U_{n+1}^{-} + V_{n+\frac{1}{2}}^{+}$$

$$\text{(2-15)}$$

$$U_n^{-} = t(n,n+1)U_{n+1}^{-} + V_{n+\frac{1}{2}}^{-}$$

with the boundary condition

$$U_{n+1}^{-} = U^{-}(a) \qquad\qquad \text{(2-16)}$$

The quantities $r(1,n+1)$, $V^+_{n+\frac{1}{2}}$, $V^-_{n+\frac{1}{2}}$ appearing in equation (2-15) are calculated by imposing the initial conditions

$$r(1,1) = 0, \qquad V^+_{\frac{1}{2}} = U^+(a) \qquad\qquad (2\text{-}17)$$

by computing recursively

$$r(1,n+1) = r(n,n+1)+t(n+1,n)r(1,n)X$$

$$[I-r(n+1,n)r(1,n)]^{-1}t(n,n+1) \qquad\qquad (2\text{-}18)$$

$$V^+_{n+\frac{1}{2}} = \hat{t}(n+1,n)V^+_{n-\frac{1}{2}} + \Sigma^+(n+1,n)+R_{n+\frac{1}{2}}\ \Sigma^-(n,n+1)$$

$$V^-_{n+\frac{1}{2}} = \hat{r}(n+1,n)V^+_{n-\frac{1}{2}} + T_{n+\frac{1}{2}}\ \Sigma^-(n,n+1) \qquad\qquad (2\text{-}19)$$

where

$$\hat{t}(n+1,n) = t(n+1,n)[I-r(1,n)r(n+1,n)]^{-1}$$

$$\hat{r}(n+1,n) - r(n+1,n)[I-r(1,n)r(n+1,n)]^{-1}$$

and $\qquad\qquad\qquad\qquad\qquad\qquad\qquad\qquad\qquad (2\text{-}20)$

$$R_{n+\frac{1}{2}} = \hat{t}(n+1,n)r(1,n)$$

$$T_{n+\frac{1}{2}} = [I-r(n+1,n)r(1,n)]^{-1}$$

also in Eqn.(2.-15)

$$t(n,n+1) = T_{n+\frac{1}{2}} \; t(n,n+1) \qquad\qquad (2-21)$$

Radiation field at internal points is calculated by adopting the following procedure:

1. The medium is divided into a large number of shells say N with N+1 boundaries.

2. The pairs of reflection and transmission operators

$$r(n+1,n); \quad r(n,n+1) \qquad\qquad \text{and}$$

$t(n+1,n); \quad t(n,n+1)$ in each shell are calculated by applying star algorithm if the optical thickness of each shell is larger than a critical value (τ_{crit}). If the medium is thick and homogeneous 'doubling method' is adopted for calculating these operators.

3. Boundary condition that $r(1,1) = 0$ and $V_{\frac{1}{2}}^{+} = U^{\dagger}(a)$ is imposed and the reflection, transmission operators mentioned above are computed recursively from shell 1 to shell N i.e. from the outermost layer at B to the innermost at A.

4. Then swept back from A to B calculating the radiation field as given in equation (2.-15) with the boundary condition

$$U_{n+1}^{-} = U^{-}(a)$$

It may be noted here that the operators $r(1,n+1)$, $t(n,n+1)$, $V^{+}_{n+\frac{1}{2}}$ and $V^{\pm}_{n+\frac{1}{2}}$ for each shell calculated are retained and utilised wherever necessary while calculating the radiation field.

For a reflecting surface we have

$$U^{-}_{n+1} = r_G U^{+}_{n+1} \qquad\qquad (2-22)$$

where r_G is the reflection operator. For a totally reflecting surface

$$r_G = 1$$

therefore we have

$$U^{+}_{n+1} = [I - r(1,n+1)r_G]^{-1} V^{+}_{n+\frac{1}{2}} \qquad\qquad (2-23)$$

from this U^{-}_{n+1} can be calculated with the help of equation (2-22).

The solution obtained within the frame work of discrete space theory can be checked for conservation of flux i.e. the system should neither create nor destroy the energy. It can effectively be checked by introducing some flux at the point A and calculating the fluxes that emerge at A and B.

If F-denotes the flux we must have

$$F^-(a) = F^-(b) + F^+(a) \qquad (2-24)$$

where $F^-(b)$ is the flux emerging at $r = b$ and $F^+(a)$ is the flux scattered back into the inner regions.

2.5 Derivation of reflection and transmission operators for the 'cell'

Radiative transfer equation in spherical symmetry is written as (Peraiah and Grant 1973)

$$\frac{\mu}{r^2} \frac{\partial}{\partial r} \{ r^2 I(r,\mu) \} + \frac{1}{r} \frac{\partial}{\partial \mu} \{ (1-\mu^2) I(r,\mu) \} + \sigma(r) I(r,\mu)$$

$$= \sigma(r) [\{ 1-\omega(r) \} \ b(r) + \frac{1}{2} \omega(r) \int_{-1}^{+1} P(r,\mu,\mu') I(r,\mu') d\mu'$$

$$(2-25)$$

where r-radius, μ is cosine of the angle made by the beam with radius vector. $\sigma(r)$ is the absorption coefficient, $\omega(r)$ is the albedo for single scattering, $b(r)$ represents the sources within the medium, $I(r,\mu)$-specific intensity of the ray and $P(r,\mu,\mu')$ is the phase function which is normalised as

$$\frac{1}{2} \int_{-1}^{+1} P(r,\mu,\mu') d\mu' = 1 \qquad (2-26)$$

$P(r, \mu, \mu')$ being a positive quantity with μ and μ' having values between -1 and $+1$. By substituting

$$I(r, \mu) = \frac{U(r, \mu)}{4\pi r^2}$$

and

$$b(r) = \frac{B(r)}{4\pi r^2}$$

then the equation of transfer for an outward going beam can be written as

$$\mu \frac{\partial U(r, \mu)}{\partial r} + \frac{1}{r} \frac{\partial}{\partial \mu} \{(1-\mu^2)U(r, \mu)\} + \sigma(r)U(r, \mu)$$

$$= \sigma(r)[\{1-\omega(r)\} B(r) + \frac{1}{2}\omega(r) \int_{-1}^{+1} P(r, \mu, \mu')U(r, \mu')d\mu'$$

(2.-27)

for an oppositely directed beam

$$-\mu \frac{\partial U(r, -\mu)}{\partial r} - \frac{1}{r} \frac{\partial}{\partial \mu} \{(1-\mu^2)U(r, -\mu) + \sigma(r)U(r, -\mu)$$

$$= \sigma(r)[\{(1-\omega(r)\} B(r) + \frac{1}{2}\omega(r) \int_{-1}^{+1} P(r, -\mu, \mu')U(r, \mu')d\mu' \qquad .$$

(2-28)

μ is restricted to lie in the interval $[0,1]$ for some discrete points.

In the 'cell' method of deriving difference equations, (2.-27) and (2-28) are integrated within the boundaries defined by

$$[r_n, r_{n+1}] \times [\mu_{j-\frac{1}{2}}, \mu_{j+\frac{1}{2}}]$$

a two dimensional grid (Carlson 1963, Lathrop and Carlson 1967).

Utilizing the roots μ_j and their corresponding weights C_j of the Gauss-Legendre quadrature formula of order J over an interval [0,1] and writing $\mu_{\frac{1}{2}} = 0$ we define

$$\mu_{j+\frac{1}{2}} = \sum_{k=1}^{J} C_k, \quad j = 1,2,\ldots J \qquad (2\text{-}29)$$

From the interpolatory character of the Gauss formula it may be seen that

$$\mu_{j-\frac{1}{2}} \leq \mu_j \leq \mu_{j+\frac{1}{2}}$$

First considering the angle integration, equation (2-27) over the interval $[\mu_{j-\frac{1}{2}}, \mu_{j+\frac{1}{2}}]$.

We obtain

$$C_i \mu_j \frac{\partial U_j^+(r)}{\partial r} + \frac{1}{r} [(1-\mu_{j+\frac{1}{2}}^2)U_{j+\frac{1}{2}}^+(r)-(1-\mu_{j-\frac{1}{2}}^2)U_{j-\frac{1}{2}}^+(r)]$$

$$+C_j \sigma(r)U_j^+(r) = \sigma(r)C_j[(1-\omega(r)B(r)$$

$$+ \frac{1}{2} \omega(r) \sum_{j'=1}^{J} \{P^{++}(r)_{jj'}C_{j'}U_{j'}^+(r)+P^{+-}(r)_{jj'}C_{j'}U_{j'}^-(r)\}]$$

$$(2-30)$$

where

$$U_j^+(r) = U(r,\mu_j), \qquad U_j^-(r) = U(r,-\mu_j)$$

$$P^{++}(r)_{jj'}=P(r,\mu_j,\mu_{j'}); \quad P^{-+}(r)_{jj'} = P(r,-\mu_j,\mu_{j'}) \text{ and so on.}$$

Similar equation can be got for (2 -28). With little loss of accuracy the terms $U_{j+\frac{1}{2}}^\pm$ are defined by writing

$$U_{j+\frac{1}{2}}^\pm = \frac{(\mu_{j+1}-\mu_{j+\frac{1}{2}}) U_j^\pm+(\mu_{j+\frac{1}{2}}-\mu_j)U_{j+1}^\pm}{\mu_{j+1} - \mu_j} \qquad (2-31)$$

where j = 1,2,....,(J-1).

for convenience if we put $U^+_{\frac{1}{2}} = U^-_{\frac{1}{2}}$ by interpolation

$$U^+_{\frac{1}{2}} = U^-_{\frac{1}{2}} = \frac{1}{2}(U^+_1 + U^-_1) \qquad (2-32)$$

Writing

$$\underset{\sim}{U}^+(r) = \begin{bmatrix} U^\pm_1(r) \\ U^\pm_2(r) \\ \cdot \\ \cdot \\ \cdot \\ U^\pm_J(r) \end{bmatrix} \qquad (2-33)$$

making use of this and also equations (2-31),(2-32) equation (2-30) can be rewritten for all the angles in the matrix form as

$$\underset{\sim}{M} \frac{\partial U^+(r)}{\partial r} + \frac{1}{r}[\underset{\sim}{\Lambda}^+\underset{\sim}{U}^+(r)+ \underset{\sim}{\Lambda}^-\underset{\sim}{U}^-(r)]+ \sigma(r)\underset{\sim}{U}^+(r)$$

$$= \sigma(r)[\{(1-\omega(r)\} \underset{\sim}{B}^+(r)+ \frac{1}{2} \omega(r) \{ \underset{\sim}{P}^{++}(r)\underset{\sim\sim}{C}U^+(r)+\underset{\sim}{P}^{+-}(r)\underset{\sim\sim}{C}U^-(r)\}]$$

$$(2-34)$$

In similar way equation (2-28) takes the form

$$-\underset{\sim}{M}\,\frac{\partial \underset{\sim}{U}^-(r)}{\partial r} - \frac{1}{r}\,[\underset{\sim}{\Lambda}^+\underset{\sim}{U}^-(r) - \underset{\sim}{\Lambda}^-\underset{\sim}{U}^+(r)] + \sigma(r)\underset{\sim}{U}^-(r)$$

$$=\sigma(r)\left[\{(1-\omega(r))\}B^-(r) + \tfrac{1}{2}\omega(r)\{\underset{\sim}{P}^{-+}(r)\underset{\sim}{C}\underset{\sim}{U}^+(r) + \underset{\sim}{P}^{--}(r)\underset{\sim}{C}\underset{\sim}{U}^-(r)\}\right]$$

$$(2-35)$$

where C and M are diagonal matrices with elements $[C_j\,\delta_{jj'}]$ and $[\mu_j\,\delta_{jj'}]$ respectively. B^+ and B^- are source vectors and Λ^+, Λ^- are curvature scattering matrices of dimension J X J as defined in chapter 3 by equations (3-27) and (3-28). These matrices should satisfy the identity

$$\sum_{j=1}^{J} \underset{\sim}{C}_j(\underset{\sim}{\Lambda}^+_{jk} - \underset{\sim}{\Lambda}^-_{jk}) = 0 \qquad\qquad (2-36)$$

Now by integrating over the radial co-ordiante from r_n to r_{n+1}, equations (2-34) and (2-35) give

$$\underset{\sim}{M}[\underset{\sim}{U}^+_{n+1} - \underset{\sim}{U}^+_n] + \tau_{n+\frac{1}{2}}\underset{\sim}{U}^+_{n+\frac{1}{2}} = \tau_{n+\frac{1}{2}}\left[(1-\omega_{n+\frac{1}{2}})\underset{\sim}{B}^+_{n+\frac{1}{2}} + (\tfrac{1}{2}\omega_{n+\frac{1}{2}}\underset{\sim}{P}^{++}_{n+\frac{1}{2}}\underset{\sim}{C}\right.$$

$$\left. - \frac{\rho\underset{\sim}{\Lambda}^+}{\tau_{n+\frac{1}{2}}}\right)\underset{\sim}{U}^+_{n+\frac{1}{2}} + (\tfrac{1}{2}\omega_{n+\frac{1}{2}}\underset{\sim}{P}^{+-}_{n+\frac{1}{2}}\underset{\sim}{C} - \frac{\rho\underset{\sim}{\Lambda}^-}{\tau_{n+\frac{1}{2}}})\underset{\sim}{U}^-_{n+\frac{1}{2}}$$

$$(2-37)$$

$$\underset{\sim}{M}[\underset{\sim}{U}^-_n - \underset{\sim}{U}^-_{n+1}] + \tau_{n+\frac{1}{2}} \underset{\sim}{U}^-_{n+\frac{1}{2}} = \tau_{n+\frac{1}{2}}[(1-\omega_{n+\frac{1}{2}})\underset{\sim}{B}^-_{n+\frac{1}{2}}$$

$$+ (\frac{1}{2}\omega_{n+\frac{1}{2}}\underset{\sim}{P}^{-+}_{n+\frac{1}{2}}\underset{\sim}{C} + \frac{\rho\underset{\sim}{\Lambda}^-}{\tau_{n+\frac{1}{2}}})\ \underset{\sim}{U}^+_{n+\frac{1}{2}}$$

$$+ (\frac{1}{2}\omega_{n+\frac{1}{2}}\underset{\sim}{P}^{--}_{n+\frac{1}{2}}\ \underset{\sim}{C} + \frac{\rho\underset{\sim}{\Lambda}^+}{\tau_{n+\frac{1}{2}}})\underset{\sim}{U}^-_{n+\frac{1}{2}}] \qquad (2-38)$$

Here $\underset{\sim}{U}^+_n = \underset{\sim}{U}^+(r_n)$ and the variables subscripted with $n+\frac{1}{2}$ are averages over the cell whose radial boundaries are r_n and r_{n+1} .

We define

$$\Delta r_{n+\frac{1}{2}} = r_{n+1} - r_{n'} \qquad \tau_{n+\frac{1}{2}} = \sigma_{n+\frac{1}{2}} \Delta r_{n+\frac{1}{2}}$$

$$\rho = \frac{\Delta r_{n+\frac{1}{2}}}{r_{n+\frac{1}{2}}}$$

where $r_{n+\frac{1}{2}}$ is a suitable mean radius such that

$$r_{n+\frac{1}{2}} = \frac{(r_n + r_{n+1})}{2}$$

The quantities $U^+_{n+\frac{1}{2}}$ and $U^-_{n+\frac{1}{2}}$ are replaced by

$$\underset{\sim}{U}^+_{n+\frac{1}{2}} = \frac{1}{2} (\underset{\sim}{U}^+_{n+1} + \underset{\sim}{U}^+_n)$$

and

$$\underset{\sim}{U}^-_{n+\frac{1}{2}} = \frac{1}{2} (\underset{\sim}{U}^-_n + \underset{\sim}{U}^-_{n+1}) \qquad\qquad (2-39)$$

This is the conventional 'diamond' difference scheme.

2.6 Equations for reflection and transmission operators and source vectors:

Substituting equation (2-39) in the previous two equations viz.(2-37) and (2-38) and rearranging the input and output intensities in the form of interaction principle, further comparing these equations with those given in Equation (2-1) we obtain $\underline{r}$ and $\underline{t}$ operators in the matrix form as

$$\underset{\sim}{r}(n+1,n) = 2\underset{\sim}{t}^- \underset{\sim}{r}^{-+} \underset{\sim}{\Delta}^+ \underset{\sim}{M}$$

$$\underset{\sim}{r}(n,n+1) = 2\underset{\sim}{t}^+ \underset{\sim}{r}^{+-} \underset{\sim}{\Delta}^- \underset{\sim}{M} \qquad\qquad (2-40)$$

and

$$\underset{\sim}{t}(n+1,n) = \underset{\sim}{t}^+[\ \underset{\sim}{\Delta}^+\underset{\sim}{s}^{++} + \underset{\sim}{r}^{+-}\underset{\sim}{r}^{-+}]$$

$$\underset{\sim}{t}(n,n+1) = \underset{\sim}{t}^-[\ \underset{\sim}{\Delta}^-\underset{\sim}{s}^{--} + \underset{\sim}{r}^{-+}\underset{\sim}{r}^{+-}] \qquad\qquad ((2\text{-}41)$$

and the source vectors are given by

$$\underset{\sim}{\Sigma}^+_{n+\frac{1}{2}} = \tau_{n+\frac{1}{2}}(1-\omega)\underset{\sim}{t}^+[\underset{\sim}{\Delta}^+\underset{\sim}{B}^+ + \underset{\sim}{r}^{+-}\underset{\sim}{\Delta}^-\underset{\sim}{B}^-]$$

$$\underset{\sim}{\Sigma}^-_{n+\frac{1}{2}} = \tau_{n+\frac{1}{2}}(1-\omega)\underset{\sim}{t}^-[\underset{\sim}{\Delta}^-\underset{\sim}{B}^- + \underset{\sim}{r}^{-+}\underset{\sim}{\Delta}^+\underset{\sim}{B}^+] \qquad\qquad (2\text{-}42)$$

where

$$\underset{\sim}{t}^+ = [\underset{\sim}{I}-\underset{\sim}{r}^{+-}\underset{\sim}{r}^{-+}]^{-1}, \qquad \underset{\sim}{t}^- = [\underset{\sim}{I}-\underset{\sim}{r}^{-+}\underset{\sim}{r}^{+-}]^{-1} \qquad (2\text{-}43)$$

$$\underset{\sim}{r}^{+-} = \underset{\sim}{\Delta}^+\underset{\sim}{s}^{+-} \qquad , \qquad \underset{\sim}{r}^{-+} = \underset{\sim}{\Delta}^-\underset{\sim}{s}^{-+} \qquad\qquad (2\text{-}44)$$

and

$$\underset{\sim}{\Delta}^+ = [\underset{\sim}{M} + \tfrac{1}{2}\tau_{n+\frac{1}{2}}(\underset{\sim}{I}-\underset{\sim}{Q}^{++}_{n+\frac{1}{2}})]^{-1}$$

$$\underset{\sim}{\Delta}^- = [\underset{\sim}{M} + \tfrac{1}{2}\tau_{n+\frac{1}{2}}(\underset{\sim}{I}-\underset{\sim}{Q}^{--}_{n+\frac{1}{2}})]^{-1} \qquad\qquad (2\text{-}45)$$

$$\underset{\sim}{s}^{++} = \underset{\sim}{M}-\tfrac{1}{2}\tau_{n+\frac{1}{2}}(\underset{\sim}{I}-\underset{\sim}{Q}^{++}_{n+\frac{1}{2}}) \qquad\qquad (2\text{-}46)$$

$$\underset{\sim}{s}^{--} = \underset{\sim}{M}-\tfrac{1}{2}\tau_{n+\frac{1}{2}}(\underset{\sim}{I}-\underset{\sim}{Q}^{--}_{n+\frac{1}{2}}) \qquad\qquad (2\text{-}46)$$

$$\underset{\sim}{S}^{-+} = \frac{1}{2} \tau_{n+\frac{1}{2}} \underset{\sim}{Q}^{-+}_{n+\frac{1}{2}}$$

$$\underset{\sim}{S}^{+-} = \frac{1}{2} \tau_{n+\frac{1}{2}} \underset{\sim}{Q}^{+-}_{n+\frac{1}{2}} \qquad (2-47)$$

while

$$\underset{\sim}{Q}^{++}_{n+\frac{1}{2}} = \frac{1}{2} \omega \underset{\sim}{P}^{++} \underset{\sim}{C} - \frac{\rho \Lambda^{+}}{\tau_{n+\frac{1}{2}}}$$

$$\underset{\sim}{Q}^{--}_{n+\frac{1}{2}} = \frac{1}{2} \omega \underset{\sim}{P}^{--} \underset{\sim}{C} + \frac{\rho \Lambda^{+}}{\tau_{n+\frac{1}{2}}} \qquad (2-48)$$

and

$$\underset{\sim}{Q}^{-+}_{n+\frac{1}{2}} = \frac{1}{2} \omega \underset{\sim}{P}^{-+} \underset{\sim}{C} + \frac{\rho \Lambda^{-}}{\tau_{n+\frac{1}{2}}}$$

$$\underset{\sim}{Q}^{+-}_{n+\frac{1}{2}} = \frac{1}{2} \omega \underset{\sim}{P}^{+-} \underset{\sim}{C} - \frac{\rho \Lambda^{-}}{\tau_{n+\frac{1}{2}}} \qquad (2-49)$$

Reflection and transmission operators must be non-negative
for satisfying this condition it is necessary that $\underset{\sim}{\Delta}^{+}, \underset{\sim}{\Delta}^{-}, \underset{\sim}{S}^{++}$
and $\underset{\sim}{S}^{--}$ must all be positive.

This positivity is possible only if

$$\tau_{n+\frac{1}{2}} \leqslant \tau_{crit}$$

where

$$\tau_{crit} = \min_{j} \left[\frac{\mu_j \pm \frac{1}{2} \rho \cdot \Lambda_{jj}^+}{\frac{1}{2}(1 - \omega_{n+\frac{1}{2}} P_{jj}^{++} C_j)} \right] \qquad (2-50)$$

By so calculating the r and t operators corresponding to this critical optical depth we can obtain the radiation field for a shell of larger optical thickness making use of the star algorithm.

CHAPTER 3

FORMATION OF SPECTRAL LINES IN THE EXPANDING STELLAR

ATMOSPHERES IN THE REST FRAME

3.1 Introduction

In the expanding atmospheres the physical proper-
ties of medium are affected by the local conditions of
the moving matter. This complicates the problem of cal-
culating the spectral lines in expanding atmospheres,
because the absorption coefficient becomes a function of
angle and frequency in the rest frame. For smaller veloci-
ties of the order of one or two mean thermal units rest
frame can be used for simulation of spectral lines. Dis-
advantage of the rest frame, is the angle-frequency mesh
increases in size with the velocities of the expanding
medium because of Doppler effect. However, in the comoving

frame, one need not worry about the Doppler effect and can employ high velocities with smaller angle-frequency mesh. Effects of photon frequency redistribution on the spectral line formation in stellar atmospheres is of greater importance. The frequency redistribution of photons after several scatterings and absorptions in the line, will change the escape probability of photon through the outer surface of the stellar atmosphere.

When the matter in the atmosphere is radially expanding the line emitted by this gas continuously gets shifted. It means that the wing photons which would have escaped from the atmosphere had the medium been stationary. Due to expansion they will be absorbed and re-emitted with redistribution in both angle and frequency at a different radial point in the atmosphere. As a result of this in a moving medium the source function is changed and the redistribution of photons in angle as well as frequency becomes more complicated to understand. The process becomes much more complicated when curvature factor is introduced. Redistribution in frequency is influenced by the velocity gradients in the gas while the redistribution in angle coupled with the sphericity will affect both photon frequency redistribution and the motion of gas itself through the radiation pressure in the line. Hence it is important to treat the problem of transfer of line radiation by taking into account angle dependent frequency redistribution in an expanding spherical atmosphere.

3.2 Line transfer in the rest frame of the star

A study of the effects of angle dependent partial redistribution functions on the formation of spectral lines in the spherically symmetric expanding medium is made. For simplicity let us first solve the line transfer in the rest frame of the star (Peraiah 1978, Peraiah and Wehrse (1978).

In this event, we have the frequency of the line photon shifted by

$$x = x' \pm v\mu \tag{3-1}$$

where $\quad x' = \dfrac{\nu - \nu_o}{\Delta\nu_D}$

$\Delta\nu_D$ being the Doppler width and v is the velocity of the gas in thermal units and μ is the cosine of the angle between the ray and the radius vector. The $+,-$ signs represent the oppositely directed beams of the photons of frequency x'. The gas is assumed to be expanding radially outwards with a steady velocity.

The mean intensity J and the net flux (F_{net}) towards the surface of the atmosphere at each boundary r_n are given by the relations

$$J = \frac{1}{2} \int_{-1}^{+1} U d\mu = \frac{1}{2} \sum_{j=1}^{J} (U_n^- + U_n^+) \, C_j \tag{3-2}$$

and

$$F_{net} = 2\pi \int_{-1}^{+1} U \, d\mu = 2\pi \sum_{j=1}^{J} (U_n^- - U_n^+) \, \mu_j C_j \qquad (3-3)$$

Calculation of the diffuse field requires the correct estimation of reflection and transmission matrices for each shell of the medium. Since the physics of the medium is being described fully by these matrices we are trying to show how these r and transmission matrices for a differentially expanding spherical medium. in which the photon redistribution occurs in a line with zero natural width.

3.3 Calculation of reflection and transmission operators in a shell of given physical properties.

The equation of line transfer describes the physical and geometrical properties of the medium. The equation is to be integrated with partial frequency redistribution.

The equation of line transfer for a two level atom in spherical symmetry is given by

$$\mu \frac{\partial I(x,\mu,r)}{\partial r} + \frac{1-\mu^2}{r} \frac{\partial I(x,\mu,r)}{\partial \mu} = K_L [\beta + \phi(x, \mu, r)] \, x$$

$$[S(x,\mu,r) - I(x,\mu,r)] \qquad (3-4)$$

47

and for an oppositely directed beam

$$-\mu \; \frac{\partial I(x,-\mu,r)}{\partial r} - \frac{1-\mu^2}{r} \; \frac{I(x,-\mu,r)}{\partial \mu} = K_L[\beta+\phi(x,-\mu,r)] \; x$$

$$[S(x,-\mu,r)-I(x,-\mu,r)] \qquad\qquad (3-5)$$

where $I(x,\mu,r)$ is the specific intensity at an angle $\theta = \cos^{-1}\mu, [\mu \; \epsilon(0,1)]$ at the radial point r and frequency $x = \frac{\nu-\nu_o}{\Delta\nu_s}$ $\Delta\nu_s$ is some standard frequency interval. The quantity $\beta = \frac{k_c}{k_L}$, is the ratio of the opacity due to conti-

nuous absorption per unit interval of frequency x to the opacity that in the line. The source functions $S(x,\mu,r)$ and $S(x,-\mu,r)$ are given by

$$S(x,\mu,r) = \frac{\phi(x,\mu,r)S_L(x,\mu,r)+ \beta S_c(r)}{\phi(x,\mu,r)+ \beta} \qquad\qquad (3-6)$$

and

$$S(x,-\mu,r) = \frac{(x,-\mu,r)S_L(x,-\mu,r)+\beta S_c(r)}{\phi(x,-\mu,r)+ \beta} \qquad\qquad (3-7)$$

where S_L and S_C are the source functions in the line and in the continuum respectively and

$$S_c(r) = \rho(r)B(\nu_o, T_e(r)) \qquad (3-8)$$

B - Planck function at frequency ν and effective temperature T_e.

ρ - is an unspecified parameter.

The line source function is given by

$$S_L(x,\mu,r) = \frac{1-\varepsilon}{\phi(x,\mu,r)} \int_{-\infty}^{+\infty} \int_{-1}^{+1} R(x,\mu;x',\mu,r) \ X$$

$$I(x',\mu,r)d\mu'dx' + \varepsilon B(r) \qquad (3-9)$$

$$S_L(x,-\mu,r) = \frac{1-\varepsilon}{\phi(x,-\mu,r)} \int_{-\infty}^{+\infty} \int_{-1}^{+1} R(x,\mu;x',\mu,r) \ X$$

$$I(x',+\mu,r)d\mu' dx' + \varepsilon B(r) \qquad (3-10)$$

$R(x,\pm\mu;x',\mu,r)$ represent partial frequency redistribution functions, $\phi(x,\pm\mu,r)$ give the profile functions of the line and

$$\varepsilon = \frac{C_{21}}{C_{21} + A_{21}[1-e^{-h\nu_e/kT_e}]^{-1}} \qquad (3.-11)$$

is the probability per scattering that a photon is lost from the line by collisional de-excitation.

The equations (3-4) and (3-5) are integrated following the methods suggested by Peraiah and Grant (1973), Grant and Peraiah (1972). Frequency, angle and space coordinates have been discretised.

For frequency discretization, we have chosen discrete points x_i and weights a_i, so that

$$\int_{-\infty}^{+\infty} \phi(x)f(x)dx \simeq \sum_{i=-I}^{I} a_i f(x_i); \quad \sum_{i=-I}^{I} a_i = 1 \qquad (3-12)$$

For angular discretization, we have chosen (μ_j) and weight (C_j) such that

$$\int_{0}^{1} f(\mu)d\mu \simeq \sum_{j=1}^{m} b_j f(\mu_j), \quad \sum_{j=1}^{m} b_j = 1 \qquad (3-13)$$

and

$$B'(\nu_o, T_e(r)) = 4\pi r_n^2 B(\nu_o, T_e(r)) \qquad (3-14)$$

The transfer equations are integrated by using the 'cell' method as given by Lathrop and Carlson (1967). Integration is performed over an interval

$$[r_n, r_{n+1}] \times [\mu_{j-\frac{1}{2}}, \mu_{j+\frac{1}{2}}]$$

defined on a two dimensional grid. The roots μ_j and weights c_j of Gauss-Legendre quadrature formula of order J over (0,1) are chosen and the set $\mu_{j+\frac{1}{2}}$ is calculated as given by

$$\mu_{j+\frac{1}{2}} = \sum_{k=1}^{j} c_k, \quad j=1,2\ldots\ldots j \tag{3-15}$$

We shall define the boundary $\mu_{\frac{1}{2}} = 0; \; \mu_{j-\frac{1}{2}} \leqslant \mu_j \leqslant \mu_{j+\frac{1}{2}}$

Angle integration of equations (3-4) and (3-5) gives

$$[c_j \, \mu_j \, \frac{\partial U^+_{i,j}(r)}{\partial r} + \frac{1}{r}\{ (1-\mu^2_{j+\frac{1}{2}})U^+_{i,j+\frac{1}{2}}(r)-(1-\mu^2_{j-\frac{1}{2}})U^+_{i,j-\frac{1}{2}}(r)$$

$$+ \, c_j K_L(r) \} \, X \{ \beta + \phi^+_{i,j}(r) \} \, U^+_{i,j}(r)] = c_j K_L(r) \; X$$

$$[\{\rho\beta + \phi^+_{ij}(r)\} \, B'(r) + \frac{1}{2} \, (1-\epsilon) \sum_{j'=1}^{J} R^+_{i,i',j,j'}(r) *$$

$$c_{j'} U^+_{i',j'}(r) + R^{+-}_{i,i',j,j'}(r) c_{j'} U^-_{i,j'}(r)] \tag{3-16}$$

and

$$[-c_j\mu_j \, \frac{\partial U^-_{i,j}(r)}{\partial r} - \frac{1}{r}\{ (1-\mu^2_{j+\frac{1}{2}})U^-_{i,j+\frac{1}{2}}(r)-(1-\mu^2_{j-\frac{1}{2}})U^-_{i,j-\frac{1}{2}}(r)\}$$

$$+c_j K_L(r)\{\beta + \phi^-_{i,j}(r)\} \, U^{-1}_{i,j}(r) \quad = c_j K_L(r) \quad X$$

$$[(\rho\beta + \phi_{ij}^{-}(r)B'(r) + \tfrac{1}{2}(1-\epsilon) \sum_{j'=1}^{j} \{R_{i,i',j,j'}^{-+}(r)C_{j'}U_{i',j}^{+}(r)$$

$$+R_{i,i',j,j'}^{--}(r)C_{j'}U_{i',j'}^{-}(r)\}] \qquad (3-17)$$

where

$$U_{i,j}^{+}(r) = U(x_i, \mu_j, r)$$

$$U_{i,j}^{-}(r) = U(x_i, -\mu_j, r)$$

$$R_{i,i';j,j'}^{++}(r) = R(x_i, \mu_j; x_i', \mu_{j'}; r)$$

$$\qquad\qquad (3-18)$$

$$R_{i,i';j,j'}^{-+}(r) = R(x_i, -\mu_j; x_{i'}, \mu_{j'}; r)$$

$$\phi_{i,j}^{+}(r) = \phi(x_i, \mu_j, r)$$

$$\phi_{i,j}^{-}(r) = \phi(x_i, -\mu_j, r)$$

We shall define $U_{j+\frac{1}{2}}^{+}$ and $U_{j+\frac{1}{2}}^{-}$ by

$$U_{j+\frac{1}{2}}^{+} = \frac{(\mu_{j+1} - \mu_{j+\frac{1}{2}})U_j^{+} + (\mu_{j+\frac{1}{2}} - \mu_j)U_{j+1}^{+}}{\mu_{j+1} - \mu_j}$$

$$j = 1,2,\ldots(J-1) \qquad (3-19)$$

and

$$U_{j+\frac{1}{2}}^{-} = \frac{(\mu_{j+1} - \mu_{j+\frac{1}{2}}) U_j^{-} + (\mu_{j+\frac{1}{2}} - \mu_j) U_{j+1}^{-}}{\mu_{j+1} - \mu_j}$$

$$j = 1, 2, \ldots (J-1) \qquad (3-20)$$

$$U_{\frac{1}{2}}^{+} = U_{\frac{1}{2}}^{-}$$

by interpolation,

$$U_{\frac{1}{2}}^{+} = U_{\frac{1}{2}}^{-} = \frac{1}{2}(U_1^{+} + U_1^{-}) \qquad (3-21)$$

$$U_{i,n}^{+} = \begin{bmatrix} U(x_i, \mu_1, r_n) \\ U(x_i, \mu_2, r_n) \\ U(x_i, \mu_3, r_n) \\ \vdots \\ U(x_i, \mu_m, r_n) \end{bmatrix} ; \quad U_{i,n}^{-} = \begin{bmatrix} U(x_i, -\mu_1, r_n) \\ U(x_i, -\mu_2, r_n) \\ U(x_i, -\mu_3, r_n) \\ \vdots \\ U(x_i, -\mu_m, r_n) \end{bmatrix}$$

and

$$M_m = (\mu_j \delta_{jk}); \quad C_m = (C_j \delta_{jk}) \qquad (3-22)$$

$$\phi_{i,m}^{+}(r) = \begin{bmatrix} \phi(x_i, \mu_1, r) \\ \phi(x_i, \mu_2, r) \\ \vdots \\ \phi(x_i, \mu_m, r) \end{bmatrix}$$

and

$$\overline{\phi}_{i,m}(r) = \begin{bmatrix} \phi(x_i,-\mu_1,r) \\ \phi(x_i,-\mu_2,r) \\ \cdot \\ \cdot \\ \cdot \\ \cdot \\ \Phi(x_i,-\mu_m,r) \end{bmatrix}$$

(3-23)

Redistribution functions are given by

$$R^{++}_{i,i'}(r) = \begin{bmatrix} R(x_i,\mu_1;x_i',\mu_1;r) \\ R(x_i,\mu_2;x_i',\mu_1;r) \\ R(x_i,\mu_3;x_i',\mu_1;r) \\ \vdots \\ R(x_i,\mu_m;x_i',\mu_m;r) \end{bmatrix}$$

$$R^{-+}_{i,i'}(r) = \begin{bmatrix} R(x_i,-\mu_1;x_i',\mu_1;r) \\ R(x_i,-\mu_2;x_i',\mu_1;r) \\ R(x_i,-\mu_3;x_i',\mu_1;r) \\ \vdots \\ R(x_i,-\mu_m;x_i',\mu_m;r) \end{bmatrix}$$

(3-24)

Equations (3-16) and (3-17) can be rewritten for the set of angles (μ_j) over $(0,1)$ as

$$M_{\dot{m}} \frac{\partial U_i^+(r)}{\partial r} + \frac{1}{r} [\Lambda_m^+ U_i^+(r) + \Lambda_m^- U_i^-(r)] + K_L(r)\{\beta + \phi_{i,m}^+(r)\} \times U_i^+(r)$$

$$= K_L(r) \{(\rho\beta + \epsilon\phi_{i,m}^+(r)B'(r) + \frac{1}{2}(1-\epsilon) \times$$

$$[R_{i,i'}^{++}(r)a_{i'}^{++}(r)C_m U_{i'}^+(r) + R_{i,i'}^{+-}(r)a_{i'}^{+-}(r)C_m U_{i'}^-(r)]\}$$

$$(3-25)$$

Similarly for an oppositely directed beam

$$-M_m \frac{\partial U_i^-(r)}{\partial r} - \frac{1}{r} [\Lambda_m^+ U_i^-(r) + \Lambda_m^- U_i^+(r)] + K_L(r)\{\beta + \phi_{i,m}^-(r)\} \times U_i^-(r)$$

$$= k_L(r) \{ (\rho\beta + \phi_{i,m}^-(r)B'(r) + \frac{1}{2}(1-\epsilon) [R_{i,i'}^{--}(r) \times$$

$$a_{i'}^{--}(r)C_m U_{i'}^-(r) + R_{i,i'}^{-+}(r)a_{i'}^{-+}(r)C_m U_{i'}^+(r)]$$

$$(3-26)$$

where Λ_m^+ and Λ_m^- are square JXJ matrices are called curvature scattering matrices and are defined by

$$\Lambda^+_{jk} = \frac{(1-\mu^2_{j+\frac{1}{2}})(\mu_{j+\frac{1}{2}}-\mu_j)}{c_j(\mu_{j+1}-\mu_j)} \qquad k = j+1, j=1,2,\ldots(J-1).$$

$$= \frac{(1-\mu^2_{j+\frac{1}{2}})(\mu_{j+1}-\mu_{j+\frac{1}{2}})}{c_j(\mu_{j+1}-\mu_j)} - \frac{(1-\mu^2_{j-\frac{1}{2}})(\mu_{j-\frac{1}{2}}-\mu_{j-1})}{c_j(\mu_j-\mu_{j-1})}$$

$$k = j, j=1,2,\ldots)J-1),J.$$

$$= -\frac{(1-\mu^2_{j-\frac{1}{2}})(\mu_j-\mu_{j-\frac{1}{2}})}{c_j(\mu_j-\mu_{j-1})} , \quad k=j-1, j=2,3,\ldots J$$

$$\tag{3-27}$$

and

$$\Lambda^-_{jk} = -\frac{1}{2c_j}\delta_{j,1} \times \delta_{k,1} \tag{3-28}$$

μ's and c's are the roots and weights of Gauss-Legendre qua-
drature on $\mu\epsilon(0,1)$.

The integration over $[r_n, r_{n+1}]$ of equations (3-25)
and (3-26) gives

$$M_m(U^+_{i,n+1} - U^+_{i,n}) + \rho_c(\Lambda^+_m U^+_{i,n+\frac{1}{2}} + \Lambda^-_m U^-_{i,n+\frac{1}{2}})$$

$$+ \tau_{n+\frac{1}{2}}(\beta + \phi^+_{m,i})U^+_{i,n+\frac{1}{2}} = \tau_{n+\frac{1}{2}}(\rho\beta + \phi \epsilon^+_{m,i})_{n+\frac{1}{2}}B'_{n+\frac{1}{2}}$$

$$+ \frac{1}{2}\tau_{n+\frac{1}{2}}(1-\epsilon)(R^{++}_{i,i',n+\frac{1}{2}}a^{++}_{i,n+\frac{1}{2}}CU^+_{i'n+\frac{1}{2}} + R^{+-}_{i,i',n+\frac{1}{2}}a^{+-}_{i',n+\frac{1}{2}} \; X$$

$$CU^-_{i',n+\frac{1}{2}}) \qquad\qquad (3-29)$$

and

$$M_m(U^-_{i,n} - U^-_{i,n+1}) - \rho_c(\Lambda^+_m U^-_{i,n+\frac{1}{2}} + \Lambda^-_m U^+_{i,n+\frac{1}{2}})$$

$$+ \tau_{n+\frac{1}{2}}(\beta + \phi^-_{m,i})U^-_{i,n+\frac{1}{2}} = \tau_{n+\frac{1}{2}}(\rho\beta + \phi^-_{m,i})B'_{n+\frac{1}{2}}$$

$$+ \frac{1}{2}\tau_{n+\frac{1}{2}}(1-\epsilon)(R^{-+}_{i,i',n+\frac{1}{2}}a^{-+}_{i,n+\frac{1}{2}}CU^-_{i,n+\frac{1}{2}} + R^{--}_{i,i',n+\frac{1}{2}} \; X$$

$$a^{--}_{i',n+\frac{1}{2}}CU^-_{i',n+\frac{1}{2}}) \qquad\qquad (3-30)$$

where ρ_c is the curvature factor defined as

$$\rho_c = \frac{\Delta r}{r_{n+\frac{1}{2}}} \qquad \text{and} \quad \tau_{n+\frac{1}{2}} = K_L(n+\frac{1}{2})\,\Delta r \qquad\qquad (3-31)$$

Subscript 'n' refers to r_n

n+1 refers to r_{n+1}

n+½ refers to $r_{n+\frac{1}{2}}$

$r_{n+\frac{1}{2}}$ refers to the parameter averaged over shell bounded by r_n and r_{n+1}. the weights are defined as

$$(\phi_i \ W_k) = a_{i,n+\frac{1}{2}} C_j \qquad (3.-32)$$

the subscript k is defined as

$$(i,j) \equiv k \equiv j+(i-1)j, \quad 1 \leqslant k \leqslant K = IJ.$$

I and J are the number of frequency and angle points respectively and i,j are the corresponding running indices.

By putting

$$U_n^+ = \begin{bmatrix} U_{1,n}^+ \\ U_{2,n}^+ \\ \vdots \\ U_{I,n}^+ \end{bmatrix}$$

$$\phi_{n+\frac{1}{2}}^+ = \left[\phi_{kk'}^+ \right]_{n+\frac{1}{2}} = [\beta + \phi^+ k]_{n+\frac{1}{2}} \ \delta_{kk'}$$

and

$$S_{n+\frac{1}{2}}^+ = [b\beta + \varepsilon \phi_k]_{n+\frac{1}{2}} B'_{n+\frac{1}{2}} \ \delta_{kk'}$$

Equations (.3.-29) and (.3*-30) are rewritten including all the frequency points as follows

$$M[U_{n+1}^+ - U_n^-] + \rho_c[\Lambda^+ \; U_{n+\frac{1}{2}}^+ + \Lambda^- U_{n+\frac{1}{2}}^-] + \tau_{n+\frac{1}{2}} \phi_{n+\frac{1}{2}}^+ \; X$$

$$U_{n+\frac{1}{2}}^+ = \tau_{n+\frac{1}{2}} S_{n+\frac{1}{2}}^+ + \frac{1}{2}(1-\epsilon)\tau_{n+\frac{1}{2}}[R^{++}W^{++}U^+ + R^{+-}W^{+-}U^-]_{n+\frac{1}{2}} \qquad (3-33)$$

and

$$M[U_n^- - U_{n+1}^-] - \rho_c[\Lambda^+ U_{n+\frac{1}{2}}^- + \Lambda^- U_{n+\frac{1}{2}}^+] +$$

$$\tau_{n+\frac{1}{2}} \phi_{n+\frac{1}{2}}^- + \frac{1}{2}U_{n+\frac{1}{2}}^- = \tau_{n+\frac{1}{2}} S_{n+\frac{1}{2}}^- + \frac{1}{2}(1-\epsilon) \; X$$

$$\tau_{n+\frac{1}{2}}[R^{-+}W^{-+}U^+ + R^{--}W^{--}U^-]_{n+\frac{1}{2}} \qquad (3-34)$$

where

$$M = \begin{bmatrix} M_m & & & \\ & M_m & & \\ & & \ddots & \\ & & & M_m \end{bmatrix}$$

and

$$\Lambda^{\pm} = \begin{bmatrix} \Lambda^{\pm}_m & & & & \\ & \Lambda^{\pm}_m & & & \\ & & \cdot & & \\ & & & \cdot & \\ & & & & \Lambda^{\pm}_m \end{bmatrix}$$

Using the 'diamond' scheme of Grant and Peraiah (1972) the average intensities $U^{+}_{n+\frac{1}{2}}$ in the above equations are replaced by

$$[I-x_{n+\frac{1}{2}}]U^{+}_n + x_n U^{+}_{n+1} = U^{+}_{n+\frac{1}{2}}$$

$$(3-35)$$

$$[I-x_{n+\frac{1}{2}}]U^{-}_{n+1} + x_{n+\frac{1}{2}}U^{-}_n = U^{-}_{n+\frac{1}{2}}$$

with $x = \frac{1}{2} I$ for diamond scheme and I is the identity matrix. By using equation (3 -35),(3 -33) and (3 - 34) can be written as

$$\begin{bmatrix} M+ \frac{1}{2} \tau [\phi^{+} - \frac{\delta}{2} R^{++}W^{++}] + \frac{1}{2}\rho_c\Lambda^{+} - \frac{\delta\tau}{4} R^{+-}W^{+-}] + \frac{1}{2}\rho_c\Lambda^{-} \\ - \frac{\delta\tau}{4} R^{-+}W^{-+} - \frac{1}{2}\rho_c\Lambda^{-} M+ \frac{\tau}{2} [\phi^{-} \frac{\delta}{2} R^{--}W^{--}] - \frac{1}{2}\rho_c\Lambda^{+} \end{bmatrix} X$$

$$
\begin{bmatrix} U_{n+1}^{+} \\ \\ U_{n}^{-} \end{bmatrix} =
$$

$$
\begin{bmatrix} M- \frac{\tau}{2} [\phi^{+} - \frac{\delta}{2} R^{++}W^{++}] - \frac{1}{2}\rho_{c}\Lambda^{+} & \frac{\delta\tau}{4}R^{+-}W^{+-} - \frac{1}{2}\rho_{c}\Lambda^{-} \\ \\ \frac{\delta\tau}{4} R^{-+}W^{-+} + \frac{1}{2}\rho_{c}\Lambda^{-} & M- \frac{\tau}{2} [\phi^{-} - \frac{\delta}{2} R^{--}W^{--}] + \frac{1}{2}\rho_{c}\Lambda^{+} \end{bmatrix} \begin{bmatrix} U_{n}^{+} \\ \\ U_{n+1}^{-} \end{bmatrix}
$$

$$
+ \begin{bmatrix} S^{+} \\ S^{-} \end{bmatrix} \qquad\qquad (3-36)
$$

where $\delta = 1 - \varepsilon$

On comparison of equation (3-36) with equation (3-1) of interaction principle two pairs of transmission and reflection operators are obtained

$$
t(n+1,n) = G^{+-} [\Delta^{+}A + g^{+-}g^{-+}]
$$

$$
t(n,n+1) = G^{-+} [\Delta^{-}D + g^{-+}g^{+-}]
$$

$$
r(n+1,n) = G^{-+}g^{-+} [I+\Delta^{+}A]
$$

$$
r(n,n+1) = G^{+-}g^{+-} [I+\Delta^{-}D] \qquad\qquad (3-37)
$$

and the shell source vectors are

$$\Sigma^+ = G^{+-} [\Delta^+ s^+ + g^{+-} \Delta^- s^-]\tau$$

$$\Sigma^- = G^{-+} [\Delta^- s^- + g^{-+} \Delta^+ s^+]\tau \tag{3.-38}$$

along with the following auxiliary quantities

$$G^{+-} = [I - g^{+-} g^{-+}]^{-1}$$

$$G^{-+} = [I - g^{-+} g^{+-}]^{-1}$$

$$g^{+-} = \frac{1}{2}\tau \Delta^+ Y_-$$

$$g^{-+} = \frac{1}{2}\tau \Delta^- Y_+$$

$$D = M - \frac{1}{2}\tau Z_-$$

$$A = M - \frac{1}{2}\tau Z_+$$

$$\Delta^+ = [M + \frac{1}{2}\tau Z_+]^{-1}$$

$$\Delta^- = [M + \frac{1}{2}\tau Z_-]^{-1}$$

$$Z_+ = \phi^+ - \frac{\delta}{2} R^{++} W^{++} + \rho_c \Delta^+/\tau$$

$$Z_- = \phi^- - \frac{\delta}{2} R^{--} W^{--} - \rho_c \Lambda^+/\tau$$

$$Y_+ = \frac{1}{2}\delta \ R^{-+}W^{-+} + \rho_c \Lambda^-/\tau$$

$$Y_- = \frac{1}{2}\delta \ R^{+-} \ W^{+-} - \rho_c \Lambda^-/\tau \qquad\qquad (3-39)$$

Transmission and reflection operators given in equations (3 -37) and (3 -38) for a shell of optical depth τ and curvature factor ρ_c , describe the radiation field in any medium either static or moving.

The hurdle in the rest frame is to restrict only to smaller gas velocities of the order of 2 or 3 mean thermal units. For higher velocities the frequency angle mesh becomes unmanageably large. Hence for objects with atmospheres expanding at larger velocities one has to adopt an alternative approach.

CHAPTER 4

LINE FORMATION IN EXPANDING STELLAR ATMOSPHERES IN THE
COMOVING FRAME

4.1 Introduction

It is a well known fact that in the outer layers
of WR stars, quasers,novae and P-cygni stars, the matter
is flowing outward with very high radial velocities.
Attempts have been made by several people to study the
line formation problem in spherically symmetric expanding
media. The rest frame calculations were to be restricted
only to lower velocities because the frequency-angle mesh
becomes quite large for higher velocity of expansion.

Hence an alternative approach to compute lines
in rapidly expanding media has been adopted. In this
approach the observer is moving along with the expanding

medium.

4.2 Comoving frame calculation of profiles

In the comoving frame the complications arising out of Doppler effect have been conveniently avoided. One can employ very high velocities with much smaller frequency-angle mesh. This method has an advantage particularly when one tries with angle dependent partial frequency redistribution.

The method of finding solution for line transfer in comoving frame has to adopt specific velocity law. Here we have considered spectral line formation with non-LTE two level atom approximation, in a spherically symmetric medium expanding with velocity

$$V(r) = V_A + \frac{V_B - V_A}{B - A} (r-A) \qquad (4-1)$$

where V_A and V_B are the velocities in mean thermal units for gas at the inner point with radius A and outer point with radius B. $V(r)$ is the velocity at any radial point r. The equation of radiative transfer for a non-LTE two level atom in the comoving frame in spherical symmetry is given as

$$\mu \frac{\partial I(x,\mu,r)}{\partial r} + \frac{1-\mu^2}{r} \frac{\partial I(x,\mu,r)}{\partial \mu} = K(x,r)S_L(r) +$$

$$K_c(r)S_c(r) - [K(x,\mu,r)+K_c(r)]I(x,\mu,r)$$

$$+[(1-\mu^2)\frac{v(r)}{r} + \frac{\mu^2 dv(r)}{dr}]\frac{\partial I(x,\mu,r)}{\partial x} \qquad (4-2)$$

and for an oppositely directed beam

$$-\mu\frac{\partial I(x,-\mu,r)}{\partial r} - \frac{1-\mu^2}{r}\frac{\partial I(x,-\mu,r)}{\partial \mu} = K(x,r)S_L(r)$$

$$+K_c(r)S_c(r)-[K(x,r)+K_c(r)]I(x,-\mu,r)$$

$$+[(1-\mu^2)\frac{V(r)}{r}+\frac{\mu^2 dV(r)}{dr}]\frac{\partial I(x,-\mu,r)}{\partial x} \qquad (4-3)$$

where $I(x,\mu,r)$ is the specific intensity of the ray making an angle $cos^{-1}\mu$ with the radius vector at the radial point r corresponding to frequency point,

$$x = \frac{\nu - \nu_0}{\Delta s}$$

ν_0 being central frequency of the line and ΔS is a standard frequency interval in the line. $K(x,r),K_c(r)$ are the absorption coefficients per unit frequency interval in the line and the continuum respectively, where as $S_L(r)$ and $S_c(r)$ represent the source functions in the line and continuum respectively and are given by

$$S_L(r) = \frac{1}{2} (1-\varepsilon) \int_{-\infty}^{+\infty} J(x,r)\phi(x)dx + \varepsilon B(r) \qquad (4-4)$$

$$\text{and } S_c(r) = \rho(r) \ B(r) \qquad (4-5)$$

$$K(x,r) = K_L(r)\phi(x) \qquad (4-6)$$

$K_L(r)$ is the absorption coefficient at the line centre and $\phi(x)$ is the normalised line profile. The profile is normalised such that

$$\int_{-\infty}^{+\infty} \phi(x)dx = 1 \qquad (4-7)$$

$B(r)$ is the Planck fucntion $\rho(r)$ is an unspecified parameter.

We have chosen Voigt profile

$$\phi(a,x) = \frac{a}{\pi} \int_{-\infty}^{+\infty} \frac{e^{-y^2}dy}{(x-y)^2+a^2}$$

and optical depth in the line is given by

$$\tau(x,r) = K(x,r) \Delta r = \frac{\pi^{\frac{1}{2}} \varepsilon^2 N(r) f}{mc \Delta \nu_D} \phi(a,x)\Delta r$$

ε is the photon destruction probability per scattering from the line due to collisional deexcitation. $J(x,r)$ is the mean intensity.

The radiative transfer equation in spherical symmetry can be solved by integrating over a shell and the discrete equations are written as

$$\underset{\sim}{M}[\underset{\sim}{U}^+_{n+1} - \underset{\sim}{U}^+_n] + \rho_c[\underset{\sim}{\Lambda}^+ \underset{\sim}{U}^+_{n+\frac{1}{2}} - \underset{\sim}{\Lambda}^- \underset{\sim}{U}^-_{n+\frac{1}{2}}] + \tau_{n+\frac{1}{2}} \phi_{n+\frac{1}{2}} \underset{\sim}{U}^+_{n+\frac{1}{2}}$$

$$= \tau_{n+\frac{1}{2}} \underset{\sim}{S}_{n+\frac{1}{2}} + \left(\frac{1-\epsilon}{2}\right) \tau_{n+\frac{1}{2}}[\underset{\sim}{\phi} \underset{\sim}{\phi}^t W][\underset{\sim}{U}^+ + \underset{\sim}{U}^-]_{n+\frac{1}{2}} + \underset{\sim}{M}_1 d \underset{\sim}{U}^+_{n+\frac{1}{2}} \qquad (4-8)$$

Similarly

$$\underset{\sim}{M}[\underset{\sim}{U}^-_n - \underset{\sim}{U}^-_{n+1}] - \rho_c[\underset{\sim}{\Lambda}^+ \underset{\sim}{U}^-_{n+\frac{1}{2}} + \underset{\sim}{\Lambda}^- \underset{\sim}{U}^+_{n+\frac{1}{2}}] \tau_{n+\frac{1}{2}} \phi_{n+\frac{1}{2}} \underset{\sim}{U}^-_{n+\frac{1}{2}}$$

$$= \tau_{n+\frac{1}{2}} \underset{\sim}{S}_{n+\frac{1}{2}} + \left(\frac{1-\epsilon}{2}\right) \tau_{n+\frac{1}{2}}[\underset{\sim}{\phi} \underset{\sim}{\phi}^t W][\underset{\sim}{U}^+ + \underset{\sim}{U}^-]_{n+\frac{1}{2}} + \underset{\sim}{M}_1 d \underset{\sim}{U}^-_{n+\frac{1}{2}} \qquad (4-9)$$

where

$$\underset{\sim}{U}^+_n = [\underset{\sim}{U}^+_{1,n}, \underset{\sim}{U}^+_{2,n}, \underset{\sim}{U}^+_{3,n} \cdots \underset{\sim}{U}^+_{i,n} \cdots \underset{\sim}{U}^+_{I,n}]^t \qquad (4-10)$$

t indicating transpose of the vector.

$$\underset{\sim}{U}^+_{i,n} = 4\pi r^2_n \times \begin{bmatrix} I(\tau_n, \mu_1, x_i) \\ I(\tau_n, \mu_2, x_i) \\ \cdot \\ \cdot \\ I(\tau_n, \mu_J, x_i) \end{bmatrix} \qquad (4-11)$$

I and J indicate the total number of frequency and angle points respectively

$$\underline{\phi}_{n+\frac{1}{2}} = [\, \phi_{kk'}]_{n+\frac{1}{2}} = (\beta + \phi_k)_{n+\frac{1}{2}} \, \delta_{kk'} \qquad (\,4-12)$$

$\beta = \dfrac{k_C}{k_L}$ the ratio of absorption coefficients at the continuum and line centre per unit frequency interval.

$k = j + (i-1)J; \qquad 1 \leqslant k \leqslant K = IJ$

i,j are the running indices of angle and frequency quadrature. $(n+\frac{1}{2})$ subscript represents the average of the parameter over the shell bounded by radii r_n and r_{n+1}; also

$$\phi_k = \phi(x_i, \mu_j)$$

$$S_{n+\frac{1}{2}} = (\rho\beta + \varepsilon\,\phi_k)B'_{n+\frac{1}{2}}\,\delta_{kk'}$$

$$B'_{n+\frac{1}{2}} = 4\pi\, r^2_{n+\frac{1}{2}}\, B(r_{n+\frac{1}{2}}) \qquad (4-13)$$

$$\phi_i W_k = a_i C_j$$

where

$$a_i = \dfrac{A_i\,\phi_i}{\sum\limits_{i=-I}^{I} A_i\phi(x_i)} \qquad (4-14)$$

A_i's are the quadrature weights for the frequency points. The matrices $\underset{\sim}{M}$ and $\underset{\sim}{\Lambda}^{\pm}$ are given by

$$\underset{\sim}{M} = \begin{bmatrix} M_m & \cdot & & & \cdot & \\ & & M_m & & & \\ \cdot & & & & & \\ & & & \cdot & & \\ \hat{} & & & & M_m \end{bmatrix} \qquad \underset{\sim}{\Lambda}^{+} = \begin{bmatrix} \Lambda_m^{+} & & & \cdot & \\ & \Lambda_m^{+} & & & \\ & & \cdot & & \cdot \\ & & & \cdot & \\ & & & & \Lambda_m^{+} \end{bmatrix}$$

$$(4-15)$$

with

$$\underset{\sim m}{M} = [\mu_j \ \delta_{jk}]$$

$\underset{\sim}{\Lambda}^{\pm}$ are the curvature matrices and are given by equation (3-27) and (3-28) μ's and c's being roots and weights, for J = 2,

$$\mu_1 = 0.21132$$

$$\mu_2 = 0.78868$$

$$C_1 = C_2 = 0.5$$

$$\Lambda^{+} = \begin{bmatrix} -0.25 & 0.75 \\ -.0.75 & -0.75 \end{bmatrix} \qquad \Lambda^{-} = \begin{bmatrix} -1 & 0 \\ 0 & 0 \end{bmatrix}$$

where as for $J = 4$

$$\mu_1 = 0.06943 \qquad\qquad \text{and} \qquad C_1 = 0.17393 = C_4$$

$$\mu_2 = .33001 \qquad\qquad\qquad\qquad C_2 = 0.32607 = C_3$$

$$\mu_3 = 0.66999$$

$$\mu_4 = 0.93057$$

$$
\Lambda^+ = \begin{bmatrix}
0.46494 & 2.2359 & 0 & 0 \\
-1.78139 & -0.04258 & 1.15005 & 0 \\
0 & -1.15005 & -0.75945 & 0.58343 \\
0 & 0 & -0.73228 & -1.09379
\end{bmatrix}
$$

$$\Lambda^- = -2.87476 \; \delta_{j,1} \; \delta_{k,1}$$

The quantity $\underset{\sim}{M} \, \underset{\sim}{d} \, \underset{\sim}{U}_{n+\frac{1}{2}}$ in the Equations (4-8) and (4-9) are the equivalents of the comoving terms in equation (4-2) and (4-3) we can write

$$\underset{\sim}{M}_1 = [\underset{\sim}{M}^1 \Delta \underset{\sim}{V}_{n+\frac{1}{2}} + \underset{\sim}{M}^2 \rho_c \underset{\sim}{V}_{n+\frac{1}{2}}] \tag{4-16}$$

$$
\underset{\sim}{M}^1 = \begin{bmatrix}
M_m^1 & & & \\
& M_m^1 & & \\
& & \ddots & \\
& & & M_m^1
\end{bmatrix}
\qquad
\underset{\sim}{M}_m^1 = [\mu_j^2 \, \delta_{jI}] \tag{4-17}
$$

$$\underset{\sim}{M}^2 = \begin{bmatrix} M_m^2 & & \\ & M_m^2 & \\ & & M_m^2 \end{bmatrix} \quad ; \quad M_m^2 = [(1-\mu_j^2)\delta_{jI}] \qquad (4-18)$$

$$j,I = 1,2,\ldots J; \quad \Delta V_{n+\frac{1}{2}} = V_{n+1} - V_n$$

The matrix d is determined from the condition of flux conservation and it is given by

$$\underset{\sim}{d} = \begin{bmatrix} -d_1 & d_1 & & & & \\ -d_2 & 0 & d_2 & & & \\ & -d_3 & 0 & & & \\ & & -d_4 & & d_{I-1} & \\ & & & -d_I & d_I \end{bmatrix} \qquad (4-19)$$

where $d_i = (x_{i+1} - x_{i-1})^{-1}$ for $i=2,3,\ldots(I-1)$.

We have set the boundary condition $d_1 = d_I = 0$ on the frequency integration.

The average intensities $\underset{\sim}{U}_{n+\frac{1}{2}}^+$, $\underset{\sim}{U}_{n+\frac{1}{2}}^-$ are approximated by the 'diamond' scheme

$$\frac{1}{2}(\underset{\sim}{U}_n^+ + \underset{\sim}{U}_{n+1}^+) = \underset{\sim}{U}_{n+\frac{1}{2}}^+ \qquad (4-20)$$

and

$$\frac{1}{2} (U_{\sim n}^- + U_{\sim n+1}^-)^\cdot = U_{\sim n+\frac{1}{2}}^-$$

4.3 Reflection and transmission operators

Substituting $M_{\sim 1}$ from equation (4-16) in equations (4-8) and (4-9) and arranging the resulting equations in the form of interaction principle equations, reflection and transmission operators for the shell are obtained by making following substitutions

$$\sigma = 1 - \epsilon$$

$$Z_{\sim} = \phi_{\sim} - Y_{\sim}$$

$$Y_{\sim} = \frac{1}{2} \sigma [\phi_{\sim} \phi_{\sim}^t w]$$

$$Y_{\sim +} = Y_{\sim} + \frac{\rho_c \Lambda_{\sim}^-}{\tau}$$

$$Y_{\sim -} = Y_{\sim} - \frac{\rho_c \Lambda_{\sim}^-}{\tau}$$

$$Z_{\sim +} = Z_{\sim} + \rho_c \Lambda_{\sim}^+/\tau - \frac{M_{\sim 1} d_{\sim}}{\tau}$$

$$Z_{\sim -} = Z_{\sim} - \rho_c \Lambda_{\sim}^+/\tau - \frac{M_{\sim 1} d_{\sim}}{\tau}$$

$$\Gamma_{\sim}^{\pm} = [M_{\sim} - \frac{1}{2} Z_{\sim \pm}]$$

$$\underset{\sim}{\beta}^{+-} = \frac{1}{2}\tau\underset{\sim}{\Delta}^{+}\underset{\sim}{Y}^{-}$$

$$\underset{\sim}{\alpha}^{+-} = [I - \underset{\sim}{\beta}^{+-}\underset{\sim}{\beta}^{-+}]^{-1} \qquad (4-21)$$

In similar way $\underset{\sim}{\beta}^{-+}$ and $\underset{\sim}{\alpha}^{-+}$ are also defined. Utilizing the above equations r and t matrices and source vectors are written as

$$\underset{\sim}{t}(n+1,n) = \underset{\sim}{\alpha}^{+-}[\underset{\sim}{\Delta}^{+}\underset{\sim}{\Gamma}^{+} + \underset{\sim}{\beta}^{+-}\underset{\sim}{\beta}^{-+}]$$

$$(4-22)$$

$$\underset{\sim}{r}(n+1,n) = \underset{\sim}{\alpha}^{-+}\underset{\sim}{\beta}^{-+}[I + \underset{\sim}{\Delta}^{+}\underset{\sim}{\Gamma}^{+}]$$

and

$$\underset{\sim n+\frac{1}{2}}{\Sigma}^{+} = \tau\underset{\sim}{\alpha}^{+-}[\underset{\sim}{\Delta}^{+} + \underset{\sim}{\beta}^{+-}\underset{\sim}{\Delta}^{-}]\underset{\sim}{S} \qquad (4-23)$$

Operators $\underset{\sim}{t}(n,n+1), \underset{\sim}{r}(n,n+1)$ and $\underset{\sim n+\frac{1}{2}}{\Sigma}^{-}$ are obtained by inter-changing the + and - signs in the above equations.

The critical optical thickness can be estimated from the condition of non-negativity of r and t operators. Radiation field can be transformed to a point at infinity or on to a rest frame. Spectral lines are calculated for both the rest frame and the comoving frames. ($V_A = V_B = 0$ corresponds to static medium).

In a static medium there are no velocity fields and velocity gradients are also assumed to be absent. We have presented the frequency dependent fluxes in the line for various τ_d and V_A values V_B with a two level atom approximation.

CHAPTER 5

EFFECTS OF VELOCITY AND DUST ON THE EQUIVALENT WIDTHS
OF SPECTRAL LINES IN THE EXPANDING STELLAR MEDIUM

5.1 Introduction:

If spherical stellar atmospheres expanding radially contain dust what impact will it have on the spectral lines.? Several properties can be ascribed to the dust, like isotropic scattering, uniform distribution throughout the medium etc.

Infrared observations of many stellar objects like gaseous nebulae,, T-tauri stars and atmospheres of cool supergiants have shown ample evidence about the presence of dust. Brehmsstrahlung (free-free radiation) and thermal emission from dust grains are the two important mechanisms in producing the observed infrared excess.

This has been revealed by the study of early type of stars by Allen (1973). Investigations in the far infrared and of S140 IRS by Schwartz et al· (1983) have shown that there is good coupling between dust and gas. Circumstellar dust envelopes are also predicted around the stars with prominent infrared continua (Allen and Swings 1972). Extensive survey of many objects such as BN and CRL 490 has shown the presence of a dusty shell around hard core of ionised gas. Though many people have studied the emission of infrared radiation from extended stellar envelopes, the study of line formation in dusty envelopes is in its early stages. A. Peraiah et al (1987) have made a study of line formation in expanding spherical medium. Hummer and Kunasz (1980), Wehrse and Kalkofen (1985), Peraiah and Wehrse (1978) have studied radiative transfer effects in a medium containing both dust and gas.

We have tried, on the lines suggested by A.Peraiah (1987), to calculate the effect of dust and also the velocity of the radially expanding medium on the equivalent width of the line. Presence of dust, sphericity of the atmosphere and variations in temperature and density of the gas radially have been considered in our calculations. Calculations have been done for both static and moving media with velocities upto 50 mtu.

5.2 Method of solution for line transfer in comoving frame

In the comoving frame the radiative transfer equation is to include the term

$$\frac{(1-\mu^2)V(r)}{r} + \frac{\mu^2 dV(r)}{r} \quad \frac{\partial I(r,\mu,x)}{\partial x} \qquad (5\text{-}1)$$

(Ref.Chandrasekhar 1945, Mihalas et al 1975, and Mihalas 1978).

where $I(r,\mu,x)$ is the specific intensity of the ray with a standarised frequency x and making an angle $\mathrm{Cos}^{-1}\mu$ with the radial vector point r. $V(r)$ is the radial velocity of the gas at the point r given in mean thermal doppler units (mtu). Now the equation of line transfer including absorption and emission due to gas and dust may be written as (Peraiah (1984),Wehrse and Kalkofen (1985))

$$\mu \frac{\partial I(r,\mu,x)}{\partial r} + \frac{1-\mu^2}{r} \quad \frac{\partial I(r,\mu,x)}{\partial \mu}$$

$$= K_L(r) [\phi(x)+\beta][S(r,\mu,x)-I(r,\mu,x)]$$

$$+[(1-\mu^2) \frac{V(r)}{r} + \frac{\mu^2 dV(r)}{dr}] \frac{\partial I(r,\mu,x)}{\partial x}$$

$$+K_{dust}(r)[S_{dust}(r,\mu,x)-I(r,\mu,x)] \qquad (5\text{-}2)$$

In similar way for an oppositely directed beam

$$-\mu \frac{\partial I(r,-\mu,x)}{\partial r} - \frac{1-\mu^2}{r} \quad \frac{\partial I(r,-\mu,x)}{\partial \mu} = K_L(r)[\phi(x)+\beta]$$

$$[S(r,-\mu,x)-I(r,-\mu,x)]+[\frac{(1-\mu^2)V(r)}{r} + \frac{\mu^2 dV(r)}{dr}]\frac{\partial I(r,-\mu,x)}{\partial x}$$

$$+ K_{dust}(r)[S_{dust}(r,-\mu,x)-I(r,-\mu,x)] \qquad (5-3)$$

Where $\cos\theta$ has values between 0 and 1.

$K_L(r)$ is the absorption coefficient at the line centre, $\phi(x)$ is the Doppler profile function. β is the ratio of continuum to line opacities (i.e. $\beta = \dfrac{k_c}{k_L}$)

The source function is given by

$$S(r,\pm\mu,x) = \frac{\phi(x)}{\phi(x)+\beta} S_L(r) + \frac{\beta}{\phi(x)+\beta} S_c(r,x) \qquad (5-4)$$

and line source fucntion is

$$S_L(r) = \frac{1-\varepsilon}{2} \int_{-\infty}^{+\infty} \phi(x) \int_{-1}^{+1} I(r,\mu',x)\,dx\,d\mu' + \varepsilon\, B(T(r),x) \qquad (5-5)$$

$S_c(r)$ the continuum source function is given by

$$S_c(r) = \rho(r)\, B(T(r)\,x) \qquad (5-6)$$

ε being the probability per scattering that a photon is lost by collisional de-excitation from the line. $B(T(r),x)$ is the Planck function at temperature $T(r)$ and $\rho(r)$ is an arbitrary quantity. $K_{dust}(r)$ absorption coefficient of dust and source function is given by

$$S_{dust}(r,\pm\mu,x) = (1-\omega)B_{dust} + \frac{\omega}{2}\int_{-\infty}^{+\infty} P(\mu,\mu',r)I(r,\mu',x)d\mu'$$

$$(5-7)$$

B_{dust} planck function for dust emission, ω-albedo of the dust and P-the scattering phase function. Since re-emission from dust is at a much different frequency from that of the line frequency B_{dust} will not contribute much to the line radiation.

Transfer equation is solved by the "cell" method using discrete frequency points x_i and weights a_i .

$$\int_{-\infty}^{+\infty} \phi(x)f(x)dx = \sum_{i=-1}^{I} a_i f(x_i)$$

$$(5-8)$$

$$\sum_{i=-1}^{I} a_i = 1$$

Angle discretization is done as

$$\int_{0}^{+1} f(x)d\mu = \sum_{j=1}^{m} c_j f(\mu_j); \quad \sum_{j=1}^{m} c_j = 1$$

$$(5-9)$$

The integration is performed over a cell bound by
$[r_n, r_{n+1}][\mu_{j-\frac{1}{2}}, \mu_{j+\frac{1}{2}}][x_i, x_{i+1}]$

where

$$\mu_{j+\frac{1}{2}} = \sum_{k=1}^{j} C_k \qquad j = 1,2, \ldots .m \qquad (5-10)$$

where μ's and c's are the roots and weights of Gauss-Legendre quadrature.

By introducing

$$\underset{\sim}{U}_{i,n}^{+} = 4\pi r_n^2 \begin{bmatrix} \underset{\sim}{I}(\mu_1, x_i, \tau_n) \\ \underset{\sim}{I}(\mu_2, x_i, \tau_n) \\ \vdots \\ \underset{\sim}{I}(\mu_m, x_i, \tau_n) \end{bmatrix} \qquad (5-11)$$

$$\underset{\sim}{U}_{i,n}^{-} = 4\pi r_n^2 \begin{bmatrix} \underset{\sim}{I}(-\mu_1, x_i, \tau_n) \\ \underset{\sim}{I}(-\mu_2, x_i, \tau_n) \\ \\ \underset{\sim}{I}(-\mu_m, x_i, \tau_n) \end{bmatrix} \qquad (5-12)$$

and

$$B'(\nu_o, T_e(r)) = 4\pi r_n^2 B(\nu_o, T_e(r)) \qquad (5-13)$$

$$\underset{\sim}{h} = [1, 1, \ldots .1]^T \qquad (5-14)$$

where T indicates the transpose.

Integration of the equations of line transfer in comoving frame with dust and gas reduce to:

$$\underset{\sim}{M}_m(\underset{\sim}{U}^+_{i,n+1} - \underset{\sim}{U}^+_{i,n}) + \rho_c(\underset{\sim m}{\Lambda}^+ \underset{\sim}{U}^+_{i,n+\frac{1}{2}} + \underset{\sim m}{\Lambda}^- \underset{\sim}{U}^-_{i,n+\frac{1}{2}})$$

$$+\tau_{g,n+\frac{1}{2}}(\beta + \phi_i)_{n+\frac{1}{2}}\underset{\sim}{U}^+_{i,n+\frac{1}{2}} + \tau_{d,n+\frac{1}{2}}\underset{\sim}{U}^+_{i,n+\frac{1}{2}}$$

$$= \tau_{g,n+\frac{1}{2}}(\rho\beta + \varepsilon\phi_i)_{n+\frac{1}{2}} \quad \underset{\sim}{B}^{',+}_{g,n+\frac{1}{2}} \quad \underset{\sim}{h}$$

$$+ \frac{1}{2}\tau_{g,n+\frac{1}{2}}\sigma_{n+\frac{1}{2}}\phi_{i,n+\frac{1}{2}} \sum_{i'-1}^{I} a_{i',n+\frac{1}{2}}(\underset{\sim}{h}\underset{\sim}{h}^T)\underset{\sim m}{C}(\underset{\sim}{U}^+ + \underset{\sim}{U}^-)_{i',n+\frac{1}{2}}$$

$$+ \frac{1}{2}\tau_{d,n+\frac{1}{2}}\omega_{n+\frac{1}{2}}(\underset{\sim m}{P}^{++}_{,n+\frac{1}{2}}\underset{\sim m}{C}\underset{\sim}{U}^+_{i,n+\frac{1}{2}} + \underset{\sim m}{P}^{+-}_{,n+\frac{1}{2}}\underset{\sim m}{C}\underset{\sim}{U}^-_{i,n+\frac{1}{2}})$$

$$+ \underset{\sim}{M}_{l,i+\frac{1}{2}}\underset{\sim}{d}_{i+\frac{1}{2}}\underset{\sim}{U}^+_{i+\frac{1}{2},n+\frac{1}{2}} + \tau_{d,n+\frac{1}{2}}(1-\omega)_{n+\frac{1}{2}}\underset{\sim}{B}^{',+}_{d,n+\frac{1}{2}} \quad \underset{\sim}{h} \qquad (5\text{-}15)$$

and

$$\underset{\sim}{M}_m(\underset{\sim}{U}^-_{i,n} - \underset{\sim}{U}^-_{i,n+1}) - \rho_c(\underset{\sim m}{\Lambda}^+\underset{\sim}{U}^-_{i,n+\frac{1}{2}} + \underset{\sim m}{\Lambda}^-\underset{\sim}{U}^+_{i,n+\frac{1}{2}})$$

$$+\tau_{g,n+\frac{1}{2}}(\beta + \phi_i)_{n+\frac{1}{2}}\underset{\sim}{U}^-_{i,n+\frac{1}{2}} + \tau_{d,n+\frac{1}{2}}\underset{\sim}{U}^-_{i,n+\frac{1}{2}}$$

$$= \tau_{g,n+\frac{1}{2}}(\rho\beta + \varepsilon\phi_i)_{n+\frac{1}{2}}B^{i,+}_{g,n+\frac{1}{2}} \quad \underset{\sim}{h}$$

$$+ \frac{1}{2}\, \tau_{g,n+\frac{1}{2}}\, \sigma_{n+\frac{1}{2}}\, \phi_{i,n+\frac{1}{2}} \sum_{i'=-I}^{I} a_{i',n+\frac{1}{2}}\, (\underset{\sim}{h}\,\underset{\sim}{h}{}^{T})\, \underset{\sim}{C}_m\, (\underset{\sim}{U}{}^{+} + \underset{\sim}{U}{}^{-})_{i',n+\frac{1}{2}}$$

$$+ \frac{1}{2}\, \tau_{d,n+\frac{1}{2}}\, \omega_{n+\frac{1}{2}}\, (\underset{\sim}{P}{}^{+}_{m,n+\frac{1}{2}}\, \underset{\sim}{C}_m\, \underset{\sim}{U}{}^{+}_{i,n+\frac{1}{2}} + \underset{\sim}{P}{}^{+-}_{m,n+\frac{1}{2}}\, \underset{\sim}{C}_m\, \underset{\sim}{U}{}^{-}_{i',n+\frac{1}{2}})$$

$$+ \underset{\sim}{M}_{1,i+\frac{1}{2}}\, \underset{\sim}{d}_{i+\frac{1}{2}}\, \underset{\sim}{U}{}^{-}_{i+\frac{1}{2},n+\frac{1}{2}} + \tau_{d,n+\frac{1}{2}}(1-\omega)_{n+\frac{1}{2}}\, B^{',+}_{d,}\, \underset{\sim}{h} \qquad (5\text{-}16)$$

where

$$\underset{\sim}{M}_m = [\mu^{\pm}_{j}\, \delta_{jk}] \quad ;$$

$$\underset{\sim}{C}_m = [\underset{\sim}{C}_j\, \delta_{jk}] \qquad\qquad (5\text{-}17)$$

$$d_{i+\frac{1}{2}} = (x_{i+1} - x_i)^{-1},$$

$$\underset{\sim}{U}{}^{\pm}_{i+\frac{1}{2}} = \frac{1}{2}\, (\underset{\sim}{U}{}^{\pm}_{i} + \underset{\sim}{U}{}^{\pm}_{i+1}) \qquad\qquad (5\text{-}18)$$

Λ^{+}_m , Λ^{-}_m are the curvature matrices.

$$\underset{\sim}{M}_{1,i+\frac{1}{2}} = \underset{\sim}{M}_{i+\frac{1}{2}} \Delta \underset{\sim}{V}_{n+\frac{1}{2}} + \underset{\sim}{M}_{i+\frac{1}{2}} \rho_c \underset{\sim}{V}_{n+\frac{1}{2}} \tag{5-19}$$

where $\Delta V_{n+\frac{1}{2}} = V_{n+1} - V_n$

$$\underset{\sim}{M}^1_{i+\frac{1}{2}} = [\mu_j^2 \, \delta_{jk}], \qquad \underset{\sim}{M}^2_{i+\frac{1}{2}} = [(1-\mu_j^2) \delta_{jk}] \tag{5-20}$$

and also

$$\tau_{n+\frac{1}{2}} = K_{gas} \cdot \Delta r, \quad \tau_{d,n+\frac{1}{2}} = K_{dust} \cdot \Delta r$$

$$\sigma_{n+\frac{1}{2}} = 1 - \varepsilon_{n+\frac{1}{2}} \tag{5-21}$$

The curvature factor is expressed as

$$\rho_c = \frac{\Delta r}{r_{n+\frac{1}{2}}} \tag{5-22}$$

The phase matrices of m dimension P^{++} , P^{+-} , P^{-+} , P^{--} will have all their elements equal to unity for the isotropic scattering case.

For I frequency points equations (5-15) and (5-16) get modified and may be written as

$$\underset{\sim}{M}(\underset{\sim}{U}^+_{n+1} - \underset{\sim}{U}^+_n) + \rho_c(\underset{\sim}{\Lambda}^+ \underset{\sim}{U}^+_{n+\frac{1}{2}} + \underset{\sim}{\Lambda}^- \underset{\sim}{U}^-_{n+\frac{1}{2}})$$

$$+\tau_{g,n+\frac{1}{2}}\, \phi_{n+\frac{1}{2}}\, \underset{\sim}{U}^+_{n+\frac{1}{2}} + \tau_{d,n+\frac{1}{2}}\underset{\sim}{E}\underset{\sim}{U}^+_{n+\frac{1}{2}}$$

$$=\tau_{g,n+\frac{1}{2}}\, \underset{\sim}{S}^+_{n+\frac{1}{2}} + \frac{1}{2}\tau_{g,n+\frac{1}{2}}\, \sigma_{n+\frac{1}{2}}(\underset{\sim}{\phi}\underset{\sim}{\phi}^T\underset{\sim}{W})(\underset{\sim}{U}^+ + \underset{\sim}{U}^-)_{n+\frac{1}{2}}$$

$$+ \frac{1}{2}\,\tau_{d,n+\frac{1}{2}}\omega_{n+\frac{1}{2}}(\underset{\sim}{P}^{++}\underset{\sim}{C}\underset{\sim}{U}^+ + \underset{\sim}{P}^{+-}\underset{\sim}{C}\underset{\sim}{U}^-)_{n+\frac{1}{2}}$$

$$+\tau_{d,n+\frac{1}{2}}(1-\omega_{n+\frac{1}{2}})\underset{\sim}{B}'^{,+}_{d,n+\frac{1}{2}} + \underset{\sim}{M}_1\underset{\sim}{d}\underset{\sim}{U}^+_{n+\frac{1}{2}} \qquad (5\text{-}23)$$

and

$$\underset{\sim}{M}(\underset{\sim}{U}^-_n - \underset{\sim}{U}^-_{n+1}) - \rho_c(\underset{\sim}{\Lambda}^+ \underset{\sim}{U}^-_{n+\frac{1}{2}} + \underset{\sim}{\Lambda}^- \underset{\sim}{U}^+_{n+\frac{1}{2}})$$

$$+\tau_{g,n+\frac{1}{2}}\phi_{n+\frac{1}{2}}\underset{\sim}{U}^-_{n+\frac{1}{2}} +\tau_{d,n+\frac{1}{2}}\, \underset{\sim}{E}\underset{\sim}{U}^-_{n+\frac{1}{2}} = \tau_{g,n+\frac{1}{2}}\, \underset{\sim}{S}^-_{n+\frac{1}{2}}$$

$$+ \frac{1}{2}\,\tau_{g,n+\frac{1}{2}}\sigma_{n+\frac{1}{2}}(\underset{\sim}{\phi}\underset{\sim}{\phi}^T\underset{\sim}{W})(\underset{\sim}{U}^+ + \underset{\sim}{U}^-)_{n+\frac{1}{2}}$$

$$+ \frac{1}{2}\tau_{d,n+\frac{1}{2}}\omega_{n+\frac{1}{2}}(\underset{\sim}{P}^{-+}\underset{\sim}{C}\underset{\sim}{U}^+ + \underset{\sim}{P}^{--}\underset{\sim}{C}\underset{\sim}{U}^-)_{n+\frac{1}{2}}$$

$$+\tau_{d,n+\frac{1}{2}}(1-\omega_{n+\frac{1}{2}})\, \underset{\sim}{B}'^{,-}_{d,n+\frac{1}{2}} + \underset{\sim}{M}_1\underset{\sim}{d}\, \underset{\sim}{U}^-_{n+\frac{1}{2}} \qquad (5\text{-}24)$$

where

$$\underset{\sim}{U}^{\pm}_n = [\underset{\sim}{U}^{\pm}_{1,n}\; \underset{\sim}{U}^{\pm}_{2,n}, \ldots \underset{\sim}{U}^{\pm}_{i,n} \ldots \underset{\sim}{U}^{\pm}_{I,n}]^T \qquad (5\text{-}25)$$

T being transpose.

$$\phi_{n+\frac{1}{2}} = [\phi_{kk'}]_{n+\frac{1}{2}} = (\beta + \phi_k)_{n+\frac{1}{2}} \, \delta_{kk'}$$

$$k = j+(i-1)m, \quad 1 \leq k \leq K = mI$$

i and j indicating the frequency and angle discretisation, and

$$S^{+}_{n+\frac{1}{2}} = (\rho\beta + \varepsilon\phi_k) B'^{+}_{n+\frac{1}{2}} \, \delta_{kk'}$$

$$\phi_i W_k == A_i C_j, \qquad A_i = \frac{a_i \phi_i}{\sum\limits_{i'=-I}^{I} A_i \, \phi(x_i)}$$

E is unit matrix of (K X K) dimension and

$$P^{++} = \begin{bmatrix} P^{++}_m & & & \\ & P^{++}_m & & \\ & & \ddots & \\ & & & P^{++}_m \end{bmatrix} \qquad (5\text{-}26)$$

Further

$$\underset{\sim}{B}{}_{d,n+\frac{1}{2}}^{',\pm} = \underset{\sim}{B}{}_{d,n+\frac{1}{2}}^{',\pm} \, \underset{\sim}{h} \tag{5-27}$$

$$\underset{\sim}{M}_1 = [\underset{\sim}{M}{}^1 \, \Delta \underset{\sim}{V}_{n+\frac{1}{2}} + \underset{\sim}{M}{}^2 \, \rho_c \underset{\sim}{V}_{n+\frac{1}{2}}] \tag{5-28}$$

$$\underset{\sim}{M}{}^1 = \begin{bmatrix} \underset{\sim}{M}_m^1 & & & \\ & \cdot & & \\ & & \cdot & \\ & & & \underset{\sim}{M}_m^1 \end{bmatrix} \quad ; \quad \underset{\sim}{M}_m^1 = \left| (\mu_j^2 \, \delta_{j1}) \right. \tag{5-29}$$

$$\underset{\sim}{M}{}^2 = \begin{bmatrix} \underset{\sim}{M}_m^2 & & & \\ & \cdot & & \\ & & \cdot & \\ & & & \underset{\sim}{M}_m^2 \end{bmatrix} \quad ; \quad \underset{\sim}{M}_m^2 = [(1-\mu_j^2)\delta_{j1}] \tag{5-30}$$

$$j,1 = 1,2,\ldots m$$

The matrix d being defined as in equation (4-19) and determined from the flux conservation conditions. By diamond scheme we have got

$$\underset{\sim}{U}^+_{n+\frac{1}{2}} = \frac{1}{2}\left(\underset{\sim}{U}^+_n + \underset{\sim}{U}^+_{n+1}\right)$$

$$\underset{\sim}{U}^-_{n+\frac{1}{2}} = \frac{1}{2}\left(\underset{\sim}{U}^-_n + \underset{\sim}{U}^-_{n+1}\right) \tag{5-31}$$

If these are substituted in equations (5-23) and (5-24) we get

$$
\begin{bmatrix}
\underset{\sim}{M} + \frac{1}{2}\rho_c\underset{\sim}{\Lambda}^+ + \frac{1}{2}\tau_g(\underset{\sim}{\phi} - \frac{1}{2}\sigma\underset{\sim}{\phi}\underset{\sim}{\phi}^T\underset{\sim}{W}) + \frac{1}{2}\tau_d(\underset{\sim}{E} - \frac{1}{2}\omega\underset{\sim}{P}^{++}\underset{\sim}{C}) - \frac{1}{2}\underset{\sim}{M}_1\underset{\sim}{d} & \\[0.3em]
\quad - \frac{1}{2}\rho_c\underset{\sim}{\Lambda}^- - \frac{1}{4}\tau_g\sigma(\underset{\sim}{\phi}\underset{\sim}{\phi}^T\underset{\sim}{W}) - \frac{1}{4}\tau_d\underset{\sim}{P}^{-+}\underset{\sim}{C} & \\[1em]
\frac{1}{2}\rho_c\underset{\sim}{\Lambda}^- - \frac{1}{4}\tau_g\sigma(\underset{\sim}{\phi}\underset{\sim}{\phi}^T\underset{\sim}{W}) - \frac{1}{4}\tau_d\omega\underset{\sim}{P}^{+-}\underset{\sim}{C} & \\[0.3em]
\underset{\sim}{M} - \frac{1}{2}\rho_c\underset{\sim}{\Lambda}^+ + \frac{1}{2}\tau_g(\underset{\sim}{\phi} - \frac{1}{2}\underset{\sim}{\phi}\underset{\sim}{\phi}^T\underset{\sim}{W}) + \frac{1}{2}\tau_d(\underset{\sim}{E} - \frac{1}{2}\omega\underset{\sim}{P}^{--}\underset{\sim}{C}) - \frac{1}{2}\underset{\sim}{M}_1\underset{\sim}{d}
\end{bmatrix}
\begin{bmatrix}
\underset{\sim}{U}^+_{n+1} \\[1.5em]
\underset{\sim}{U}^-_n
\end{bmatrix}
$$

$$
=
\begin{bmatrix}
\underset{\sim}{M} - \frac{1}{2}\rho_c\underset{\sim}{\Lambda}^+ - \frac{1}{2}\tau_g(\underset{\sim}{\phi} - \frac{1}{2}\sigma\underset{\sim}{\phi}\underset{\sim}{\phi}^T\underset{\sim}{W}) - \frac{1}{2}\tau_d(\underset{\sim}{E} - \frac{1}{2}\omega\underset{\sim}{P}^{++}\underset{\sim}{C}) + \frac{1}{2}\underset{\sim}{M}_1\underset{\sim}{d} & \\[0.3em]
\quad \frac{1}{2}\rho_c\underset{\sim}{\Lambda}^- + \frac{1}{4}\tau_g(\underset{\sim}{\phi}\underset{\sim}{\phi}^T\underset{\sim}{W}) + \frac{1}{4}\tau_d\omega\underset{\sim}{P}^{-+}\underset{\sim}{C} & \\[1em]
\quad - \frac{1}{2}\rho_c\underset{\sim}{\Lambda}^- + \frac{1}{4}\tau_g\sigma(\underset{\sim}{\phi}\underset{\sim}{\phi}^T\underset{\sim}{W}) + \frac{1}{4}\tau_d\underset{\sim}{P}^{+-}\underset{\sim}{C} & \\[0.3em]
\underset{\sim}{M} + \frac{1}{2}\rho_c\underset{\sim}{\Lambda}^+ - \frac{1}{2}\tau_g(\underset{\sim}{\phi} - \frac{1}{2}\sigma\underset{\sim}{\phi}\underset{\sim}{\phi}^T\underset{\sim}{W}) - \frac{1}{2}\tau_d(\underset{\sim}{E} - \frac{1}{2}\omega\underset{\sim}{P}^{--}\underset{\sim}{C}) + \frac{1}{2}\underset{\sim}{M}_1\underset{\sim}{d}
\end{bmatrix}
\begin{bmatrix}
\underset{\sim}{U}^+_n \\[1.5em]
\underset{\sim}{U}^-_{n+1}
\end{bmatrix}
$$

$$+ \tau_g \begin{bmatrix} \underset{\sim}{S}^+ \\ \\ \underset{\sim}{S}^- \end{bmatrix} + \tau_d(1-\omega) \begin{bmatrix} \underset{\sim}{B}'^{,+} \\ \\ \underset{\sim}{B}'^{,-} \end{bmatrix} \tag{5-32}$$

E is a unit matrix $\tag{5-33}$

With the help of the quantities as defined below in the following equations, we can write the reflection and transmission matrices.

$$\underset{\sim}{Z}^{++} = (\underset{\sim}{\phi} - \tfrac{1}{2}\sigma \underset{\sim}{\phi} \underset{\sim}{\phi}^T \underset{\sim}{W}) + \frac{\tau_d}{\tau_g}(\underset{\sim}{E} - \tfrac{1}{2}\omega \underset{\sim}{P}^{++}\underset{\sim}{C}) - \frac{\underset{\sim 1}{M}\underset{\sim}{d}}{\tau_g} + \frac{\rho_c \underset{\sim}{\Lambda}^+}{\tau_g}$$

$$\tag{5-34}$$

$$\underset{\sim}{Z}^{--} = (\underset{\sim}{\phi} - \tfrac{1}{2}\underset{\sim}{\sigma}\underset{\sim}{\phi}\underset{\sim}{\phi}^T \underset{\sim}{W}) + \frac{\tau_d}{\tau_g}(\underset{\sim}{E} - \tfrac{1}{2}\omega \underset{\sim}{P}^{--}\underset{\sim}{C}) - \frac{\underset{\sim 1}{M}\underset{\sim}{d}}{\tau_g} - \frac{\rho_c\underset{\sim}{\Lambda}^+}{\tau_g}$$

$$\tag{5-35}$$

$$\underset{\sim}{\Delta}^+ = (\underset{\sim}{M} + \tfrac{1}{2}\tau_g\underset{\sim}{Z}^{++})^{-1}; \qquad \underset{\sim}{\Delta}^- = (\underset{\sim}{M} + \tfrac{1}{2}\tau_g\underset{\sim}{Z}^{--})^{-1}$$

$$\tag{5-36}$$

$$\underset{\sim}{Y}^{+-} = \tfrac{1}{2}\sigma \underset{\sim}{\phi} \underset{\sim}{\phi}^T \underset{\sim}{W} + \tfrac{1}{2}\frac{\tau_d}{\tau_g}\omega \underset{\sim}{P}^{+-}\underset{\sim}{C} - \frac{\rho_c\underset{\sim}{\Lambda}^-}{\tau_g} \tag{5-37}$$

$$\underset{\sim}{Y}^{-+} = \frac{1}{2} \sigma \underset{\sim}{\phi} \underset{\sim}{\phi}^T \underset{\sim}{W} + \frac{1}{2} \frac{\tau_d}{\tau_g} \omega \underset{\sim}{P}^{-+} \underset{\sim}{C} + \frac{\rho_c}{\tau_g} \underset{\sim}{\Lambda}^- \qquad (5\text{-}38)$$

$$\underset{\sim}{A} = \underset{\sim}{M} - \frac{1}{2} \tau_g \underset{\sim}{Z}^{++} \quad , \quad \underset{\sim}{D} = \underset{\sim}{M} - \frac{1}{2} \tau_g \underset{\sim}{Z}^{--} \qquad (5\text{-}39)$$

$$\underset{\sim}{g}^{+-} = \frac{1}{2} \tau_g \underset{\sim}{\Delta}^+ \underset{\sim}{Y}^{+-} \quad , \quad \underset{\sim}{g}^{-+} = \frac{1}{2} \tau_g \underset{\sim}{\Delta}^- \underset{\sim}{Y}^{-+} \qquad (5\text{-}40)$$

$$\underset{\sim}{G}^{+-} = [\underset{\sim}{E} - \underset{\sim}{g}^{+-} \underset{\sim}{g}^{-+}]^{-1} , \quad \underset{\sim}{G}^{-+} = [\underset{\sim}{E} - \underset{\sim}{g}^{-+} \underset{\sim}{g}^{+-}]^{-1} \qquad (5\text{-}41)$$

$$\underset{\sim 1}{S}^+ = \underset{\sim}{S}^+ + \frac{\tau_d}{\tau_g} (1-\omega) \underset{\sim d}{B}'^{,+} \qquad (5\text{-}42)$$

$$\underset{\sim 1}{S}^- = \underset{\sim}{S}^- + \frac{\tau_d}{\tau_g} (1-\omega) \underset{\sim d}{B}'^{,-} \qquad (5\text{-}43)$$

Hence reflection and transmission matrices are

$$t(n+1,n) = \underset{\sim}{G}^{+-} (\underset{\sim}{\Delta}^+ \underset{\sim}{A} + \underset{\sim}{g}^{+-} \underset{\sim}{g}^{-+}) \qquad (5\text{-}44)$$

$$t(n,n+1) = \underset{\sim}{G}^{-+} (\underset{\sim}{\Delta}^- \underset{\sim}{D} + \underset{\sim}{g}^{-+} \underset{\sim}{g}^{+-}) \qquad (5\text{-}45)$$

$$r(n+1,n) = \underset{\sim}{G}^{-+} \underset{\sim}{g}^{-+} (\underset{\sim}{E} + \underset{\sim}{\Delta}^+ \underset{\sim}{A}) \qquad (5\text{-}46)$$

$$r(n,n+1) = \underset{\sim}{G}^{+-} \underset{\sim}{g}^{+-} (\underset{\sim}{E} + \underset{\sim}{\Delta}^- \underset{\sim}{D}) \qquad (5\text{-}47)$$

Corresponding source vectors are given by

$$\underset{\sim}{\Sigma}^+ = \tau_g \underset{\sim}{G}^{+-} (\underset{\sim}{\Delta}^+ \underset{\sim 1}{S}^+ + \underset{\sim}{g}^{+-} \underset{\sim}{\Delta}^- \underset{\sim 1}{S}^-) \qquad (5\text{-}48)$$

$$\underset{\sim}{\Sigma}^- = \tau_g \underset{\sim}{G}^{-+} (\underset{\sim}{\Delta}^- \underset{\sim 1}{S}^- + \underset{\sim}{g}^{-+} \underset{\sim}{\Delta}^+ \underset{\sim 1}{S}^+) \qquad (5\text{-}49)$$

These reflection and transmission operators as well as the source vectors are estimated in each shell with its thickness not exceeding a critical thickness, (τ_{crit}). This critical thickness is determined on the basis of the physical characteristics of the stellar medium.

Radiation field at the internal points is calculated using the procedure described in chapter II [see A.Peraiah (1984)]. Frequency dependent radiation field so calculated may be transformed on to the observer's frame at infinity.

5.3 Effect of dust in line formation

We have studied the effect of dust in different amounts present in the atmosphere in the formation of lines. We have also tried how the velocity of the expanding stellar medium affects the line formation. Computation is done for various velocities of the order upto 50 mean thermal units. Rest frame and comoving frames have been considered and the effects on equivalent widths is shown.

Since the variable parameters are large, we have got huge number of line profiles. In our calculations we have chosen trapezoidal points for frequency integration and Gauss-Legendre points for angle integration. Nine frequency points (2-9) with one point always at the line centre and two angles in each half space ($m = 2$). The

whole stellar atmosphere is divided into N = 100 layers
and the size of the matrix is (18 X 18). The calculations
are performed for flux conservation. Dust present in the
atmosphere is assumed to scatter the radiation isotropi-
cally. Dust is assumed to be distributed uniformly through-
out. We have selected ten dust optical depths ranging
from 0, 0.01,0.02,0.03,0.05,0.1,0.5,0.75,2.0 and 5.0.
The ratio of outer to inner radii of the atmospheric shell
is chosen B/A = 16.6 Velocity of expansion of the medium
is assumed to satisfy the equation of continuity given
by

$$4 \pi r^2 \rho(r) \ V(r) = \text{constant} \hspace{3cm} (5\text{-}50)$$

$\rho(r)$ and $V(r)$ are the density and velocity of expansion
at the radial point r. Velocity is expressed in Doppler
units. Electron density is taken as 10^{10} at the core and
is assumed to vary radially as $(1/r)$. Optical depth of
each shell and the total optical depth of the entire spheri-
cal shell is calculated using the electron density.

5.4 Boundary conditions

Conditions have been imposed such as (1) no radia-
tion is incident on to the spherical shell from outside
at the outermost shell and the optical depth is zero for
this shell i.e.at r = B, no incident radiation from outside
and τ = 0. (2) unit intensity radiation is incident at the
innermost layer at r = A and the optical depth is maximum
for this point i.e. $\tau = \tau_{max} = T$, for a pure scattering

(3) for a medium where there is internal emission within the medium radiation is given at neither the inner nor at the outer boundaries.

In other words we have

$$U^-(\tau = T, \mu_j) = 1$$

$$(\beta = \epsilon = 0) \qquad\qquad (5-51)$$

$$U^+(\tau = 0, \mu_j) = 0$$

$$U^-(\tau = T, \mu_j) = 0 \qquad\qquad \left\{ \begin{array}{l} \beta = 0 \\ \\ \epsilon = 10^{-4} \end{array} \right\} \qquad (5-52)$$

$$U^+(\tau = 0, \mu_j) = 0$$

and

$$U^-(\tau = T, \mu_j) = 0 \qquad\qquad \left\{ \begin{array}{l} \beta = 10^{-5} \\ \\ \beta = 10^{-4} \end{array} \right\} \qquad (5-53)$$

$$U^+(\tau = T, \mu_j) = 0$$

β is the ratio of absorption coefficients per unit frequency interval in the continuum and at the line centre ($\beta = {}^k c/k_L$).

ϵ- probability of destruction per scattering of a photon by collisional de-excitation. The frequency derivative for boundary condition is

$$\frac{\partial U^+}{\partial X} = 0 \text{ at } (X = X_{max}) \qquad (5\text{-}54)$$

Velocity at $\qquad r = A \rightarrow V_A$

$$r = B \rightarrow V_B$$

For velocity gradients in the medium we have set $V_A \neq V_B$

i.e. $\qquad V_A = 0$

$$V_B > 0 \qquad (5\text{-}55)$$

and for spherical shell moving with constant velocity

$$V_A = V_B \qquad (5\text{-}56)$$

In this case we have tried the velocities $0,5,10,20,30,40$ and 50 Doppler units for both V_A and V_B and for velocity gradient case we have kept $V_A = 0$ and V_B is given all velocities from 5 upto 50 mtu. The profiles are shown interms of fluxes integrated over the whole stellar disc versus the normalised frequency.

5.5 Calculation of line profiles

Since the equation of line transfer in comoving frames has found its solution in the normalised frequency co-ordinates, profiles are conveniently described in the frequency co-ordiantes. Traditionally

also the theoretical line profiles are shown in such co-ordinates (see Avrett 1966; Kunasz and Hummer 1975). Pro-files are shown as plots of $(^Fx/F_c) \to X$ where F_x - F_c are the integrated fluxes at the frequency point X and at the continuum respectively.

We have also made the study of the variation of equivalent widths with dust optical depth (Equi.Width $\to$ τ_d) for $V_A = 0$, and $V_B = 5,10,20,30,40,50$ three sets of curves for

$$\epsilon = 0, \qquad \beta = 0$$

$$\epsilon = 10^{-4}, \qquad \beta = 0$$

$$\epsilon = 10^{-4}, \qquad \beta = 10^{-5}$$

are obtained.

Similar set of plots for $V_A = V_B$ also are shown. These curves show how the equivalent width undergoes variation with the presence of different quantities of dust in the atmos-phere. The variation in the equivalent widths with velo-city for the same amount of dust in the atmosphere is also shown in the figures.

τ_d - dust optical depth

T - total gas optical depth at the line centre.

In our calculations we have divided the spherical atmos-pheric shell into 100- elementary shells. Internal radia-tion field and also the emergent radiation fields are cal-

culated by using "Interaction principle and star product" algorithm as described in the 'Discrete Space Theory' (A.Peraiah 1984).

Gas optical depth of each shell according to the variation of density at different radial points is calculated. Dust optical depth of each shell will be

$$\tau_{d \text{ shell}} = \frac{\tau_d}{N(=100)}$$

The profiles that we have plotted show maximum optical depth $\tau_{gas} = 322$ when the gas density is changing as (r^{-1}) τ_d represents the dust optical depth due to scattering alone ($\omega = 1$, refers to the pure scattering case). The profiles are symmetric for static medium and the symmetry is lost when velocity is increased for the outer layers. We also see tht the increased dust content in the medium shows increase in the absorption core. It is found to be maximum for (τ_d - maximum). As the velocity of expansion is increased dust scatters more photons back into the line core. It is observed that the dust in an expanding medium changes the profiles in a variety of ways.

CHAPTER 6

EQUIVALENT WIDTHS OF SPECTRAL LINES IN EXPANDING

DUSTY SPHERICAL ATMOSPHERES

6.1.1. Introduction

In recent years the problem of velocity fields in the outer layers of stars has become important because of the stellar winds which cause mass loss, which in turn affects the process of stellar evolution. The ultra-violet absorption in strong lines indicates the magnitude of the terminal velocities of the flows. However, the problem is the interaction of the velocity fields in the deeper layers where the stellar photospheres merge with the outer layers and the stellar winds. The flow gets accelerated through the sonic point and becomes supersonic flow.

The flow becoming supersonic depends on the complex interaction of dynamical processes of the matter and radia-

tion. Therefore one requires the knowledge of the velocity profiles to study the internal dynamics of the matter in the outer layers and in deeper layers.

The line profiles which we observe in early type stars and supergiants are the result of large scale expansion of the matter in the outer layers, rotation of the atmospheres and perhaps the turbulent velocity fields which are responsible for the non-thermal line broadening. The line broadening may be due to microturbulence or macroturbulence or the velocity gradient effects in an expanding atmospheres (Sletteback 1956). There is possibility, of non-radial pulsational modes (Stothers and Chin 1977; Vemury and Stothers 1977). This physical effect produces asymmetry and broadening while stellar rotation produces symmetric broadening of the lines.

By means of very sensitive analytical techniques or by constructing physically meaningful models one might be able to unravel the different effects described above. Recently Fourier analysis has been employed to find out the detailed velocity structure in the outer layers. In the case of static atmospheres this technique yields fairly reliable estimates of both stellar radial velocity and turbulent velocity (Gray 1975; 1976, 1978; Smith and Gray 1976). These techniques have been employed by Ebbets (1978) and Duval and Karp (1978) for the expanding atmospheres and however, the accuracy of the results remain open to question.

The calculations of line profiles in expanding atmospheres is more complicated than for the static atmospheres (see Pecker and Thomas (1961) for general discussion).

Underhill (1947) calculated the profiles of the lines in an atmosphere with plane parallel stratification with a depth independent expanding velocity. She showed that with such a velocity field the equivalent width of a line does not change although the shape of the flux profiles becomes asymmetric by the variation of the projected line of sight velocity over the stellar disc. Van Hoof and Deurnick (1952) calculated line profiles with a constant expansion velocities by convolving an intrinsic line profile. with a broadening function which accounts for the variation of line of sight velocity over a limb darkening disc. They found that weak lines are more affected than strong lines in producing the asymmetry of the lines. None of the above methods have taken velocity gradients correctly into account. Kubikowski and Ciurla (1965) calculated the equivalent widths in an atmosphere. moving with velocity gradients; they showed that the velocity gradients increase the equivalent widths and they also show that velocity grdients tend to desaturate strong lines and prolong the linear part of the curve of growth. They also show that the flat part of the curve of growth is raised and the difference in the raise is attributed to the turbulence, which is actually due to the velocity gradients. Ciurla (1966) has given a more detailed discussion on these things. He showed that in an atmosphere expanding outward with increasing velocity, lines tend to be skewed towards the shorter wavelengths. This result is exactly opposite to the geometrical distortion effect produced by model with constant depth independent expanding velocity. In this case it is assumed that the velocity was increasing linearly with geometrical height and lines

were calculated in LTE which is in pure absorption. This approximation is good only for very thin layers. If one desires to employ thick layers and scattering is to be taken into account (non-LTE effects) one has to study a more complicated transfer problem. Karp (1973) calculated the line profiles assuming LTE and again using hydrodynamic model atmospheres of Cephieds he found that the effects in strong lines are much smaller (1975). More recenlty Karp (1978) calculated the observed flux from a stellar atmosphere with velocity gradients by using an analytical solution. He used a slowly varying source function which he assumes that it represents scattering process. Worrall (1969) and Canfield (1970) followed the method. These assumptions are not correct concpetually. All the above calculations are done assuming LTE. So one must consider the correct physics in such media. The scattering in the line is important mechanism in formation of the lines. Rybicki (1970), Grant and Peraiah (1972), Simonneau (1973), Noerdlinger and Rybicki (1974), Mihalas, Kunasz, Hummer (1976) have treated the line calculations in non-LTE.

When the velocities are considered in the expanding medium it is important to treat high velocities and solve velocity gradients. If we treat the equation of transfer in the observer's frame (Kunasz and Hummer (1974), Kalkofen (1970), Peraiah and Wehrse (1978), Wehrse and Peraiah (1978) it becomes difficult to treat high velocities. Therefore it is necessary to treat such high velocities. In the comov-

ing frame of the gas. Such calculations were first started by Chandrasekhar (1945), Abhyankar (1964a,b and 1965). However, they have treated only coherent scattering by the atom and two stream approximation. The latter assumption is not adequate and gives unphysical results (Noerdlinger and Rybicki 1974). These latter authors have developed a general technique for plane parallel geometry with arbitrary velocity gradients by using a Feautrier type elimination scheme. Based upon Rybicki type elimination scheme, Mihalas and Kunasz (1975) developed the solution of transfer equation in a comoving frame. These methods require large scale computational facilities. Peraiah (1980) developed a solution of the transfer problem in the lines in the comoving frame of the fluid, based on the Discrete space theory and this requires minimum computer time. This method has been employed in calculating the lines in a comoving frame in the moving atmospheres which contains dust (Peraiah, Varghese and M.S.Rao 1987). In the following chapter we shall be using the above technique in estimating the equivalent widths of lines formed in expanding atmospheres with dust.

6.1.2. Hydrogen Lyman Alpha Line

Curve of growth yield important and reasonably good information regarding the chemical abundances in the stellar atmospheres. Generally curves of growth are made use of stationary stellar atmospheres. However observations have established the existance of stellar winds in many types of stars. The matter in the atmospheres of

stars is in continuous radial motion. Absorption and scattering of radiation by the moving medium creates complications which cannot be revealed through the ordinary curve of growth. Therefore one must study the problem by constructing theoretical models of curves of growth.

The effective optical depth is limited by the velocity gradient in a moving medium. For an electron scattering atmosphere the optical depth is defined as.

$$\tau = \sigma v_{th}(\frac{dv}{dr})^{-1} \qquad (6.-1-1)$$

where σ is the electron scattering coefficient v_{th} the thermal velocity of the medium in motion and $(\frac{dv}{dr})$ is the velocity gradient. As the radiation force on the lines becomes negligibly small the above relation is used to a fairly good approximation though it is invalid for stellar photospheres. In such situations it is difficult to obtain the information about the number density that is influencing the line formation. We have made investigations based on the effect of expansion velocities of the atmospheres and the presence of dust on the equivalent widths of resonance lines. For this purpose we have chosen Hydrogen Lyman Alpha line whose parameters are well known. We have assumed a spherically symmetric atmosphere containing varying amounts of dust.

6.1.3.Calculations

We have made calculations for a comoving frame and the equation of transfer is written as Peraiah et al

(1987) and aimed at the investigation of the effects of dust and radial expansion of the outer layers on the equivalent widths. These equivalent widths in turn indicate the total amount of absorption or emission.

Temperature distribution at different radial points of the atmosphere is calculated by assuming that

$$B_\nu (T_r) = (\frac{r_o}{r})^2 B_\nu (T_{r_o}) \qquad\qquad (6-1.2)$$

where B_ν is the Planck function at frequency ν and T_r is the temperature at radial point r in the spherical shell. T_{r_o} indicates the temperature at the inner radius of the shell. From the above equation

$$(\frac{2h\nu^3}{c^2}) (\frac{1}{e^{h\nu/KT_r}-1}) = (\frac{r_o}{r})^2 (\frac{2h\nu^3}{c^2}) (\frac{1}{e^{h\nu/KT_{r_o}}-1})$$

$$(e^{h\nu/KT_r}-1) = (\frac{r}{r_o})^2 (e^{h\nu/KT_{r_o}} -1)$$

$$e^{h\nu/KT_r} = 1+ (\frac{r}{r_o})^2 (e^{h\nu/KT_{r_o}}-1)$$

which simplifies to

$$T(r) = \frac{h\nu}{K} (\frac{1}{\ln[1+(\frac{r}{r_o})^2 (e^{h\nu/KT_{r_o}} -1)]}) \qquad\qquad (6-1.3)$$

A temperature of 15,000° K has been assumed at the inner shell $r = r_o$. For the assumed electron density figure 6.1.2 we have obtained the temperature distribution as shown in Figure 6.1.1.

Stellar atmospheres consist of a mixture of atoms at various stages of ionization and excitation. In normal stellar atmospheres hydrogen is the most abundant constituent. At high temperatures hydrogen is appreciably ionised, it contributes most of the electrons to the gas. Hence for a pure hydrogen gas the electron density is given by (Mihalas 1978)

$$ne(H) = \phi_H^{-1}[(N\phi_H+1)^{\frac{1}{2}}-1]$$

(6-1.4)

Where

$$\phi_H = \frac{U_1(T)}{U_2(T)} \quad C_1 T^{-3/2} \quad e^{X_1/KT}$$

(6-1.5)

and

$$C_1 = 2.07 \times 10^{-16} \text{ CGS units}$$

(6-1.6)

U_1 and U_2 are partition functions.

Total number of particles is given by

N = Neutral atoms (N_o) + Number of ions + number of electrons. i.e

$N = N_o + n_p + n_e$ (for hydrogen $n_p = n_e$)

hence

$N = N_o + 2n_e$

(6-1.7)

Substituting this in (6-1.4)

$$n_e(H) = \frac{1}{\phi_H} \; [\{(N_o + 2n_e)\phi_H + 1\}^{\frac{1}{2}} - 1] \qquad (6-1.8)$$

$$n_e\phi + 1 = [(N_o + 2n_e)\phi + 1]^{\frac{1}{2}}$$

$$(n_e\phi + 1)^2 = (N_o + 2n_e)\phi + 1$$

or

$$n_e^2 \, \phi = N_o$$

Hence

$$N_o = \phi n_e^2 \qquad (6-1.9)$$

Distribution of neutral atoms in the atmosphere is plotted in Figure (6.1.3).

For obtaining absorption coefficient we need to know the number of hydrogen atoms in level 1 (n_1) . This is done by using Boltzmann law which gives the fundamental relationship of the fraction of atoms in r^{th} level of excitation in terms of the total number N_i in the ith stage of ionization namely

$$\frac{N_{i,r}}{N_i} = \frac{g_{i,r}}{U_i(T)} \cdot e^{-\epsilon_{i,r}/KT} \qquad (6-1.10)$$

where $\epsilon_{i,r}$ is excitation energy of the level above ground level and $g_{i,r}$ is the statistical weight of that level, T is the temperature U_i is the partition function. If N_1 and N_2 are the number of hydrogen atoms in level 1 and 2 respectively and g_1 , g_2 are the corresponding statistical

weights comparision of population of 2nd level to that in ground level is given by Boltzmann equation (Aller 1963)

$$\log \frac{N_2}{N_1} = -\theta\epsilon + \log \frac{g_2}{g_1} \qquad (6-1.11)$$

where $\theta = \dfrac{5040}{T}$ and ϵ the excitation energy in eletron volts.

Total number of neutral atoms

$$N_o = N_1 + N_2$$

Let $\dfrac{N_2}{N_1} = a$

hence $N_o = N_1 + aN_1$

or $\qquad N_1 = \dfrac{N_o}{1+a} \qquad (6-1.12)$

Number of neutral atoms N_o is obtained from Saha's equaion by defining the electron pressure and temperature T (Aller 1963) $\qquad P_e = N_e KT$

$$\log \frac{N_I}{N_o} P_e = -\frac{5040}{T} I + 2.5 \log T - 0.48 + \log \frac{2U_1(T)}{U_o(T)}$$

$$(6-1.13)$$

where

I = ionization potential in volts

P_e = Electron pressure in dynes/cm^2

N_I = density of ionized atoms

N_o = density of neutral atoms

$U_I(T)$ = Partition function for the neutral atoms

$$N_I = n_p + n_e = 2n_e \tag{6.-1.14}$$

for a given P_e and T we can calculate $\left(\dfrac{N_I}{N_0} \right)$.

For hydrogen Lymann Alpha Line we can calculate the absorption coefficient

$$\chi_1(\nu) = \frac{n_1 B_{12} h\nu}{4\pi} \phi_\nu \left(1- \frac{n_2}{n_1} \frac{g_1}{g_2}\right) \tag{6.-1.15}$$

but $\quad A_{21} = \dfrac{2h\nu^3}{c^2} B_{21}$

and

$$g_2 B_{21} = g_1 B_{12} \qquad\qquad B_{21} = \frac{g_1}{g_2} B_{12}$$

or

$$A_{21} = \frac{2h\nu^3}{c^2} \frac{g_1}{g_2} B_{12}$$

i.e

$$B_{12} = A_{21} \frac{g_2}{g_1} \frac{c^2}{2h\nu^3}$$

hence

$$\chi_1(\nu) = n_1 A_{21} \frac{c^2}{2\nu^2} \frac{\phi_\nu}{4\pi} \left(\frac{g_2}{g_1} - \frac{n_2}{n_1} \right) \tag{6.-1.16}$$

where A_{21} is Einstein coefficient for spontaneous emission, c is speed of light and ν is the central frequency of Hydrogen Lyman Alpha Line and ϕ_ν is the profile function of the line such that

$$\int_{-\infty}^{+\infty} \phi_\nu \, d\nu = 1 \qquad\qquad (6-1.17)$$

We have employed Doppler profile.

Optical depth in each shell of the medium is plotted in Figure 6.1.4 and the total optical depth upto every shell is plotted in Figure 6.1.5. The medium is assumed to contain dust in addition to gas. The amount of dust and its distribution is represented by the dust optical depth. The spherically symmetric medium is expanding radially outwards. We have studied the expansion with and without velocity gradients. Line Transfer equations (5-2) and (5-3) are solved in a comoving frame as explained in the Chapter 5.

In solving the transfer equations phase function of dust is assumed to be isotropic.

6.1.4. Results

We have adopted a non-LTE line with a two-level atom approximation, set $\varepsilon = 0$, hence no internal source is assumed.

Following boundary conditions are imposed:

$$\varepsilon = 0, \qquad \beta = 0 \quad B(T(r),x) = 0$$

and

$$U^+(\tau = 0, \mu_j, x_i) = 0$$

V_A and V_B are the velocities in Doppler units at A and B Figure 1.2.

We have considered two cases viz.

(1) $V_A = V_B$ and

(2) $V_A = 0$, $V_B > 0$

In the first case we have an expanding spherical shell and in the second case we have expanding shell with velocity gradients. The profiles of Hydrogen Lymann Alpha Line are shown in Figures from 6.1.6 to 6.1.10 for specific dust optical depths $\tau = 0,0.1,0.5,1,5$. The figures give the relation between the ratio $\dfrac{F_x}{F_c}$ and x where

$$F_x = 2\pi \int I_x \, \mu d\mu \qquad\qquad (6-1.18)$$

$$F_c = 2\pi \int I_c \, \mu d\mu \qquad\qquad (6.-1.19)$$

I_x and I_c being the intensities in the line and continuum respectively.

Figure 6.1.6 is for $V_A = V_B = 0$ i.e. for a static medium for various dust optical depths. It is observed that as the dust optical depth increases more and more photons are scattered into the line centre indicating in diminution of absorption depth.

Figure 6.1.7 is for outer velocity $V_B = 5$ mean thermal units while $V_A = 0$ introducing a velocity gradient. Here we notice P-Cygni type profiles. Absorption is being

shifted towards violet side while emission peak remains at the centre of the line. When dust optical thickness is increased the emission is reduced considerably while more photons are scattered by the dust into the absorption core of the line. It may yield an obvious inference that dust has opposite effects in emission wing as compared to that in the absorption core.

In Figure 6.1.8 the expansion velocity is increased to V_B = 10 mtu, same effect is observed as in the previous case.

In Figure 6.1.9 and 6.1.10 we have considered the spherical shell to be expanding with constant velocities V_A = V_B = 5 mtu and 10 mtu respectively. Here we observe that the emission wing has become broader and the absorption core has been narrowed. Further the shifts of absorption cores in both the cases from the centre of the line are almost the same as that of the expansion velocities used. Almost symmetrical broadening of the emission wing is also noticed.

In Figures 6.1.11 to 6.1.15 we have shown the relation between neutral atoms and the equivalent width of the line which has been explained in Chapter 1.4 in detail.

In Figure 6.1.11 we have the relation plotted for a static medium. This has a close resemblance to the curve of growth. We have a linearly increasing portion then a flat part and further increasing linearly.

In Figure 6.1.12 we have velocity gradient V_B = 5 mtu and V_A = 0.

This shows a slight modification in the flat portion of the curve of growth. It may be noticed here that for same equivalent width with a dusty medium results in a larger number of neutral atoms. This is a very important observation. It hints that caution is to be exercised in deriving the number of neutral atoms producing the line if the presence of dust is noticed through infrared observations or by any other means. Figure 6.1.13 is for increased expansion velocity with dust. It is showing similar effect. In Figures 6.1.14 and 6.1.15 we have considered steadily expanding spherical shell with velocities of expansion 5 mtu and 10 mtu respectively without velocity gradients. In these cases though the increasing part of the curve of growth is the same as one expects in static medium, however after equivalent width reaches a maximum with the increasing number of neutral atoms, the width falls and the line becomes more of emission, which means that the emission part of P-Cygni type of profiles is larger than the absorption part. The presence of dust increases the equivalent width.

6.1.5. Conclusion

Calculations have been performed to show the effect of velocity of expansion of the stellar atmospheres and the presence of dust in the atmosphere on the equivalent width of Hydrogen Lymann Alpha line simultaneously. It is found that there is noticeable change in the equivalent widths due to presence of dust in the expanding medium.
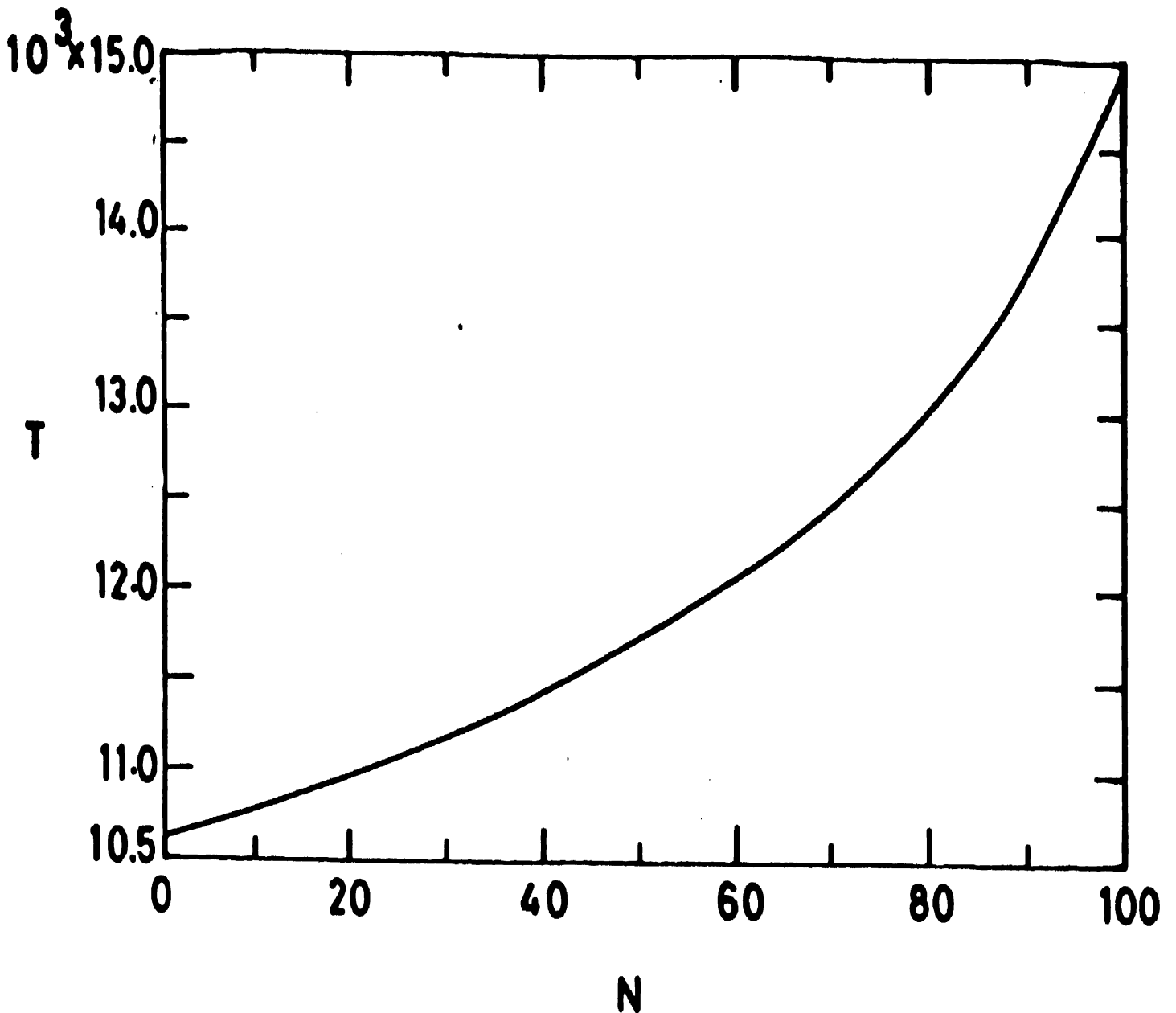
Figure 6.1.1.   Temperature at various points in the spherical shell in which hydrogen Lyman α line is forming. Here $T(r_o) = 15000$ K.   Shell No.1 is at $r = r_{max}$ and shell No.100 is at $r = r_o$.
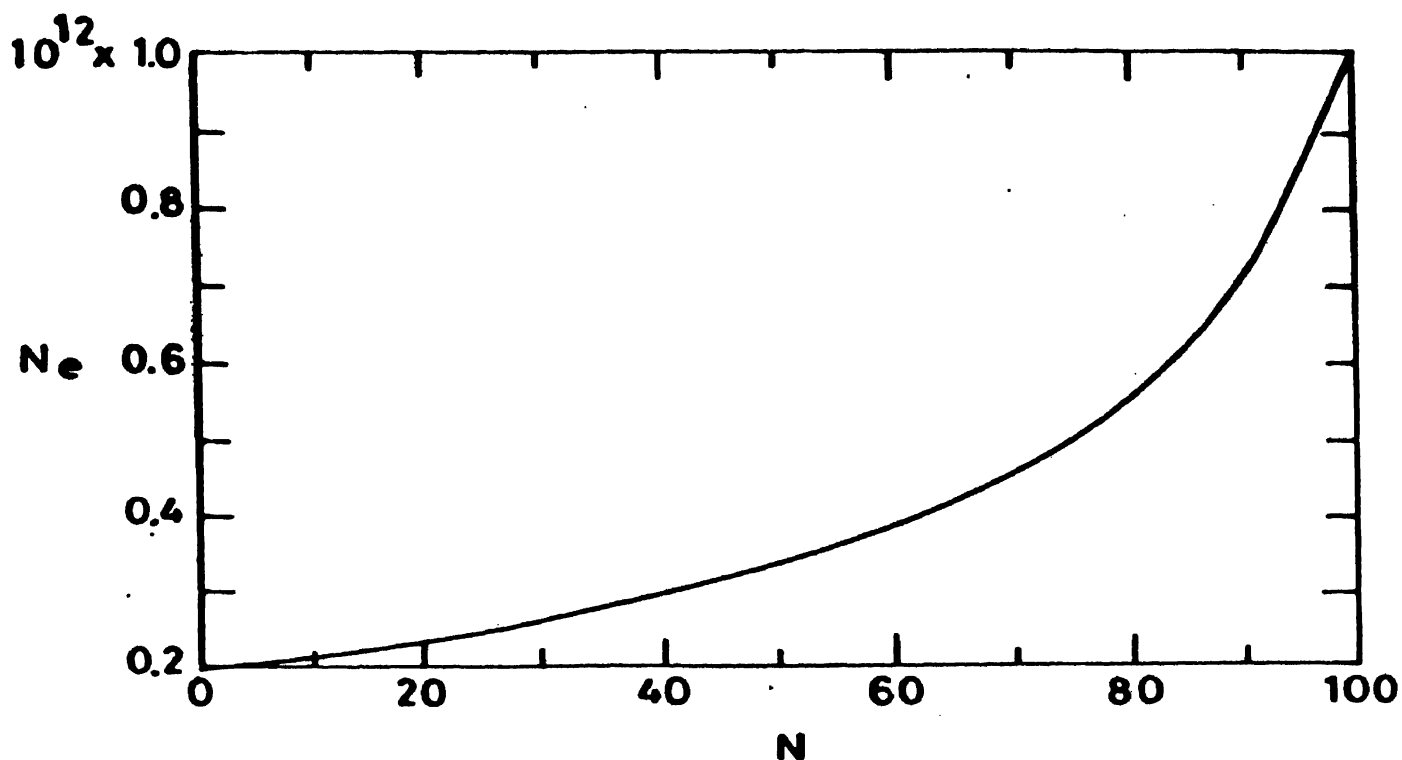
Figure 6.1.2.   Electron density (Ne) at different shells N.
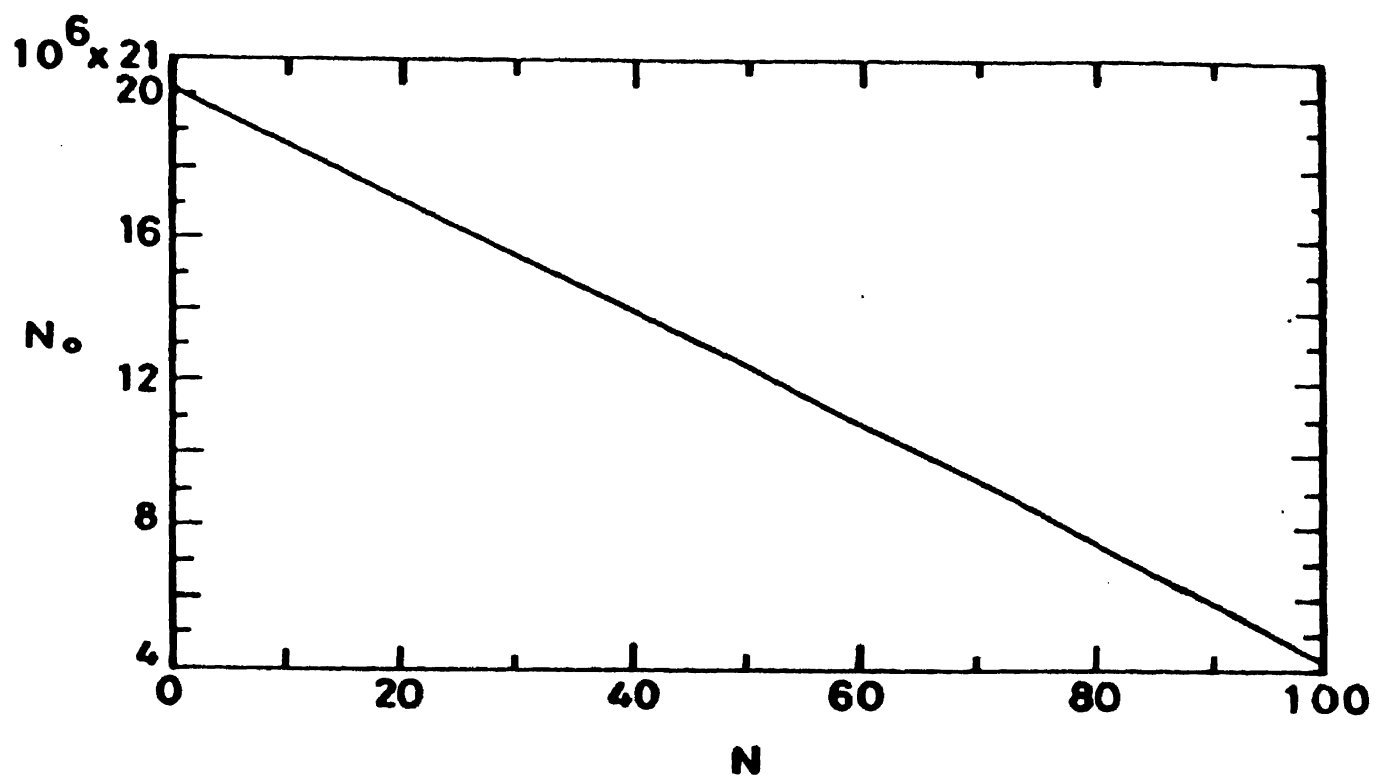
Figure 6.1.3.   Number of neutral atoms (No) at different layers
(N) of the stellar atmosphere in Hydrogen Lyman α
line calculations.
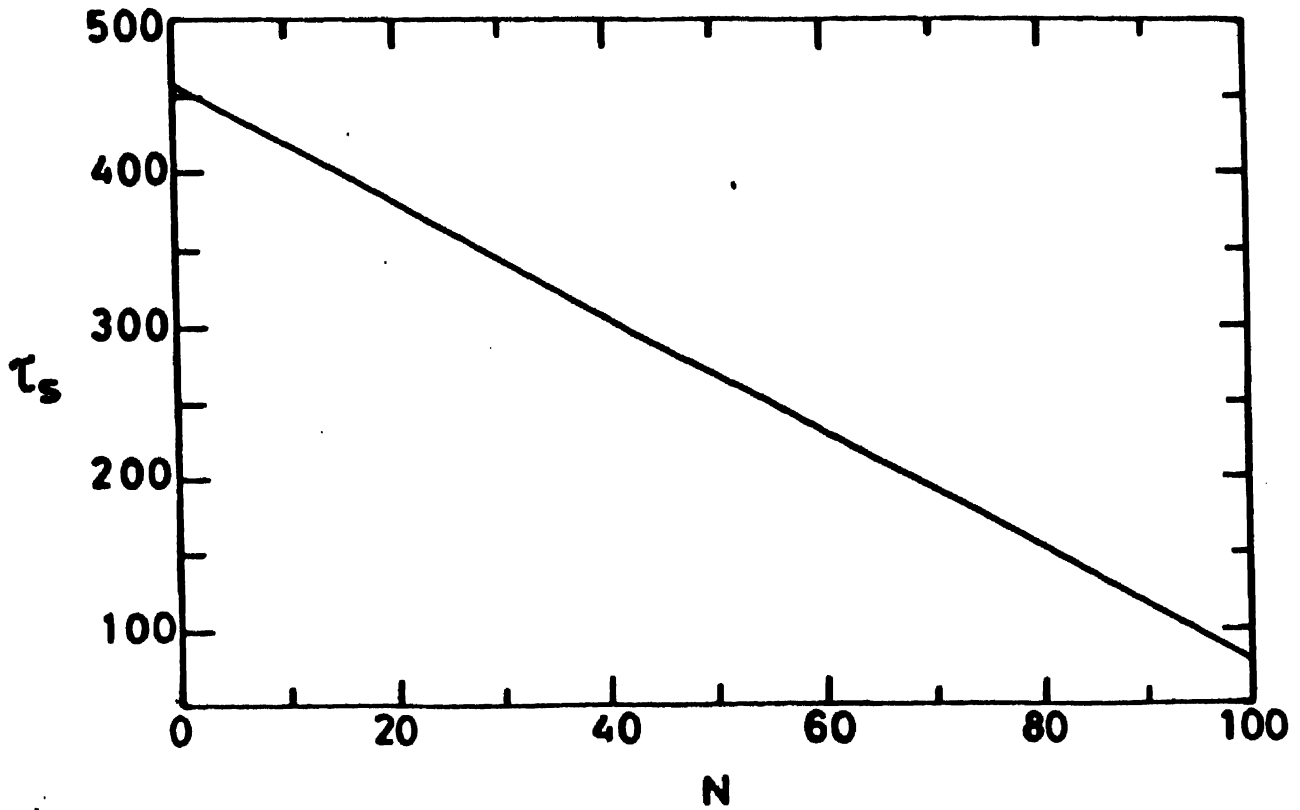
Figure 6.1.4.   Optical depth in each shell of the stellar medium.
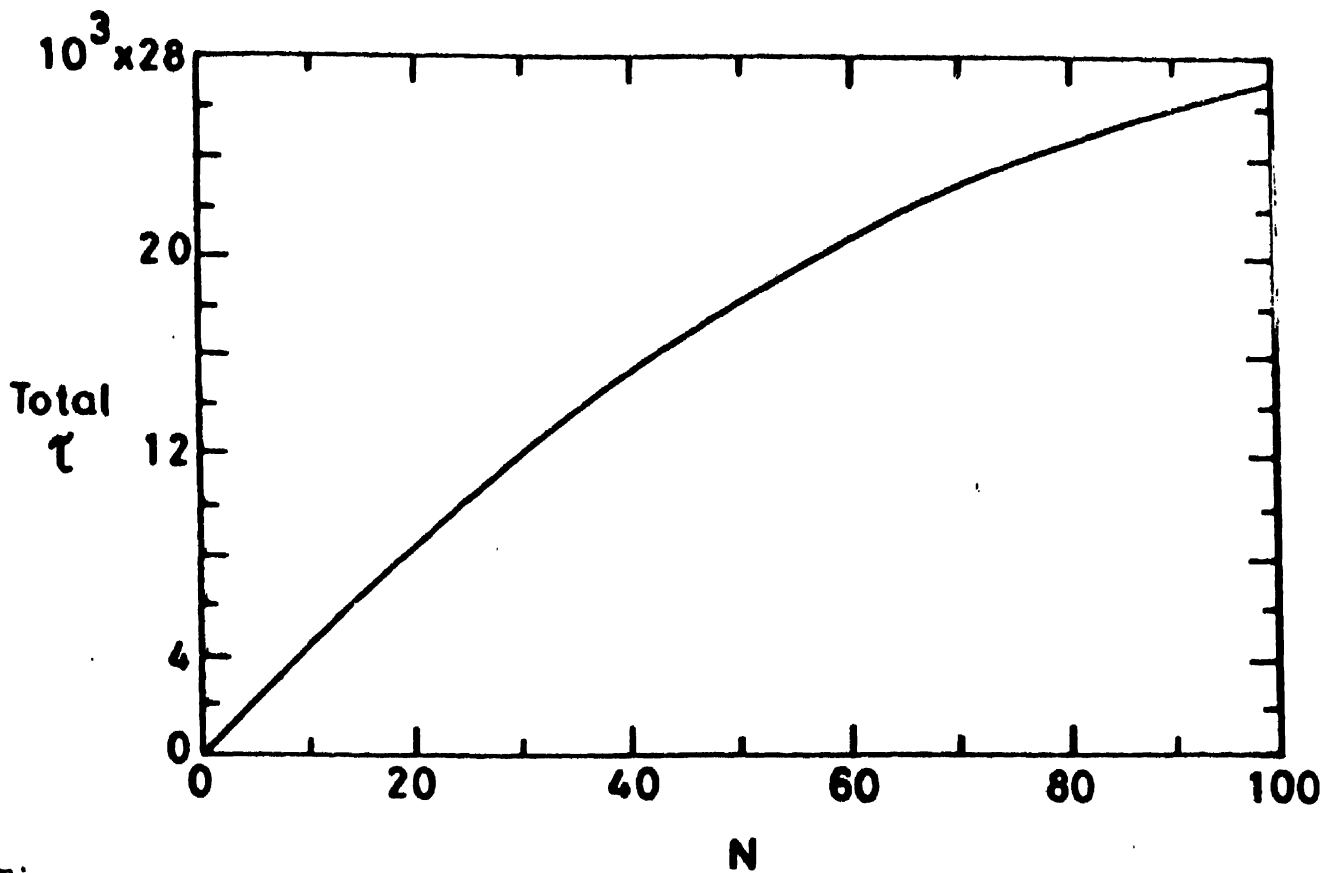
Figure 6.1.5.   Total optical depth at various layers of the medium.
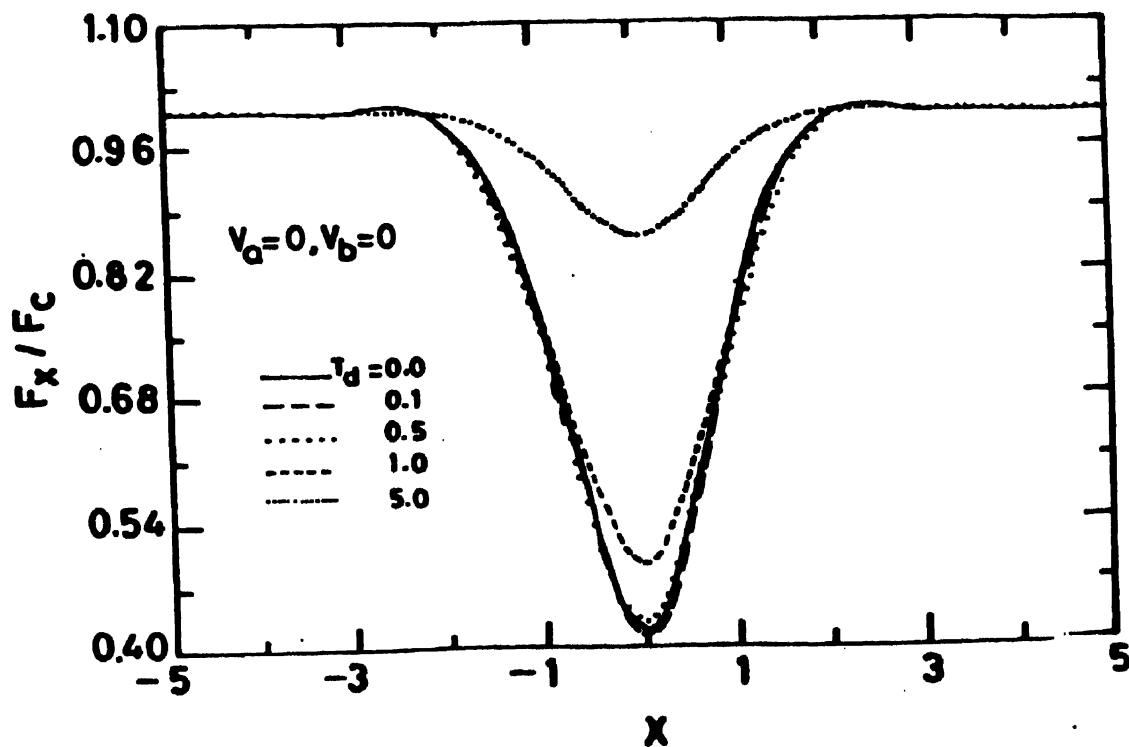
Figure 6.1.6   Hydrogen Lyman α line profiles formed in a static medium with different amounts of dust (τ_d). Distribution of dust is constant throughout the atmosphere.
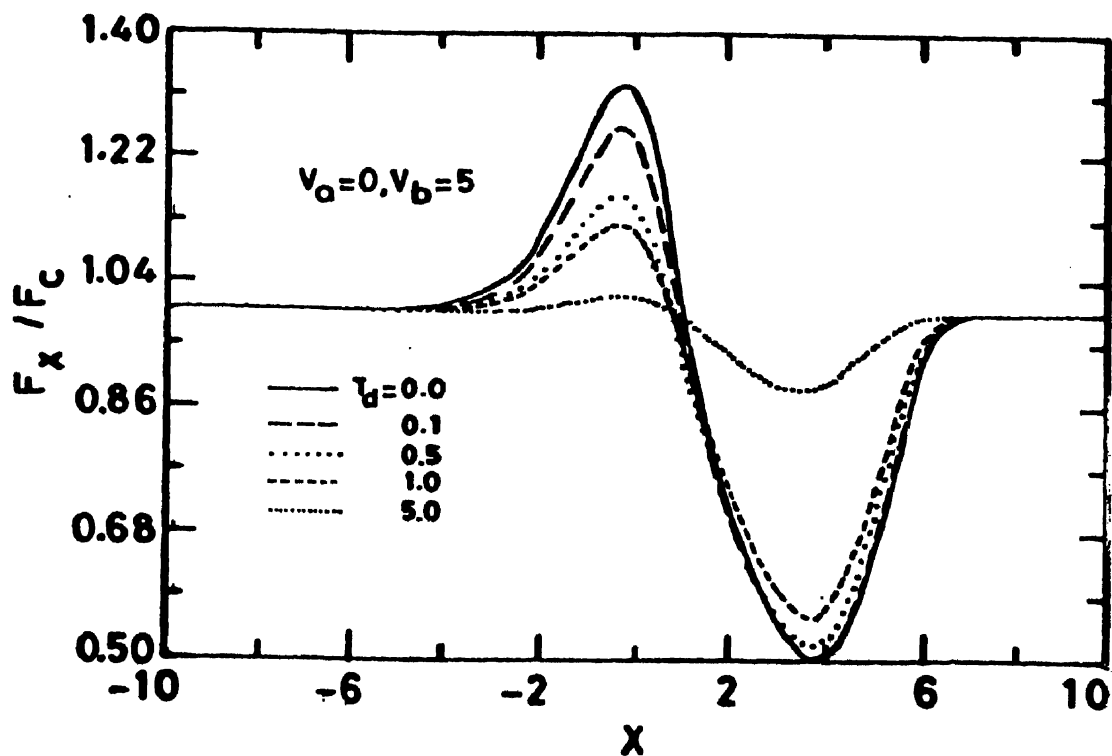
Figure 6.1.7.   Line profiles of hydrogen Lyman α formed in a medium moving with velocity of expansion V_b= 5 mtu (with velocity gradient).
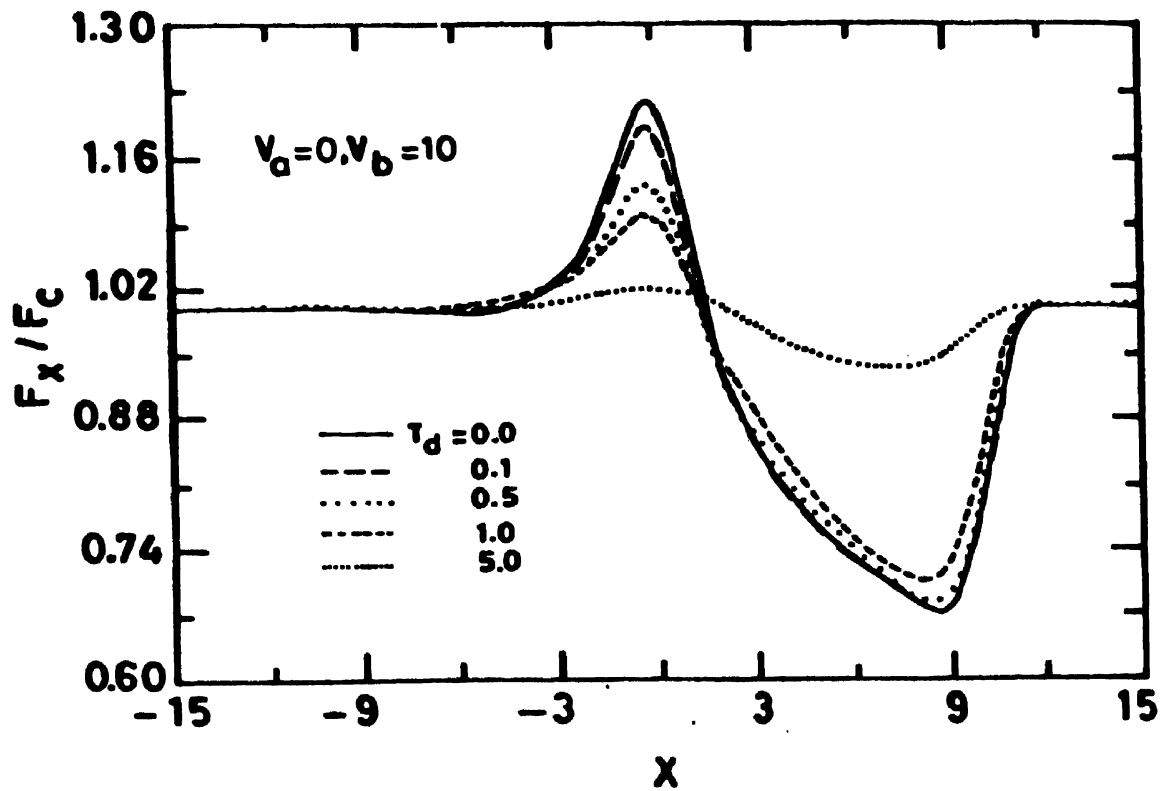
Figure 6.1.8. Same as in Figure.6.1.7 but the velocity of expansion is equal to 10 mtu.
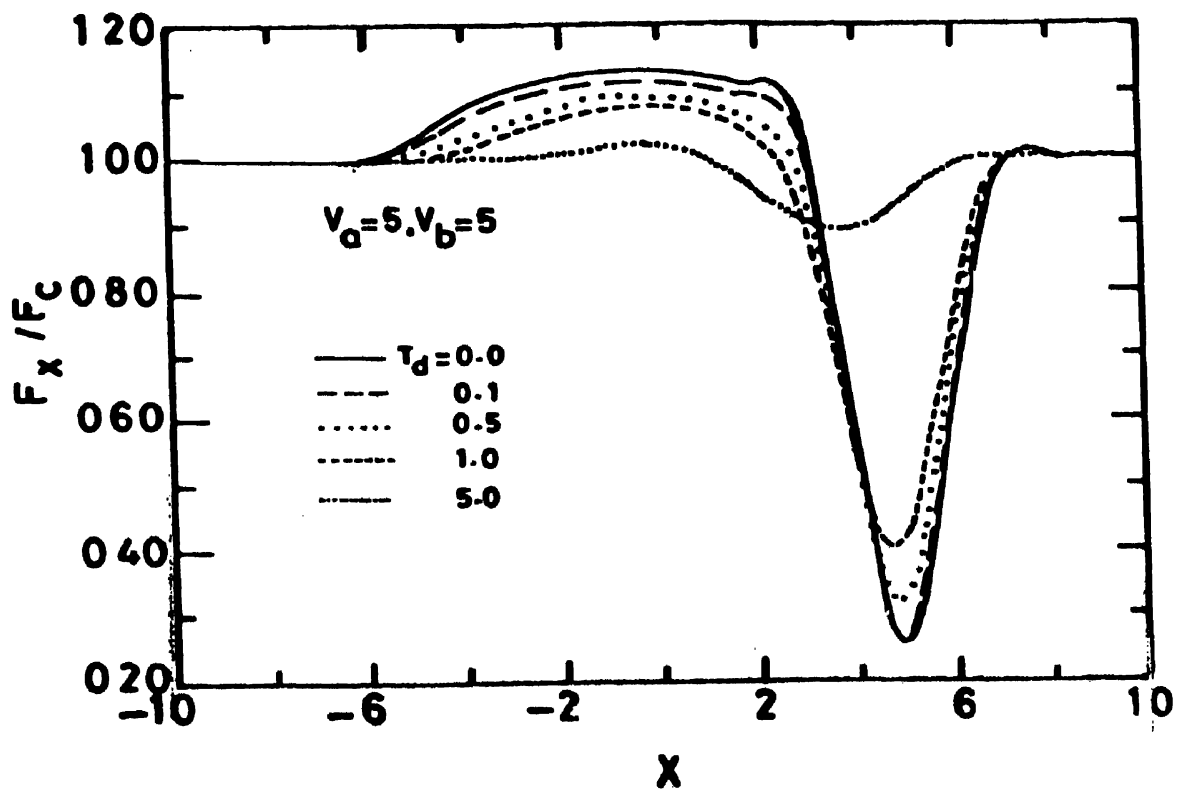
Figure 6.1.9. Hydrogen Lyman α line profiles formed in a medium expanding with velocity 5 mtu and without velocity gradients.
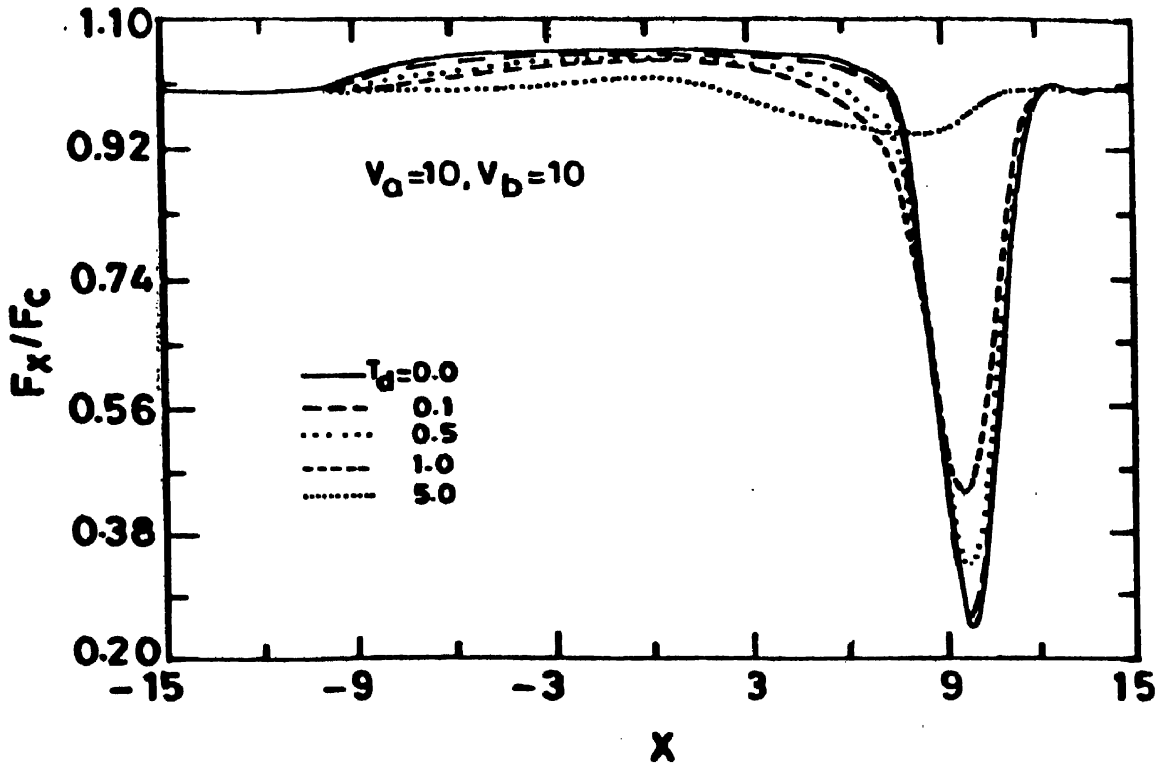
Figure 6.1.10. Same as in Figure 6.1.9.but the velocity of expansion is equal to 10 mtu.
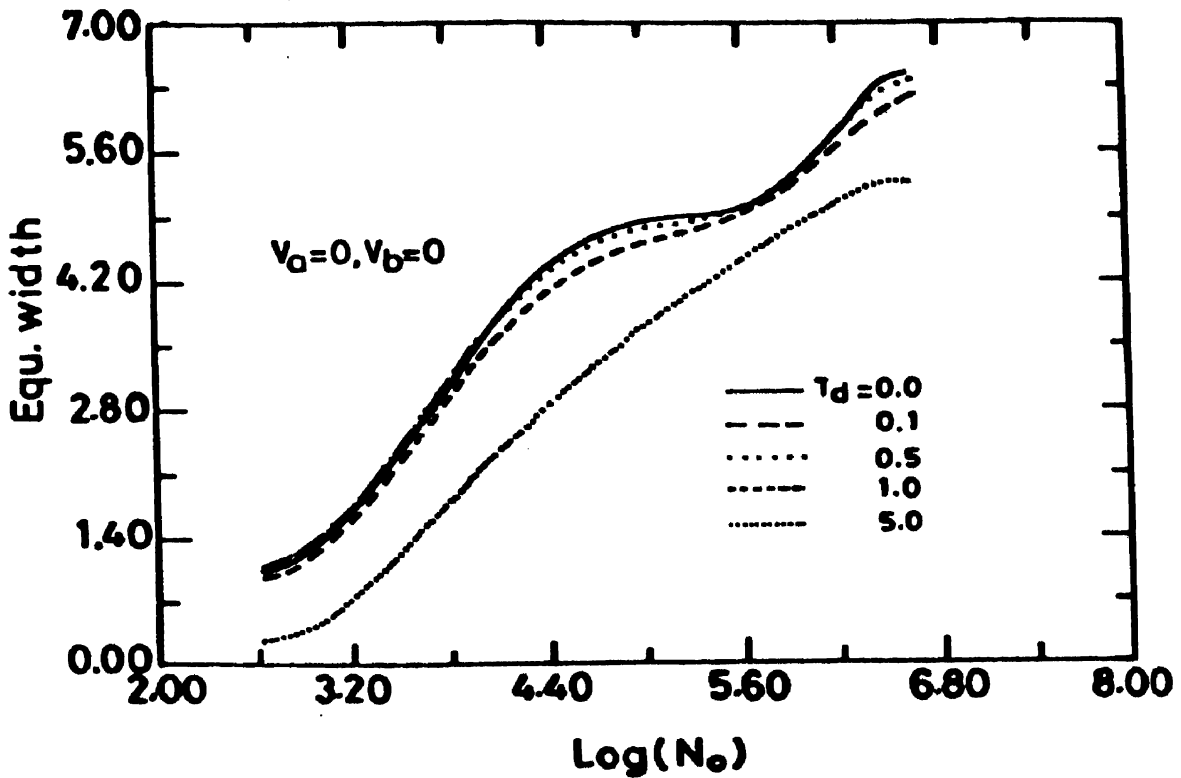
Figure 6.1.11. Variation of equivalent widths of the hydrogen Lyman α line with the increasing number of neutral atoms (log No) for a static medium and for various dust optical depths (τ_d).
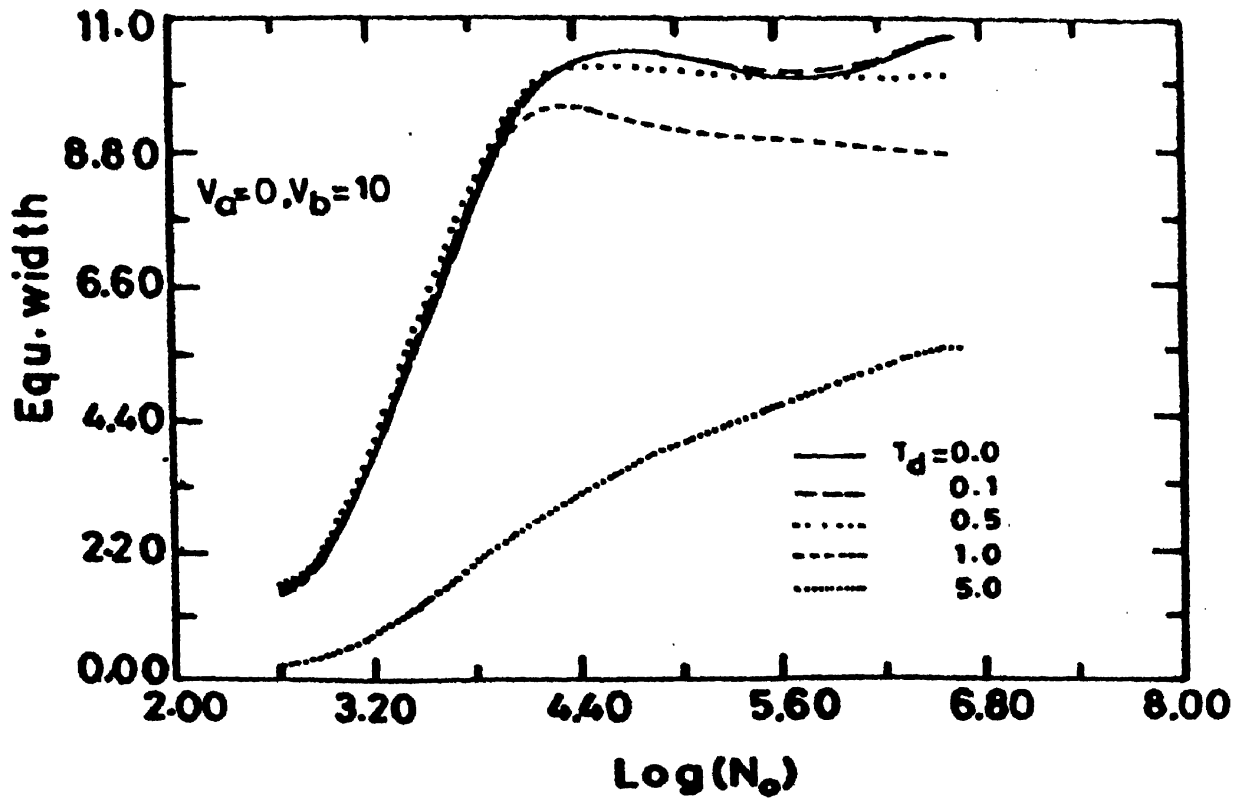
Figure 6.1.12. Same as in Figure 6.1.11 but the atmosphere is expanding with velocity gradient, expansion velocity is equal to 5 mtu.
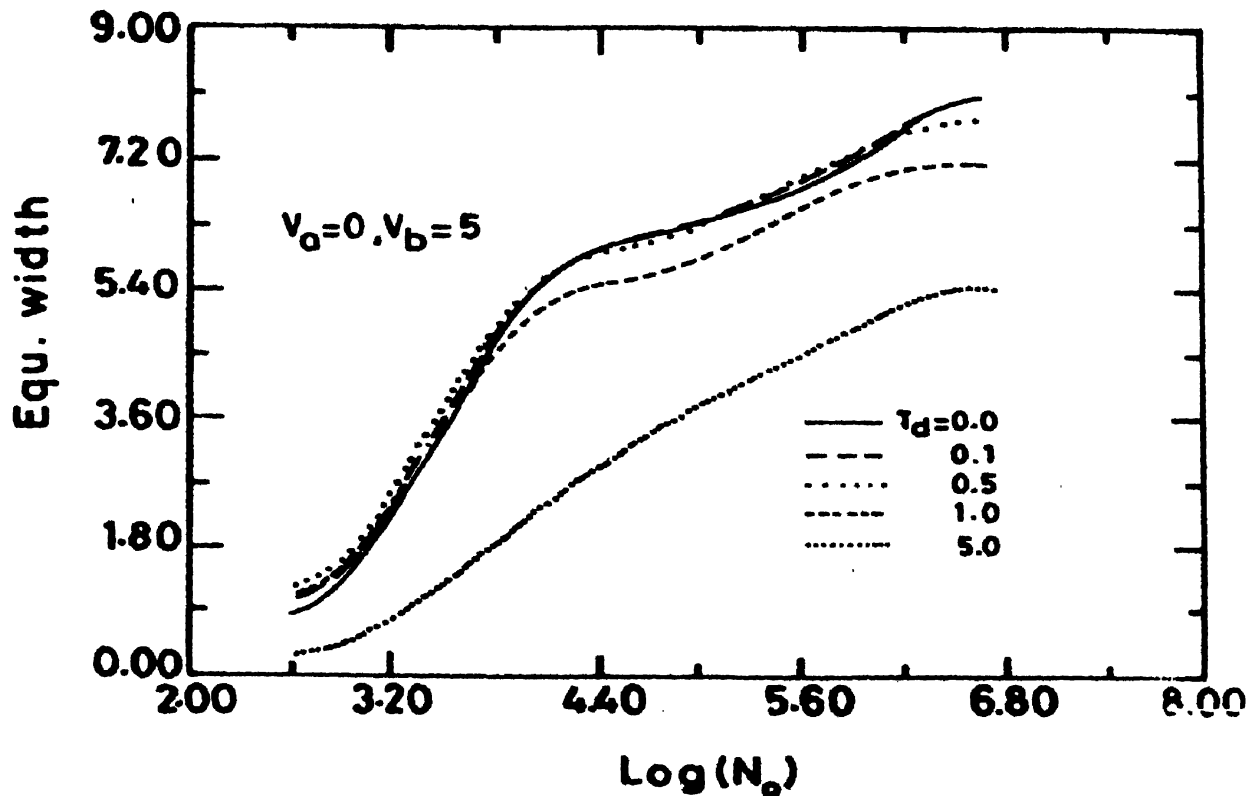
Figure 6.1.13. Same as in Figure 6.1.12 but velocity of expansion is equal to 10 mtu.
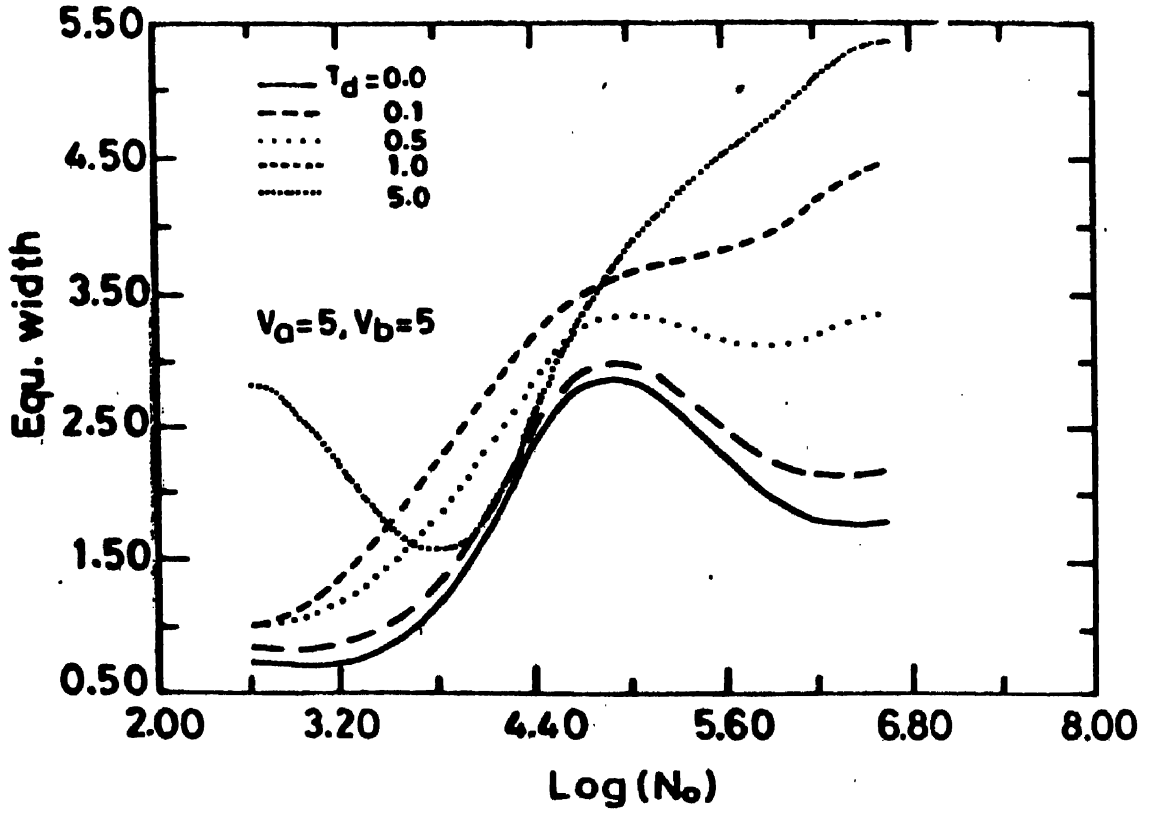
Figure 6.1.14. Same as in Figure 6.1.12 .but without velocity gradient i.e. $V_A = V_B = 5$.
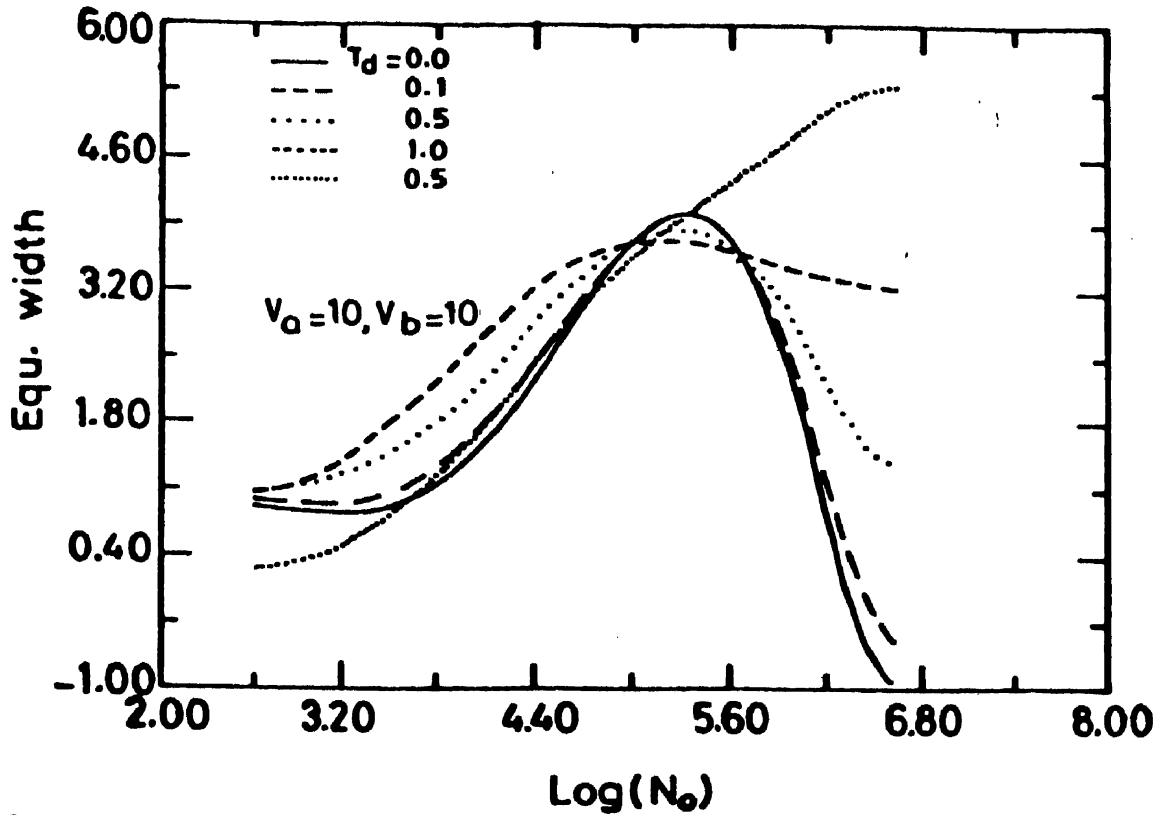
Figure 6.1.15. Same as in Figure 6.1.12 but the velocity expansion is 10 mtu.

6.2.1 Dust in the Spherical Shells

Presence of dust in the outer layers of stars has been inferred from the infrared observations of these stars. B_r Alpha line radiation was observed in Becklin-Neugebauer (BN) object in Orion by Grasdalen (1976). These objects show the presence of ionised gas and several of such objects as BN and CRL 490 seen to Posess dusty shells around a hard ionised gas core. The majority of Be stars have circumstellar dust to give rise to an infrared excess over and above that of free-free emission. Br_ν , Bf_ν Br_ν infra-red lines have been observed in the compact molecular clouds by Simon et al (1981,1985). Persi et al (1983) derived mass loss rates for 15 α-type stars based upon infrared photometric observations from 2.3 μm to 10 μm. Infrared observations of several objects such as gaseous nebulae, active galactic nuclei, T-Tauri stars, atmospheres of cool super giants show the presence of dust in the outer layers of these objects. Allen's study (1973) of several early type emission line stars has revealed that Bremmsstrahlung and thermal emission from dust grains are the causes of infrared excess. Giesel (1970), Allen and Pol Swings (1972) have found that almost all stars with prominent infrared continua appear to have circumstellar envelopes. Schwartz et al (1983) studied the far infrared and submillimeter mapping of S140 IRS and have concluded that there is a good coupling between the dust and gas. Huggins et al (1984) derived abundances in the envelopes of IRC+10216 line analysis following the approach of Kwan and Hill (1977)

and Henkel et al (1983). Felli studied the infrared emission from extended stellar envelopes.

Line formation calculations have taken into account of the velocity of expansion, presence of dust, geometrical extension of outer shell and the chemical species present. We have considered non-LTE, two-level atom approximation and the dust is assumed to scatter isotropically. The envelope is divided into 100 shells and the total optical depth is about 300. We have neglected absorption due to dust by setting albedo ω = 1. We have tried two types of expanding shell (1) with velocity gradient and (2) with out velocity gradients. Recently there have been calculations including dust and velocity of expansion (Peraiah and Wehrse 1978, Wehrse and Peraiah 1979, Hummer and Kunasz 1980, Wehrse and Kalkofen 1985, Peraiah et al 1987). Observer's frame method of solving is disadvantageous if scattering is to be considered because of large number of angles and frequencies that have to be used to obtain accurate results. For such flows, a solution in the comoving frame is better suited.

6.2.2. Calculations

Radiative transfer equation in a comoving frame were first explored by S.Chandrasekhar (1945), Abhyankar (1964,1965), Mihalas et al (1975) and Mihalas (1978). Here we perform the calculations taking the equation of transfer written as (Peraiah et al 1987)

$$\mu \frac{\partial I(r,\mu,x)}{\partial r} + \frac{1-\mu^2}{r} \frac{\partial I(r,\mu,x)}{\partial \mu} = K_L(r)[\phi(x)+\beta][S(r,\mu,x)-I(r,\mu,x)]$$

$$+ \left\{(1-\mu^2) \frac{V(r)}{r} + \mu^2 \frac{dV(r)}{dr}\right\} \frac{I(r,\mu,x)}{\partial x}$$

$$+ K_{dust}(r)\{S_{dust}(r,\mu,x)-I(r,\mu,x)\} \qquad (6.-2.1)$$

Similarly for an oppositely directed beam we have

$$-\mu\frac{\partial I(r,-\mu,x)}{\partial r} + \frac{1-\mu^2}{r} \frac{\partial I(r,-\mu,x)}{\partial \mu} = K_L(r)[\phi(x)+\beta][S(r,-\mu,x)$$

$$-I(r,-\mu,x)]$$

$$+\left\{(1-\mu^2) \frac{V(r)}{r} + \mu^2 \frac{dV(r)}{dr}\right\}\frac{\partial I(r,-\mu,x)}{\partial x}$$

$$+K_{dust}(r)\{S_{dust}(r,-\mu,x)-I(r,-\mu,x)\} \qquad (6-2.2)$$

where $\mu = \cos\theta \epsilon (0,1)$ and $K_L(r)$, β , $\phi(x)$, S etc have usual meaning as explained in Chapter V.

ϵ the probability per scatter that a photon is thermalized due to collisional de-excitation is given by

$$\epsilon = \frac{C_{21}}{C_{21}+A_{21}[1-e^{-h\nu_o/KT_e^0}]} \qquad (6-2.3)$$

where C_{21} is collisional de-excitation rate and A_{21} is spontaneous emission rate. $I(r, \mu,x)$ is the specific intensity of the ray making an angle $\theta = \cos^{-1} \mu$ with the radius vector r at a standardised frequency x given by

$$X = \frac{\nu - \nu_o}{\Delta} \tag{6 -2.4}$$

Δ being mean thermal Doppler width. $V(r)$ is the velocity of expansion of gases in Doppler units. Normalised line profile (Doppler) $\phi(x)$ is employed

$$\int_{-\infty}^{+\infty} \phi(x)dx = 1 \tag{6 -2.5}$$

For a two-level atom approximation the statistical equilibrium equation is given by

$$N_1 \left(B_{12} \int_{-\infty}^{+\infty} \phi(x)J_x dx + C_{12} \right) = N_2 \left\{ B_{21} \int_{-\infty}^{+\infty} \phi(x)J_x dx + C_{12} + A_{24} \right\} \tag{6 -2.6}$$

where B_{12} and B_{21} are Einstein coefficients and N_1 , N_2 are the population densities in levels 1 and 2 respectively.

The quantity $S_{dust}(r, \pm\mu, x)$ is the source function due to dust and is given by

$$S_{dust}(r, \pm\mu, x) - (1-\omega)B_{dust} + \frac{\omega}{2} \int_{-\infty}^{+\infty} P(\mu, \mu', r)I(r, \mu', x)d\mu' \tag{6 -2.7}$$

Where B_{dust} is the Planck function for the emission, ω is the albedo for single scattering and $P(\mu, \mu', r)$ is the phase function. Emission from dust is not having much influence on the profile shape hence is neglected. Equivalent width is calculated by using the formula

$$W = \int_{-\alpha}^{+\alpha} (1 - \frac{F_x}{F_c})dx \tag{6 -2.8}$$

Where α is half band width of the line i.e. $\alpha = \max |x|$, F_c is the flux in the immediate neighbourhood continuum of the line and F_x is the flux at point x.

Solution to equations (6-2.1 and 6-2.2) is obtained on the lines explained in detail in Chapter 5.

6.2.3 Results and Discussions

The equation of transfer is solved as described earlier. We have chosen trapezoidal points for frequency integration and Gauss-Legendre points for angle integration. We have employed nine frequency points with one point always at the line centre and two angles; i.e. $I = 9$ and $m = 2$ in each half space. This brings the working matrix of calculations (18x18). This is accurate enough to give precision permitted by the computer (Mighty Frame II located at the Indian Institute of Astrophysics, Bangalore). We have several physical situations to study, hence the number of parameters will be quite large and therefore we have to restrict to physically meaningful parameters. We have set the dust density constant throughout the medium.

Boundary Conditions: In the case of a purely scattering medium it is assumed that there is no radiation entering the shell from outside where the radius r = B and the optical depth at this point is 0 ($\tau = 0$) while radiation of unit intensity is incident at r = A and the optical depth

here is maximum i.e. τ_{max} = T.   Further when there is emission from within the medium radiation is assumed to be incident neither at A nor at B.   Boundary conditions imposed here are

$$U^-(\tau = T, \ \mu_j) = 1$$

$$(\epsilon = 0, \beta = 0) \qquad\qquad (6-2.9)$$

$$U^+(\tau = 0, \mu_j) = 0$$

and for internal emission

$$U^-(\tau = T, \mu_j) = 0$$

$$(\epsilon > 0, \beta > 0) \qquad\qquad (6-2.10)$$

$$U^+(\tau = 0, \mu_j) = 0$$

In the case of the boundary condition of the frequency derivative it is taken

$$\frac{\partial U^+}{\partial x} (\text{at } X = |X_{max}|) = 0 \qquad\qquad (6-2.11)$$

and the velocities at A and B are set as V_A and V_B respectively.   For the case of shell which is expanding with constant velocity we have

$$V_A = V_B \qquad\qquad (6-2.12)$$

for a static medium

$$V_A = V_B = 0 \qquad\qquad (6-2.13)$$

while for the expanding medium with velocity gradients we have taken

V_A = 0 and V_B > 0 (5,10,20,30,40 and 50 mtu)

Profiles are described in terms of the integrated fluxes over the whole disc versus the normalised frequency. We have varied the parameters in the following way and the corresponding results have been presented graphically.

$\frac{B}{A}$ = Ratio of the outer to inner radii of the spherical shell.

ε is the probability per scattering that a photon is thermalised by collisional de-excitation.

β is the ratio of the absorption coefficient per unit frequency interval in the continuum to that at the line centre.

V_A = Velocity in Doppler units at the point r = A.

V_B = Velocity of the expanding spherical medium at a point with radius r = B.

V = Velocity of expansion of the shell.

τ_d = Total dust optical depth.

T = Total gas optical depth at the line centre.

The spherical shell has been divided into 100 subshells. Optical depth of each shell and the total optical depth upto any internal point as well as the emergent and the internal radiation fields are calculated by using the algorithm suggested by Peraiah (1984). We have chosen the ratio B/A to be 20 and is kept constant for all cases stu-

ied.. Total gas optical depth at the line centre has worked out to be 300 in all the calculations.

Figures 6.2.1 to 6.2.4 show the line profiles plotted with respect to the normalised frequency x in a static medium (V_A = V_B = 0). Dust optical depths 0,0.5,2 and 5 are considered. It is observed that the emission in the wings falls rapidly for increased dust optical depth. For dust optical depth τ_d = 5 there is hardly any emission and the absorption core is reduced to almost half of that when there was no dust and the absorption core is very wide extending upto 3 Doppler units on either side of the line center. Substantial emission is observed in the wings when there is no dust. This shows that dust scatters photons mostly into the cores of the absorption lines and removes them from the wings.

In Figures 6.2.5 to 6.2.8 expansion velocity 5 mtu is given with velocity gradients. Lines have become asymmetric. Here also we observe the wing emission eroding rapidly with the presence of dust in the atmospheres. For dust optical depth 5 the emission in the wings is almost nil and the absorption core becomes too narrow indicating that the photons have been removed due to scattering by dust and they have been added to the cores. These lines are for a medium in which the radiation is scattered by dust and gas without any emission.

For Figures 6.2.9 to 6.2.12 thermal emission is included by setting ε = 10^{-4} in the static medium. These curves show us how the dust scatters radiation when we

have thermalisation of photons. Substantial amount of emission is seen on either side of the absorption core at the centre. Though the presence of dust reduces the emission in the wings gradually and vanishes completely for τ_d = 5, the absorption core width is observed to be unaffected. In Figures 6.2.13 to 6.2.16. we have considered expansion velocity with velocity gradient. This brings in a sudden asymmetry in the lines. In case of dust free medium we see two peaks of unequal hights, the larger among them is observed on the lower frequency side of the centre. P-Cygni type profiles develop when τ_d = 0.5 with substantial reduction in emission. Absorption core developed is obser-ved to be shifted towards violet side while emission peak remains on the red side of the line centre. On increasing the dust furthr (τ_d= 2) emission is found to reduce further while absorption core persists. For dust optical depth 5 the absorption core deepens to such an extent that it becomes almost dark with hardly any emission in the wings.

In Figures 6.2.17 to 6.2.20 the velocity of expan-sion has been increased to 10 mtu. We observe the same effect as observed for lower velocity of expansion 5 mtu with a diference of lowering of absorption depth compariti-vely.

In figures 6.2.21 to 6.2.24 we have plotted the profiles for an expanding spherical shell with constant velocity without velocity gradients i.e.$V_A = V_B$ = 5 mtu.

As observed in the previous case we see two peaks of emission. The peak on the red side is larger is comparision with that on violet side but it is flat-topped. When dust is introduced τ_d = 0.05 emission reduced to 1/3 the previous retaining its flat-top. Further increase in dust causes disappearance of emission peak and deepening of absorption core.

Increasing the velocity of expansion to 10 mtu is showing almost the same behaviourwhich has been shown in Figure 6.2.25 to 6.2.28.

Figures 6.2.29 to 6.2.44 are drawn for the profiles formed in a medium which has continuum emission together with the line emission. These have similar features as seen in the earlier figures 6.2.9 to 6.2.28.

In Figures 6.2.45 and 6.2.46 we have plotted the equivalent widths of different lines against different dust optical depths. While Figure 6.2.45 shows the equivalent widths corresponding to the lines formed in a medium without velocity gradients those in Figures 6.2.46 are for a medium expanding with velocity gradients. In both these cases we have considered scattering of radiation by both dust and gas. We have observed quite a noticeable difference in the equivalent widths of the lines formed in a medium without velocity gradients as compared to those formed in a medium with velocity gradients. In 6.2.45 we see that the equivalent width increases with the increase in dust optical depth while in Figure 6.2.46

it is the reverse i.e. the equivalent width is reduced with increasing optical depth when velocity gradients are considered.

Figure 6.2.47 is to show how the ratio of the heights of two emission peaks varies with expansion velocities. We have studied this behaviour for different dust optical depths. In Figures 6.2.48 and 6.2.49 we have shown how this behaviour changes with the constant velocity of expansion of the spherical shell ($V_A = V_B$) we observe that this ratio gets reduced as the dust optical depth is increased.

In Figure 6.2.50 we have shown the relation between the velocity of expansion and equivalent widths of lines for expanding atmospehres with velocity gradients. We have compared dust optical depth $\tau_d = 2$ with that of dust free atmosphere. It may be noticed that the equivalent width increases steadily with the velocity of expansion.

In Figure 6.2.51 we have considered the same relation for a medium moving without velocity grdients ($V_A = V_B$). In this case we see that the equivalent width is decreasing with velocity of expansion upto 15 mtu and thereafter it increses linearly with velocity.

Figure 6.2.52 is similar to those of 6.2.50 with a difference that there exists a thermal emission in the line ($\epsilon = 10^{-4}$). Here we notice that all the lines are in emission and the emission reduces as the amount of

dust is increased. Figure 6.2.53 shows the relation between equivalent width and expansion velocities of the expanding medium without velocity gradients. We observe similar behaviour of the plots.

Figures 6.2.54 and 6.2.55 are to show the reltion between velocities of expansion and equivalent widths of the lines formed in medium expanding with and without velocity gradients respectively. In this case there is emission both in the line and also in the continuum. There is similarity in behaviour between this and for the medium in which emission was considered only in the line and not in the continuum. We observe that the widths of the lines are different in the two cases.
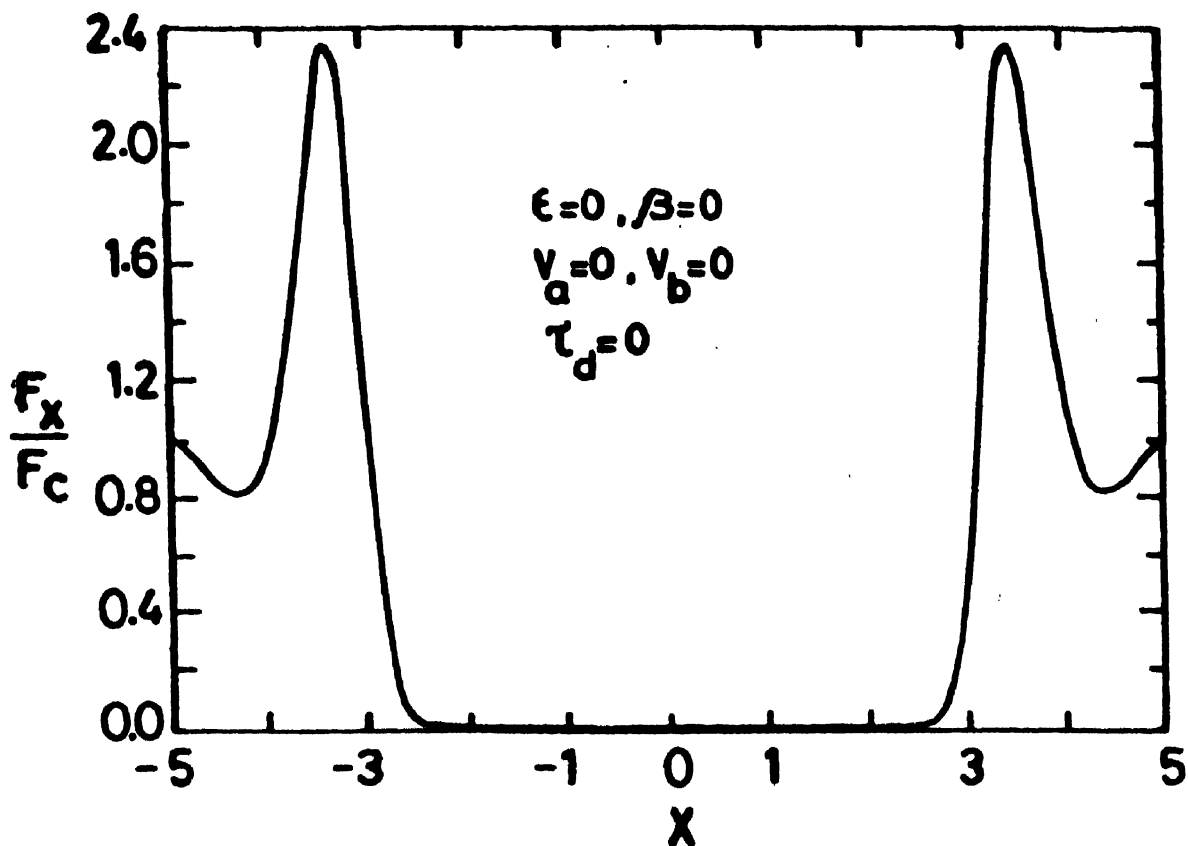
Figure 6.2.1   Line profiles formed in a static medium without
                dust ($\tau_d=0$).
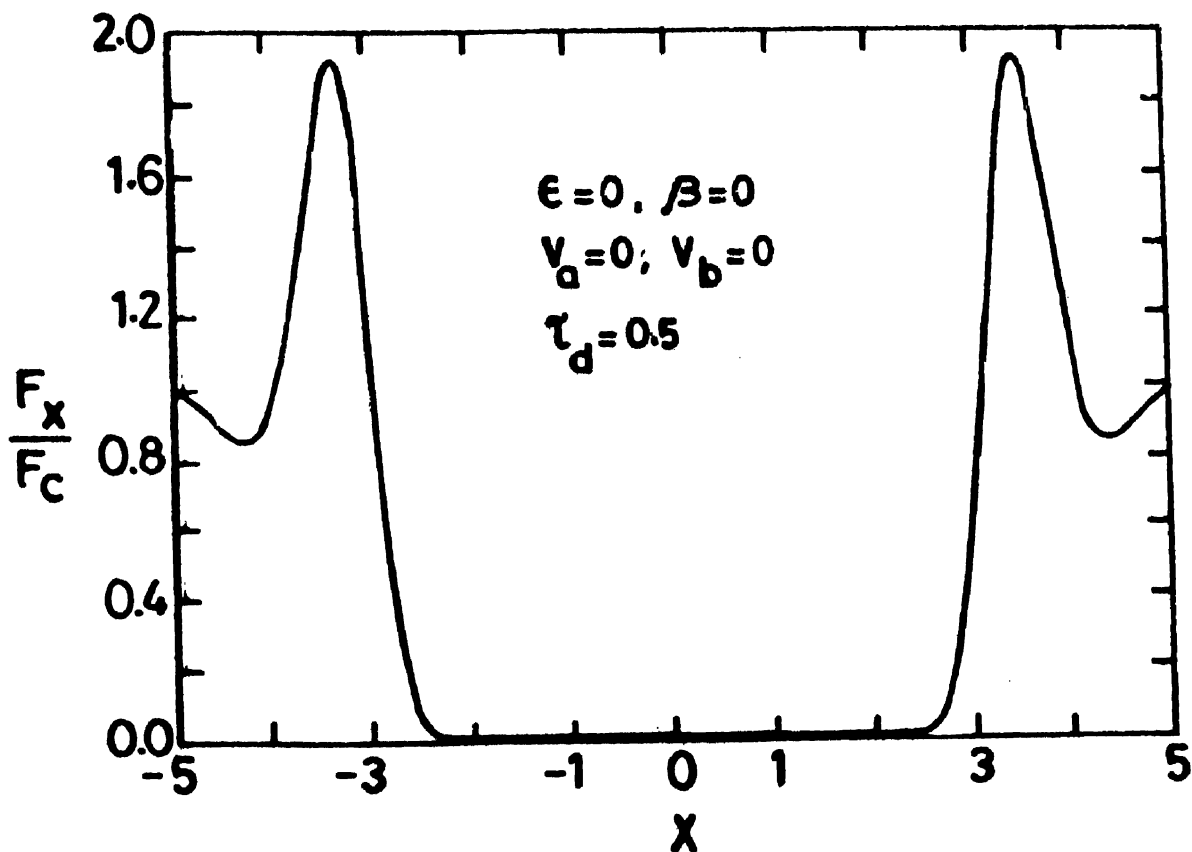
Figure 6.2.2   Same as in Figure 6.2. 1 for $\tau_d=$ 0.5 dust
                being distributed uniformly.
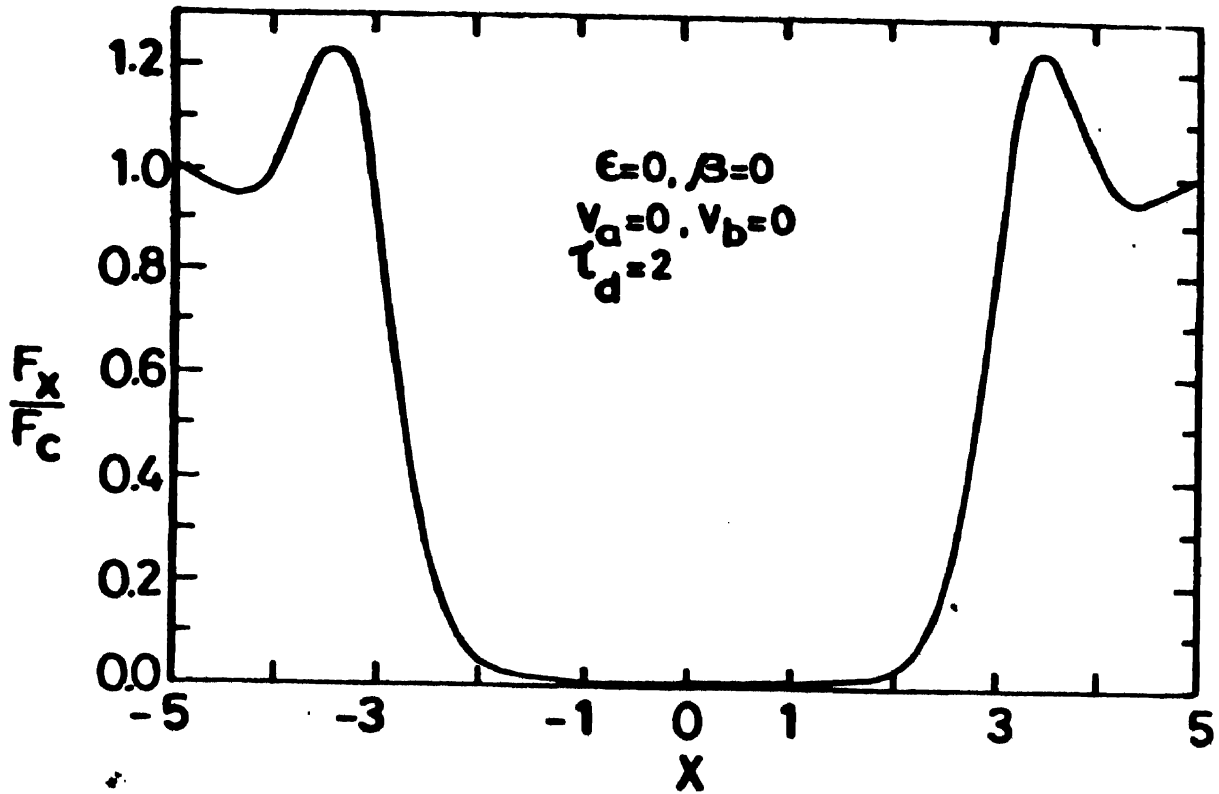
Figure 6.2.3   Same as in Figure 6.2.2 with dust optical depth, $\tau_d = 2$.
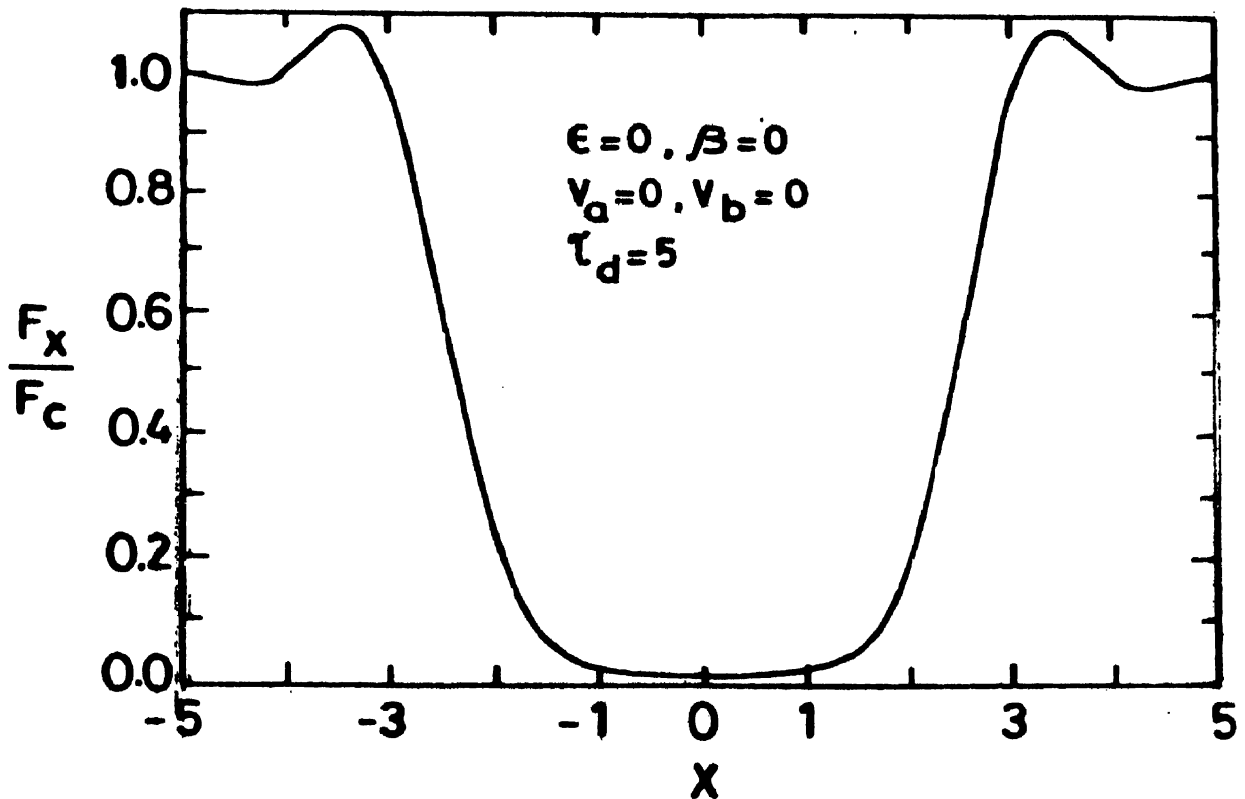
Figure 6.2.4   Same as in Figure 6.2.2 with dust optical depth $\tau_d = 5$.
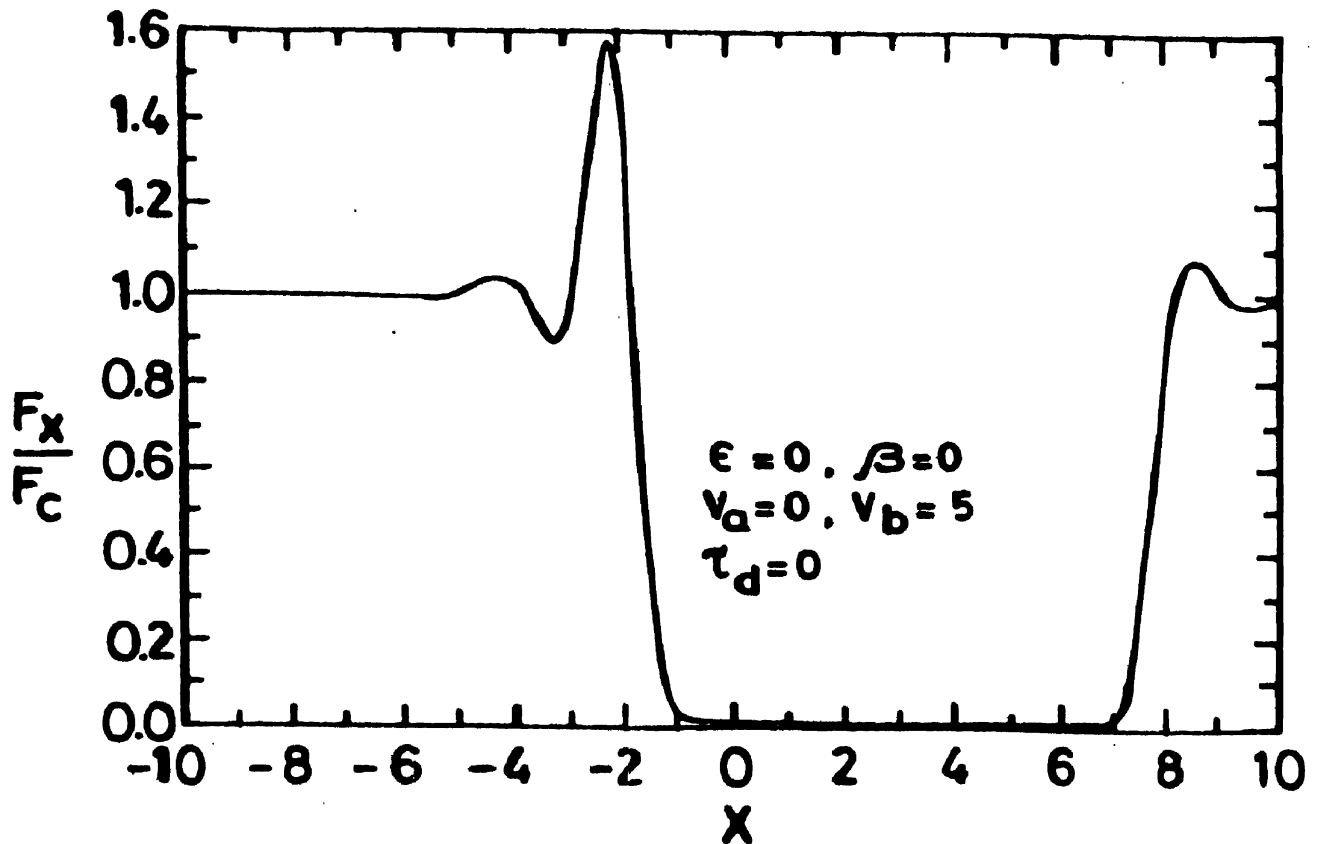
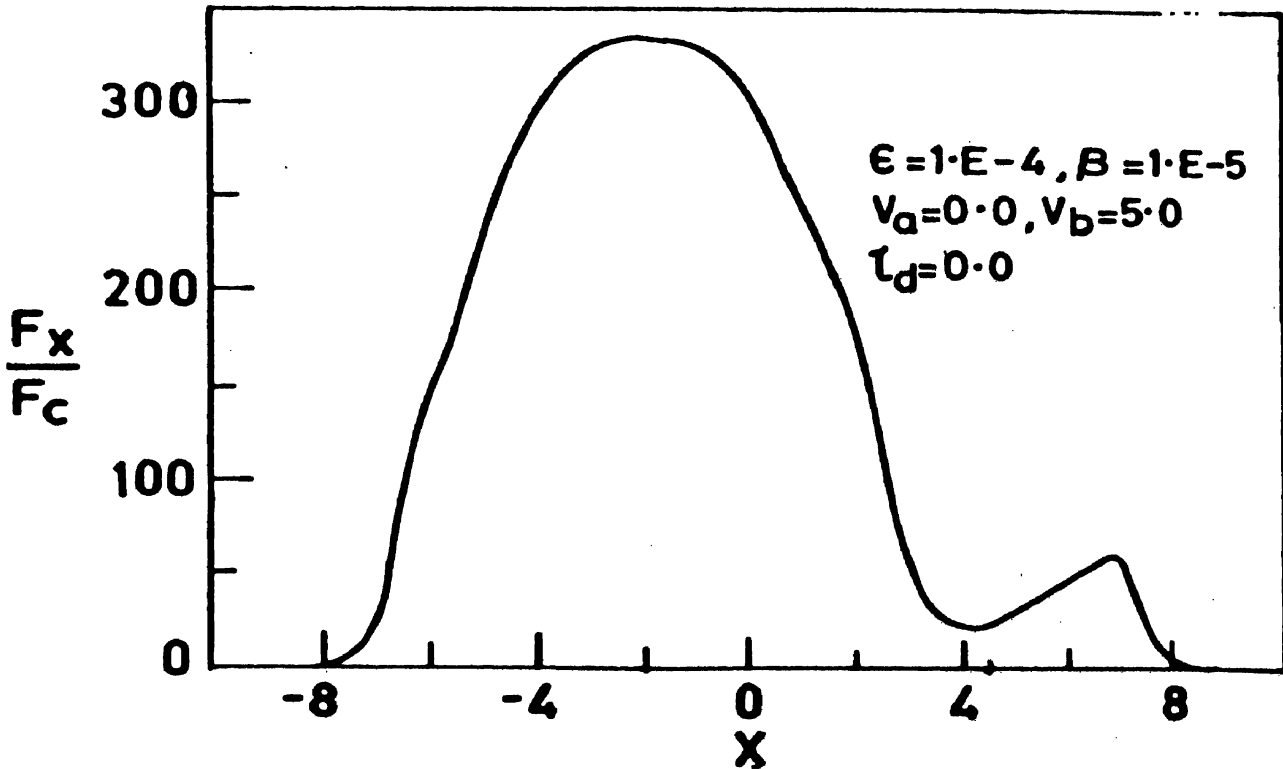Figure 6.2.5   Line profiles formed in an expanding medium with velocity gradients and velocity of expansion V_b=5 mtu and with no dust.
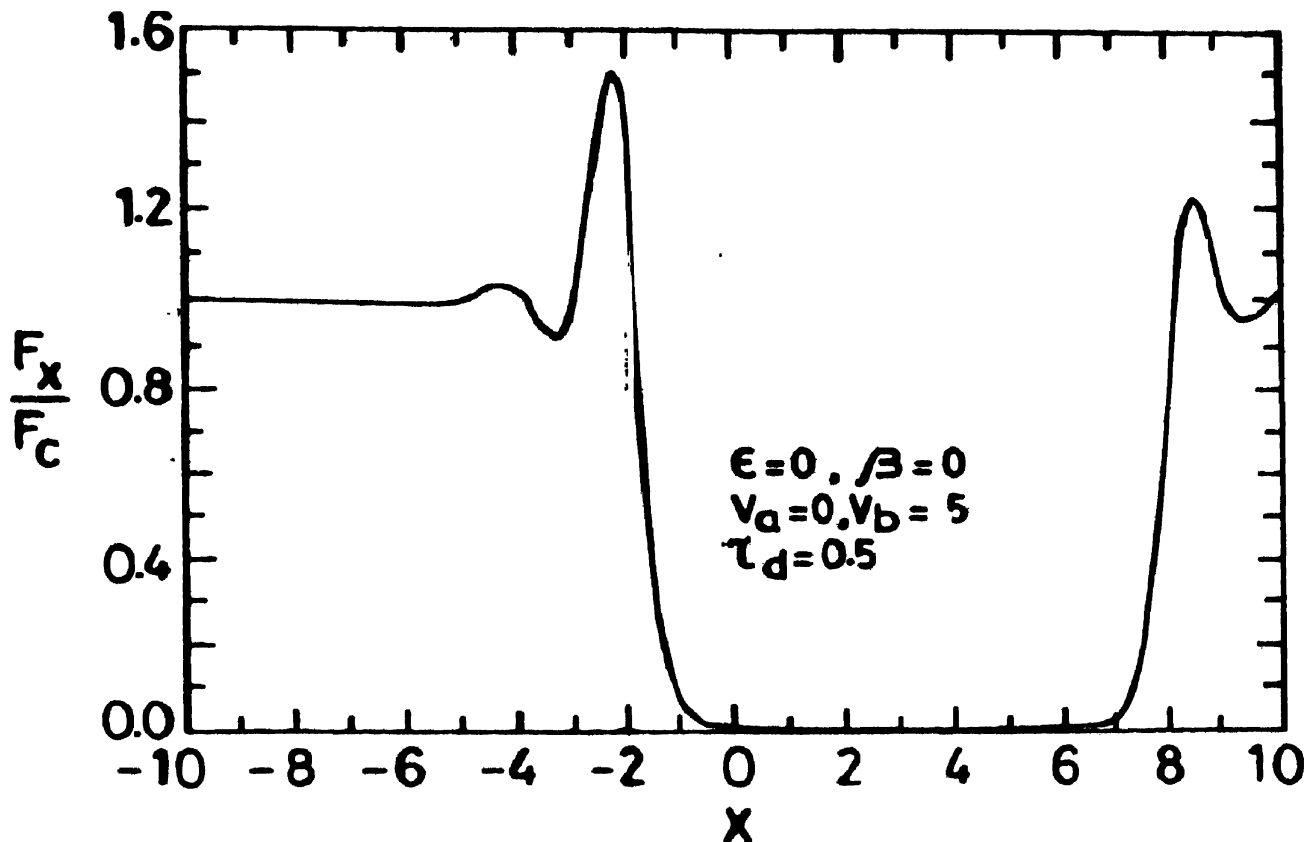
Figure 6.2.6   Same as in Figure 6.2.5 with dust distributed uniformly having τ_d= 0.5.
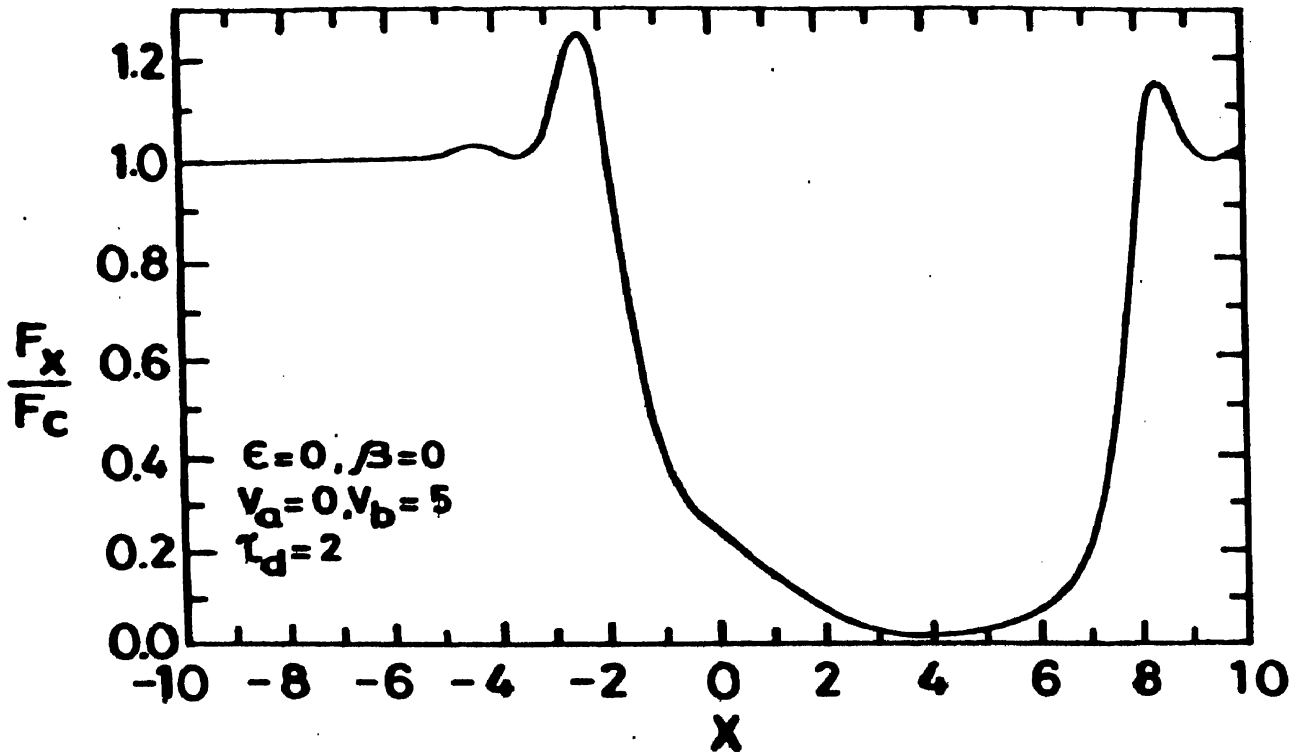
Figure 6.2.7　Same as in Figure 6.2. 5 with dust distributed uniformly having $\tau_d = 2$.
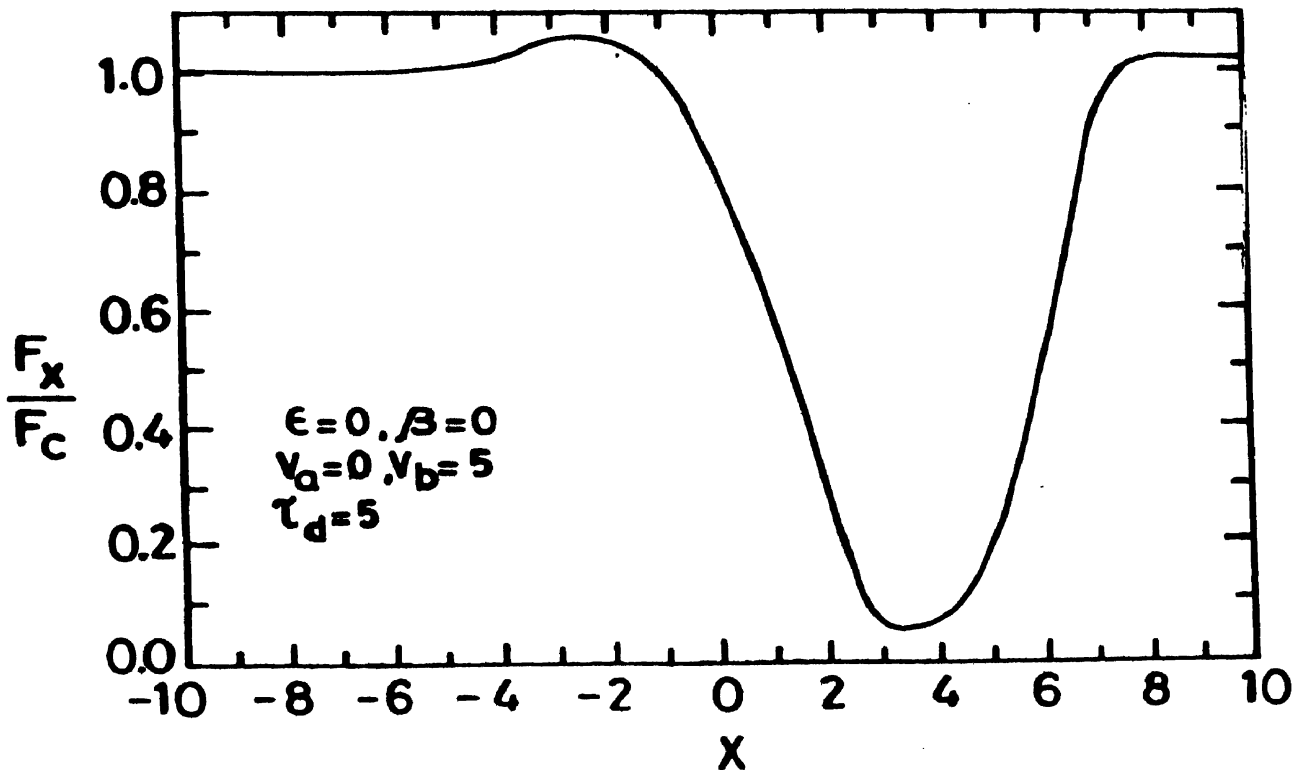
Figure 6.2.8　Same as in Figure 6.2. 5 with dust distributed uniformly having $\tau_d = 5$
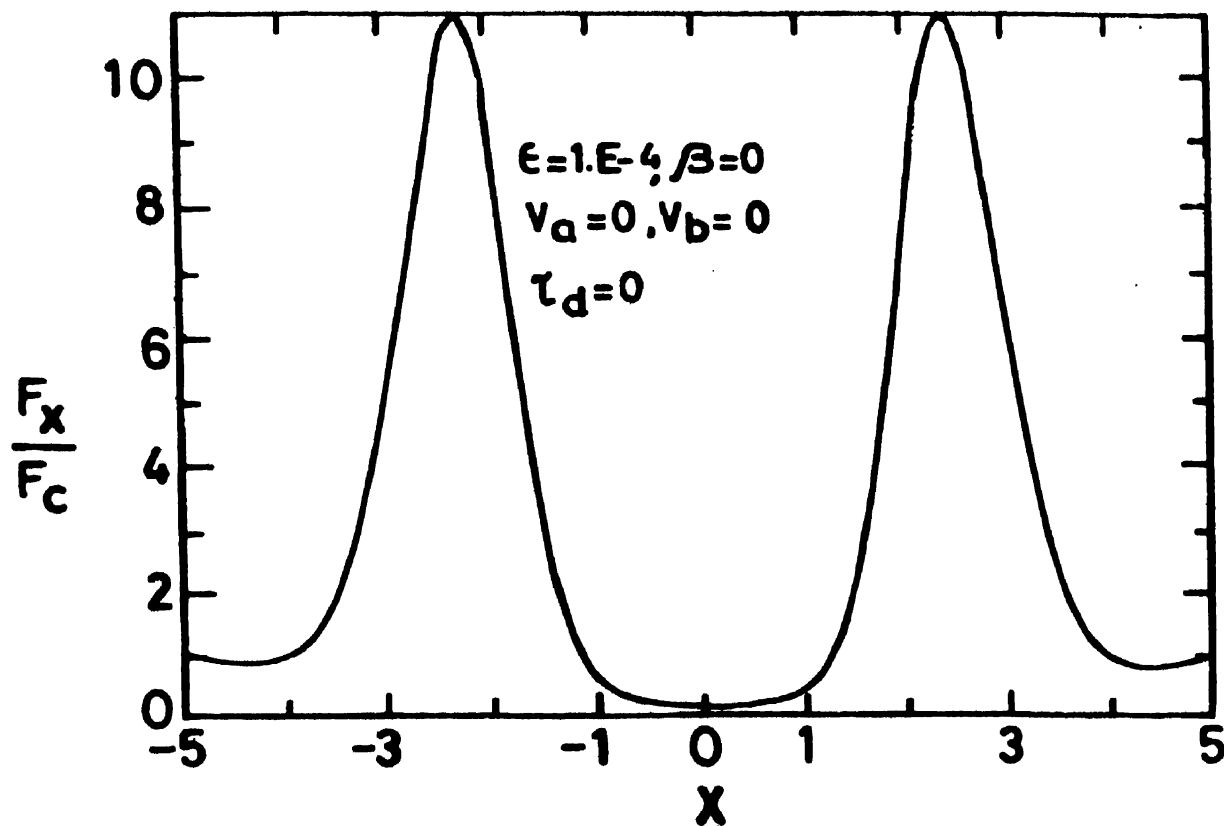
Figure 6.2.9   Line profiles formed in a static medium in which there is line emission and no dust included.
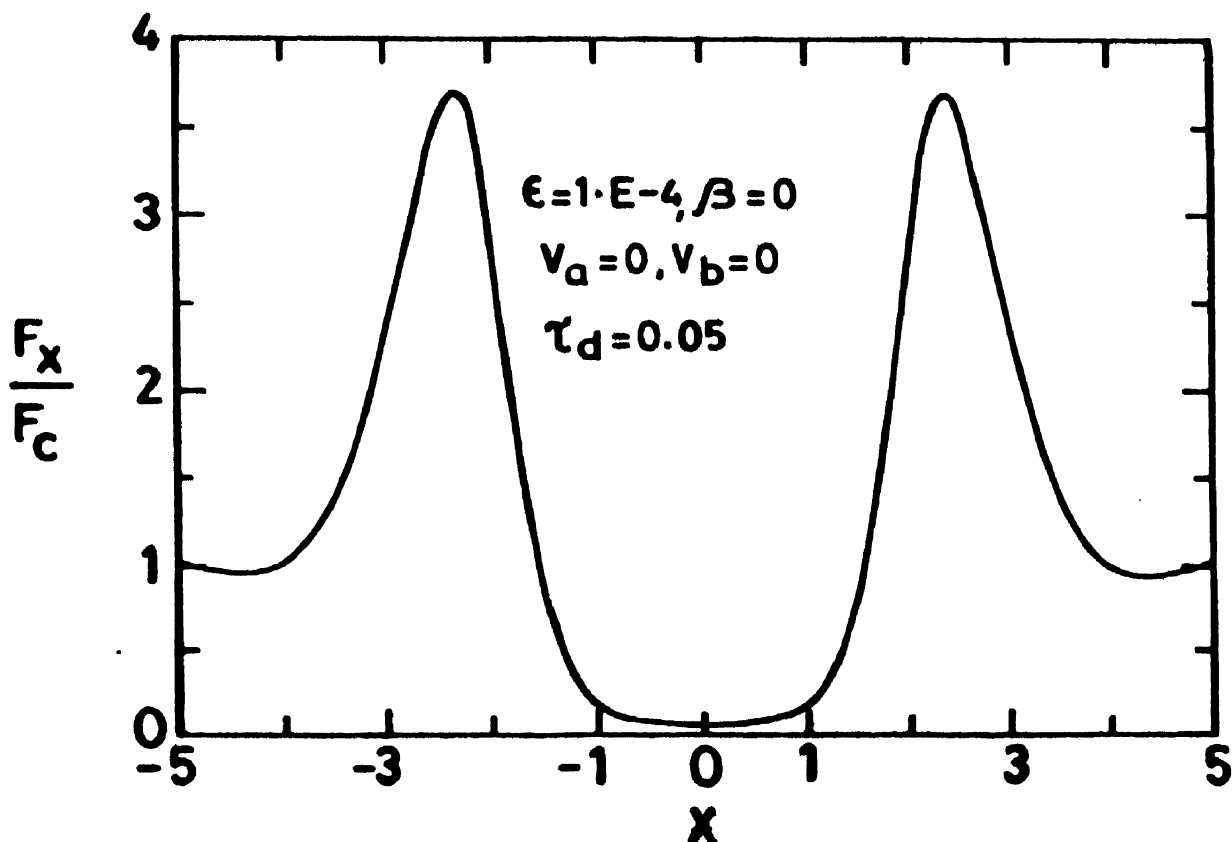
Figure 6.2.10   Same as in Figure 6.2.9 with uniform dust distribution giving a total $\tau_d = 0.05$.

$\epsilon = 1.E-4, \beta = 0$
$V_a = 0, V_b = 0$
$\tau_d = 0.5$
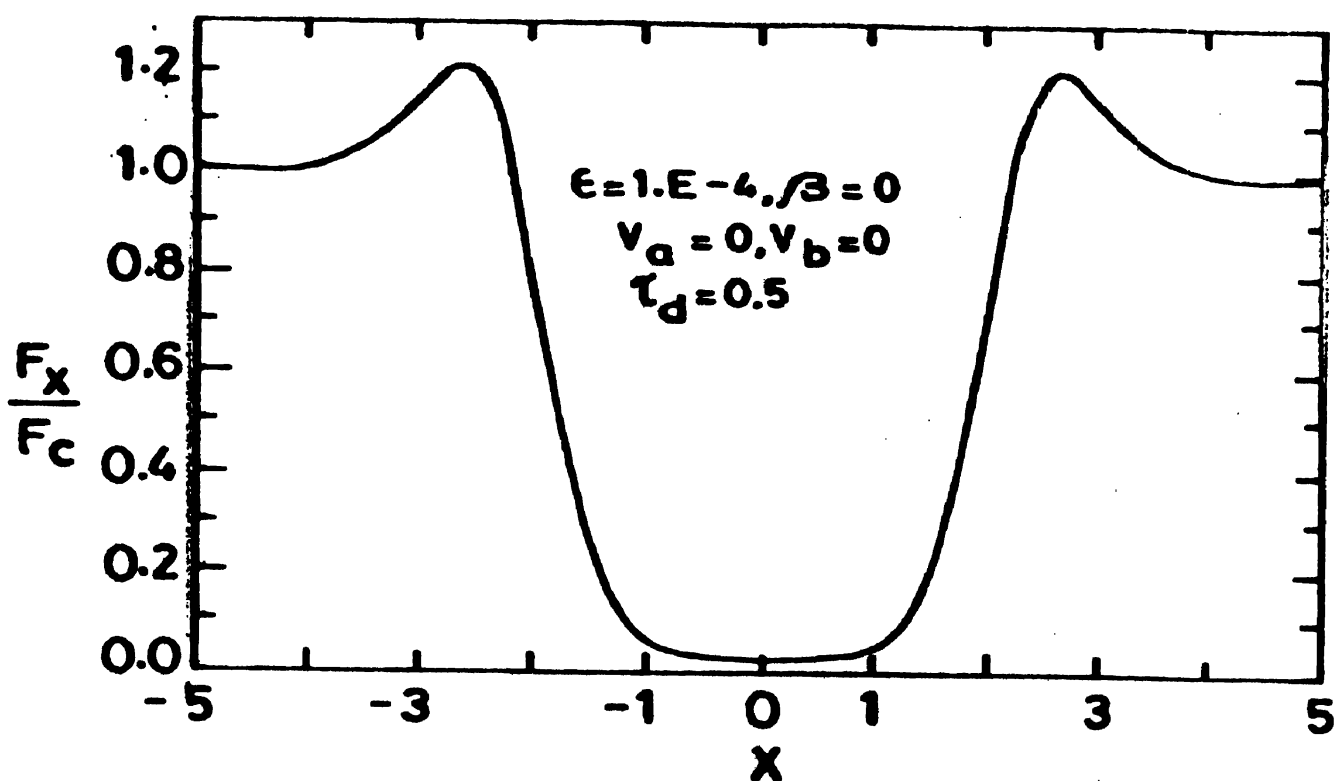
Figure 6.2.11   Same as in Figure 6.2.9 with $\tau_d = 0.5$.

$\epsilon = 1.E-4, \beta = 0$
$V_a = 0, V_b = 0$
$\tau_d = 5$
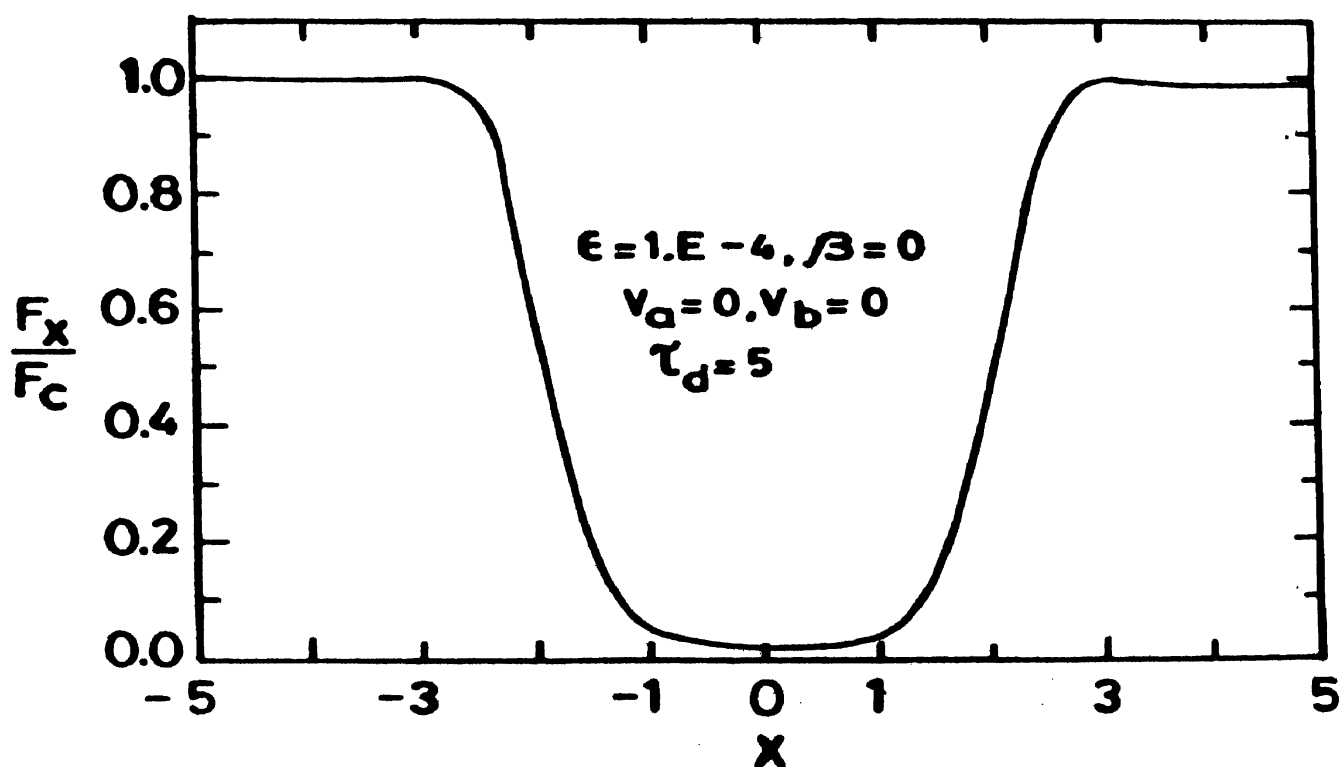
Figure 6.2.12   Same as in Figure 6.2.9 with $\tau_d = 5.0$.
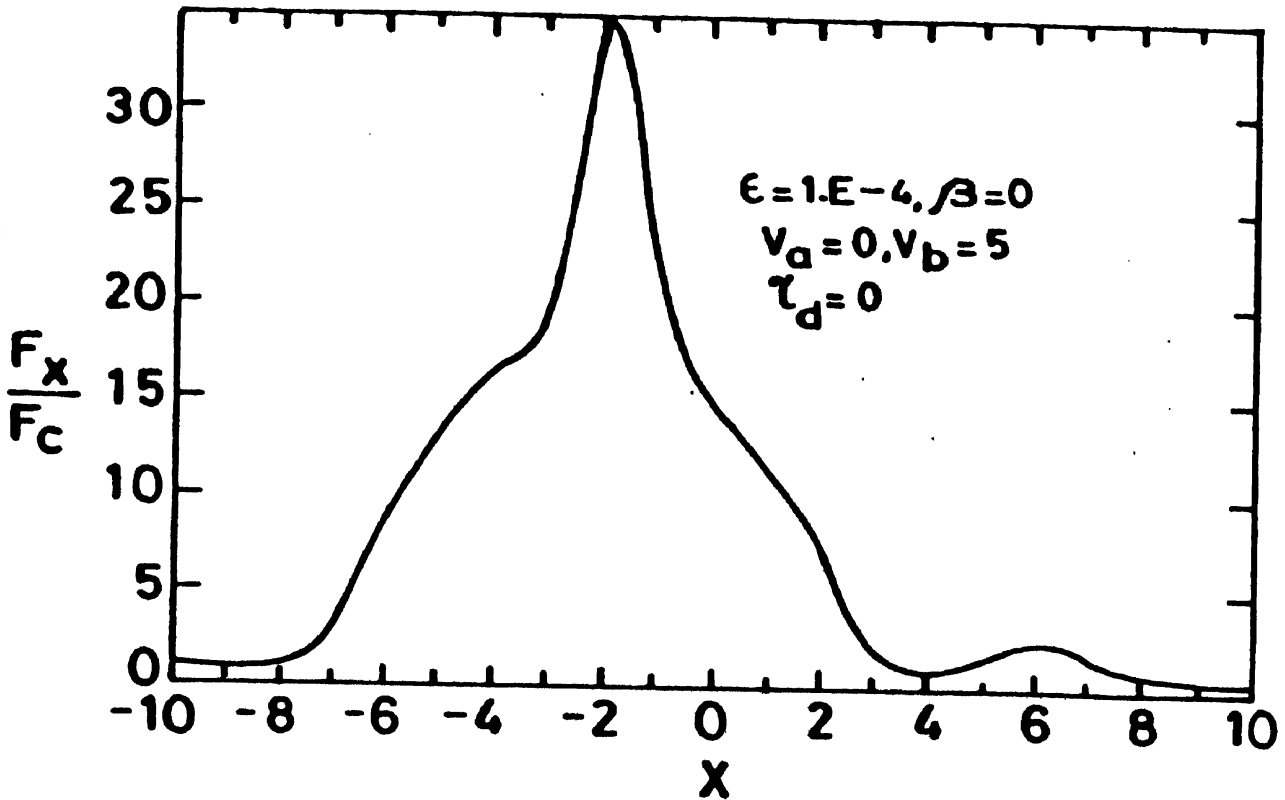
Figure 6.2.13   Line profiles formed in an expanding medium with
velocity gradients and velocity of expansion V_b= 5
τ_d= 0.
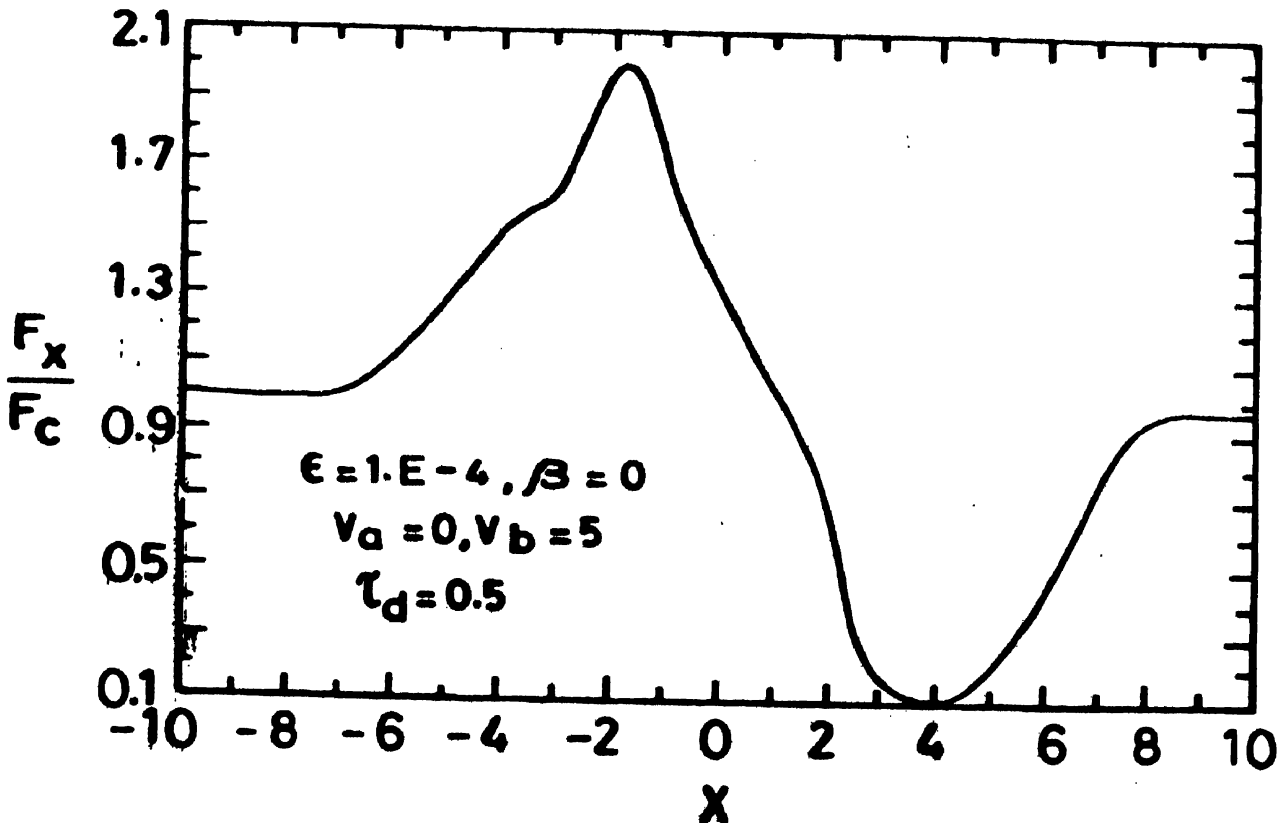
Figure 6.2.14   Line profiles formed in an expanding medium with
velocity gradients and velocity of expansion V_b= 5
τ_d= 0.5.
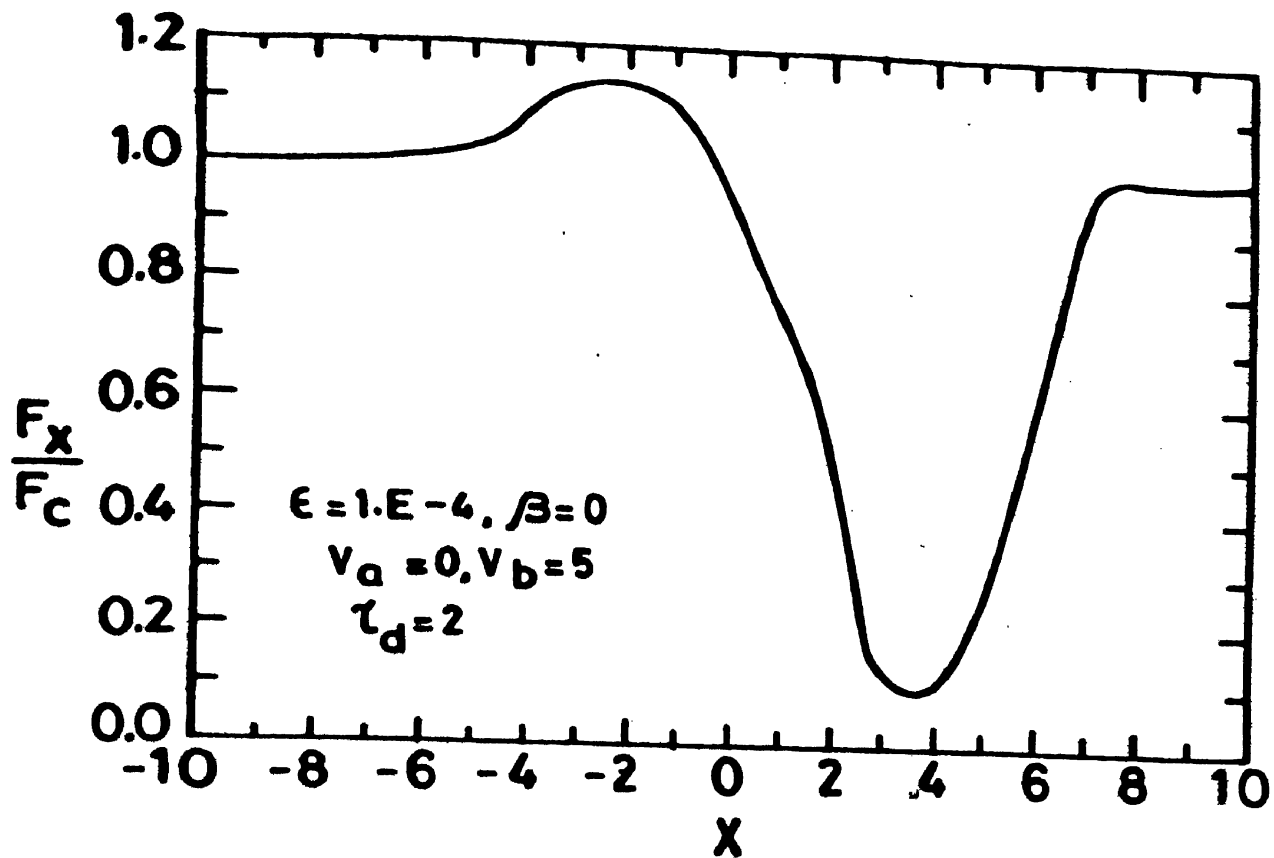
Figure 6.2.15   Line profiles formed in an expanding medium with velocity of expansion V_b= 5 mtu, τ_d= 2.0.

In the graph above:
- Y-axis: $\frac{F_x}{F_c}$ from 0.0 to 1.2
- X-axis: X from -10 to 10
- Text in plot: $\epsilon = 1.E-4, \beta=0$; $V_a = 0, V_b = 5$; $\tau_d = 2$
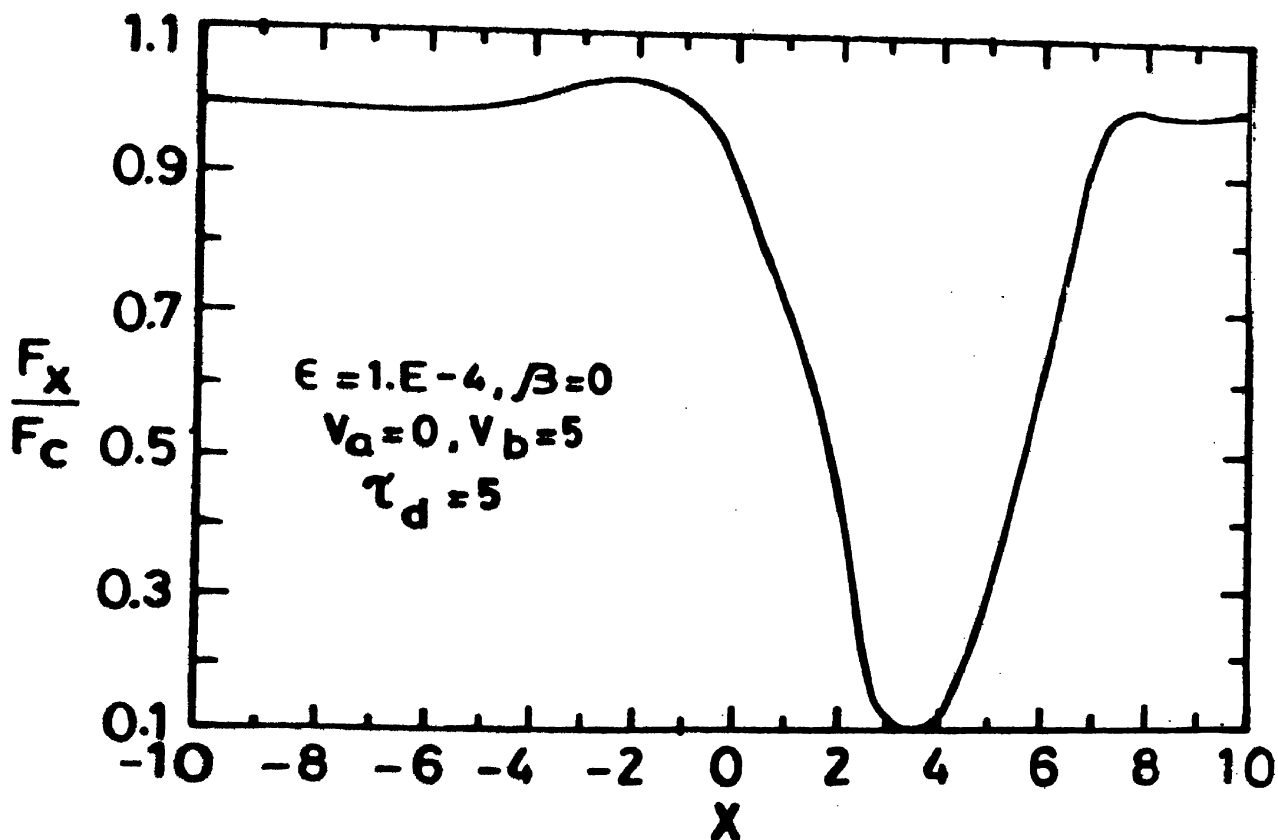
Figure 6.2.16   Line profiles formed in an expanding medium with velocity of expansion V_b= 5 mtu, τ_d= 5.0.

In the graph above:
- Y-axis: $\frac{F_x}{F_c}$ from 0.1 to 1.1
- X-axis: X from -10 to 10
- Text in plot: $\epsilon = 1.E-4, \beta=0$; $V_a = 0, V_b = 5$; $\tau_d = 5$
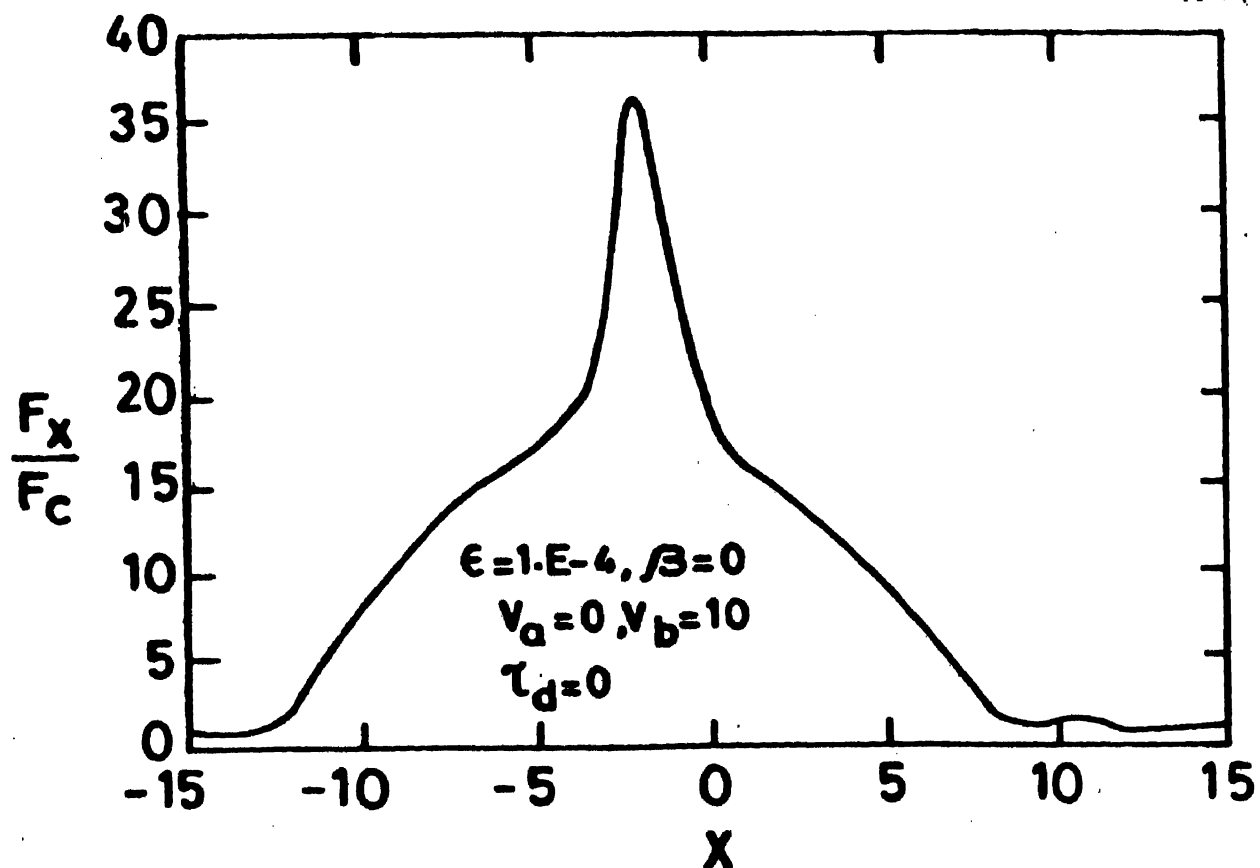
Figure 6.2.17   Same as in Figure 6.2.13 but velocity of expansion
is equal to 10 mtu.
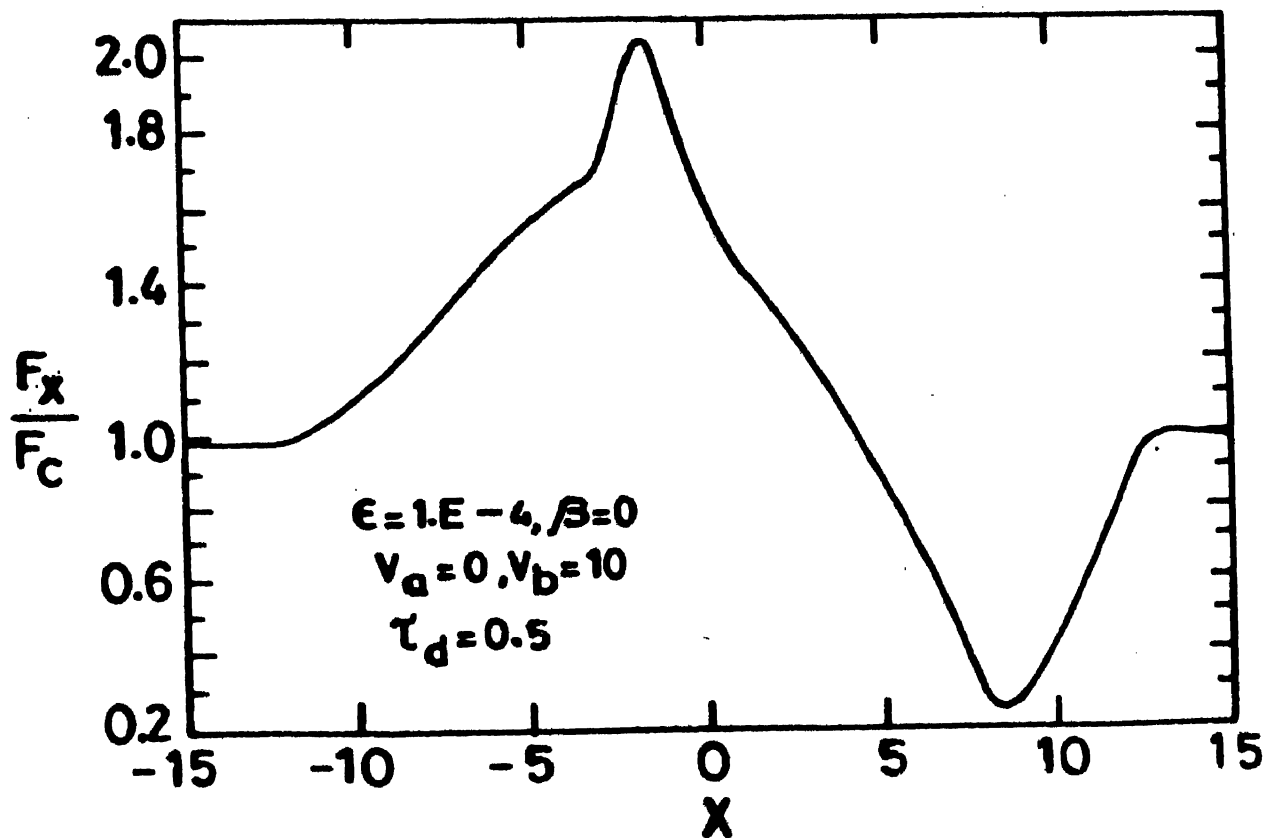
Figure 6.2.18   Same as in Figure 6.2.14 with velocity of
expansion V_b= 10 mtu.
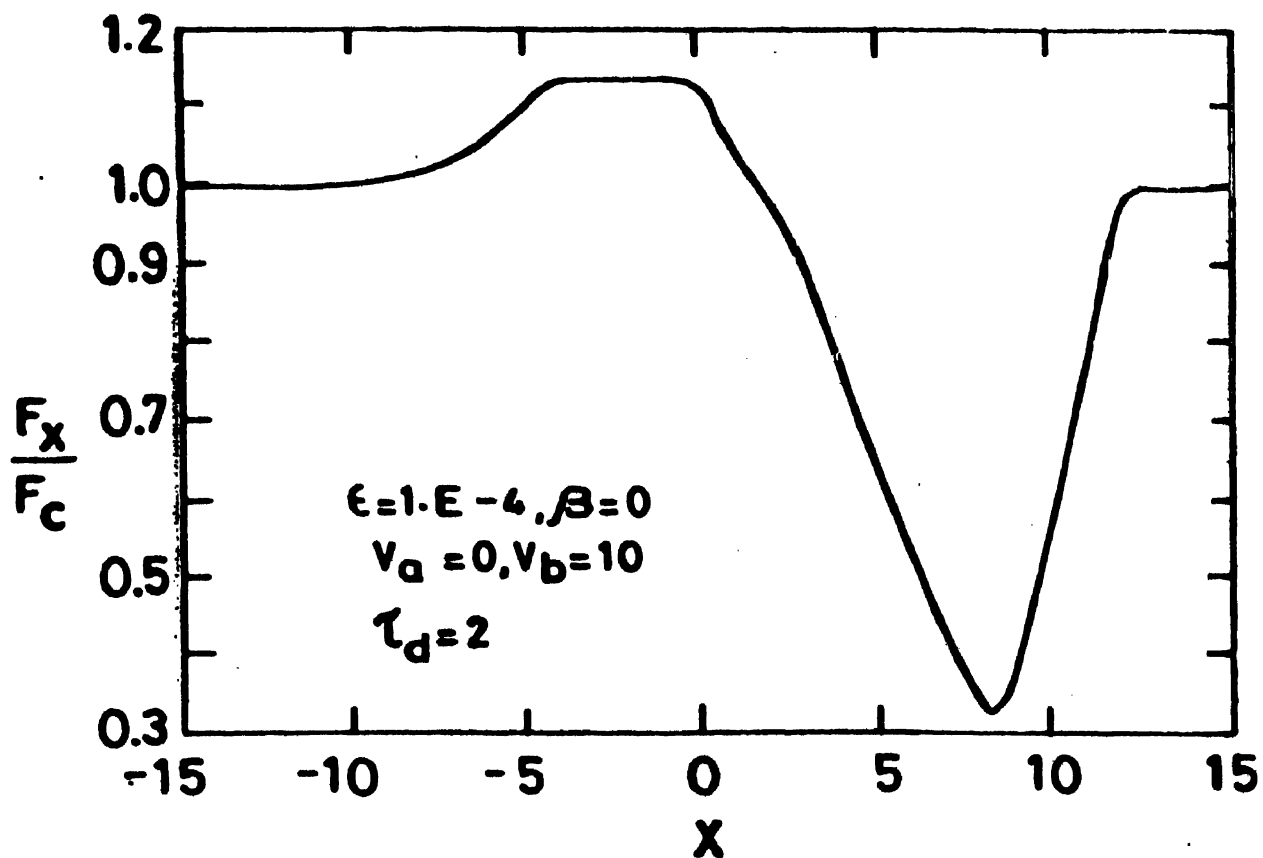
Figure 6.2.19   Same as in Figure 6.2.15 with velocity of expansion V_b= 10 mtu.
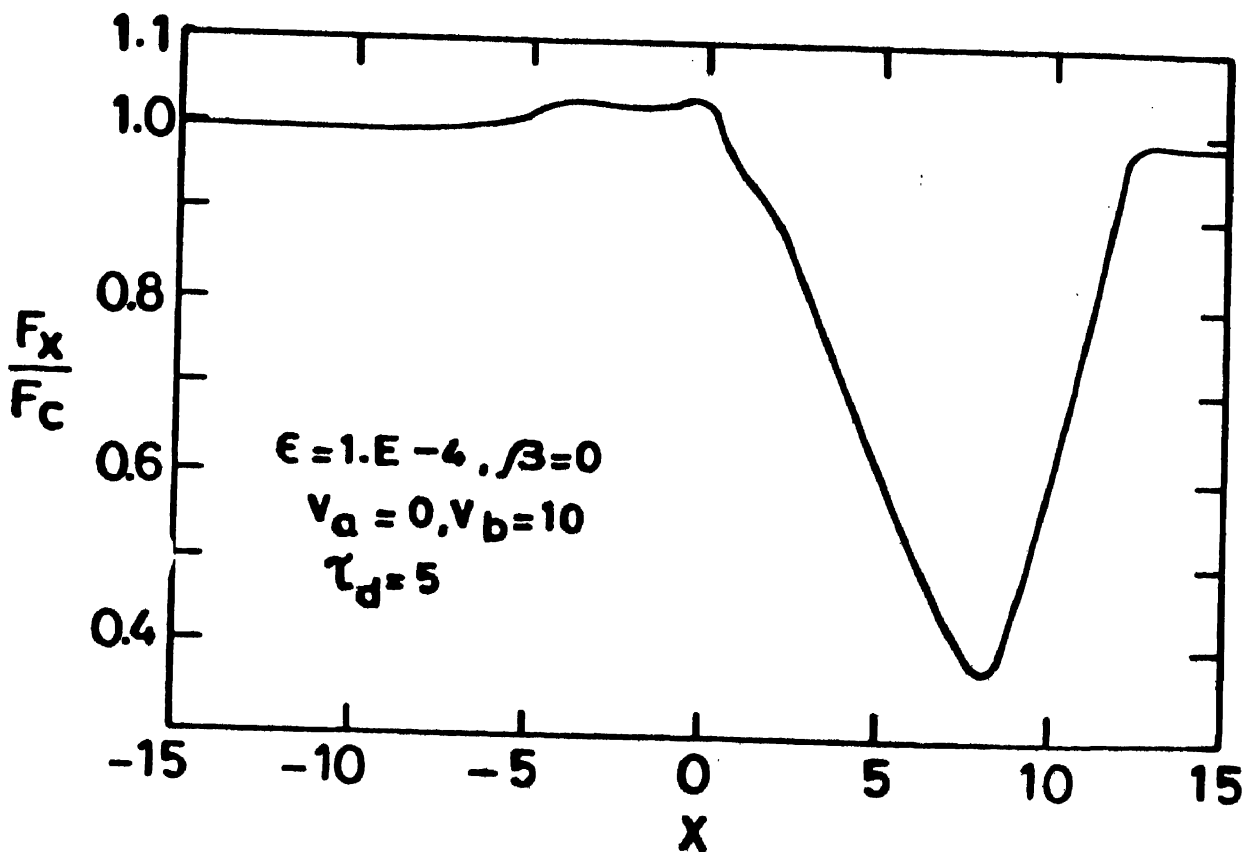
Figure 6.2.20   Same as in Figure 6.2.16 with velocity of expansion V_b= 10 mtu.
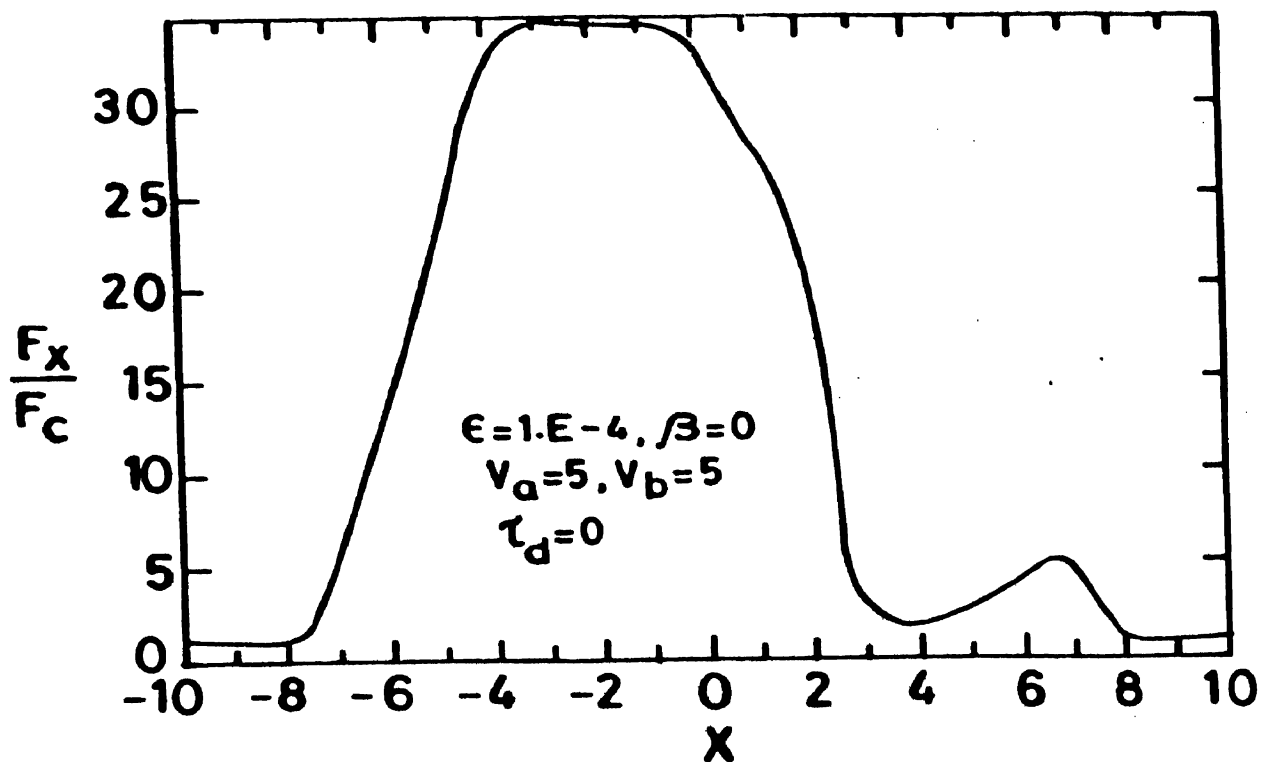
Figure 6.2.21   Line profiles formed in an expanding medium with o ut velocity gradients and velocity of expansion v_b= 5 mtu, medium containing no dust (τ_d= 0).
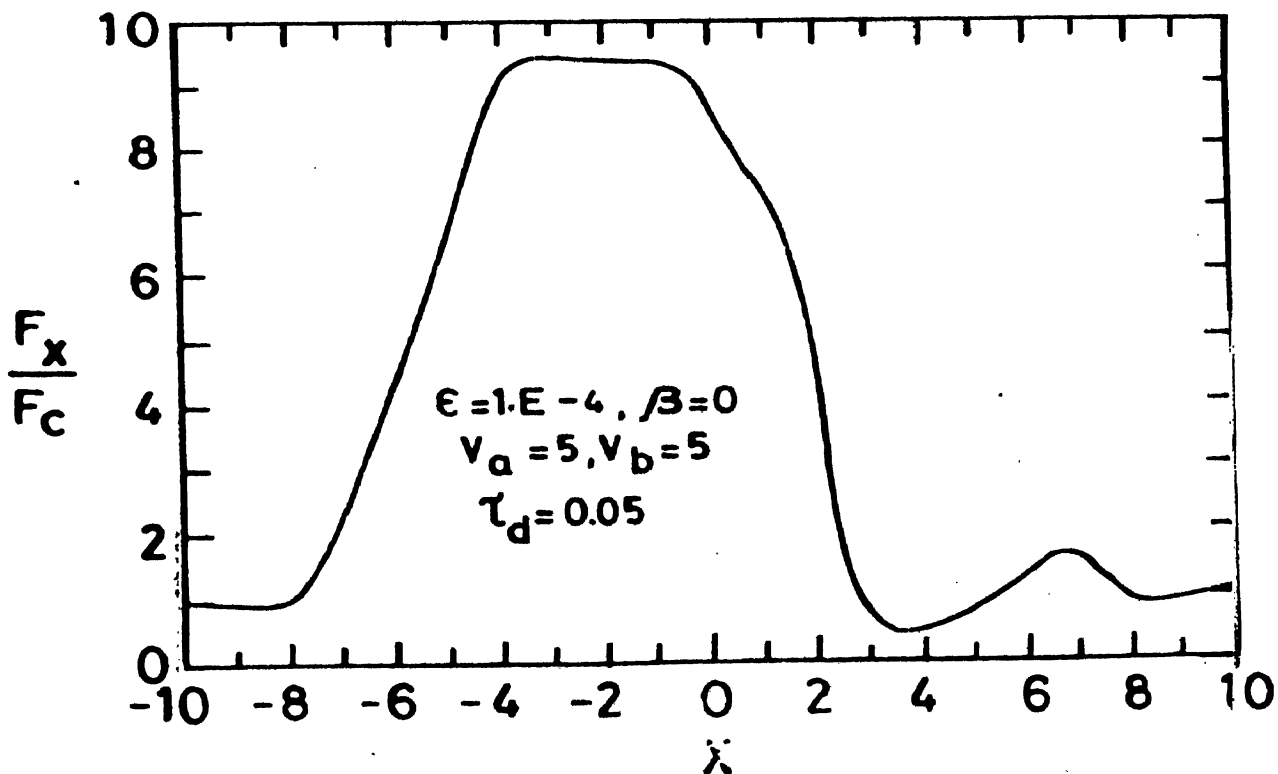
Figure 6.2.22   Same as in Figure 6.2.21 but dust content is given as optical depth τ_d 0.05.
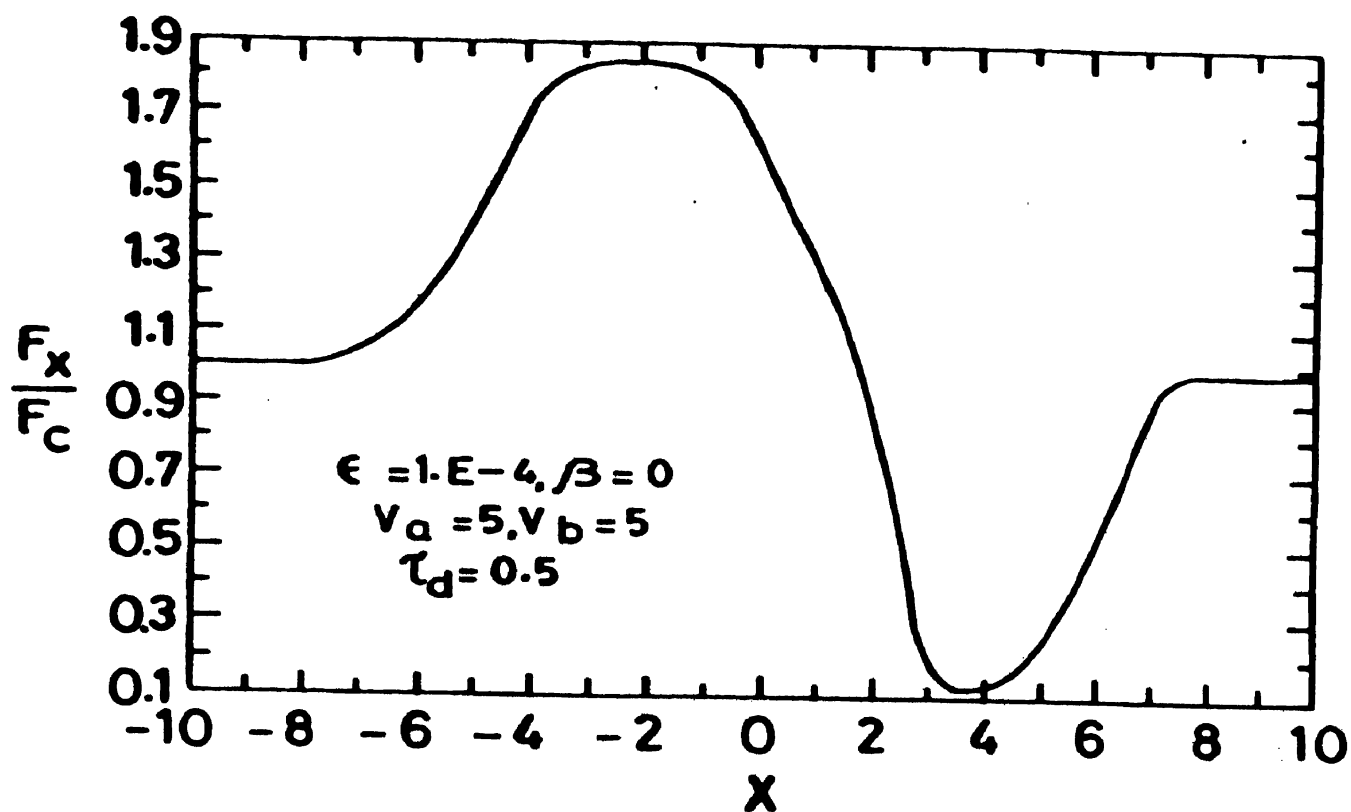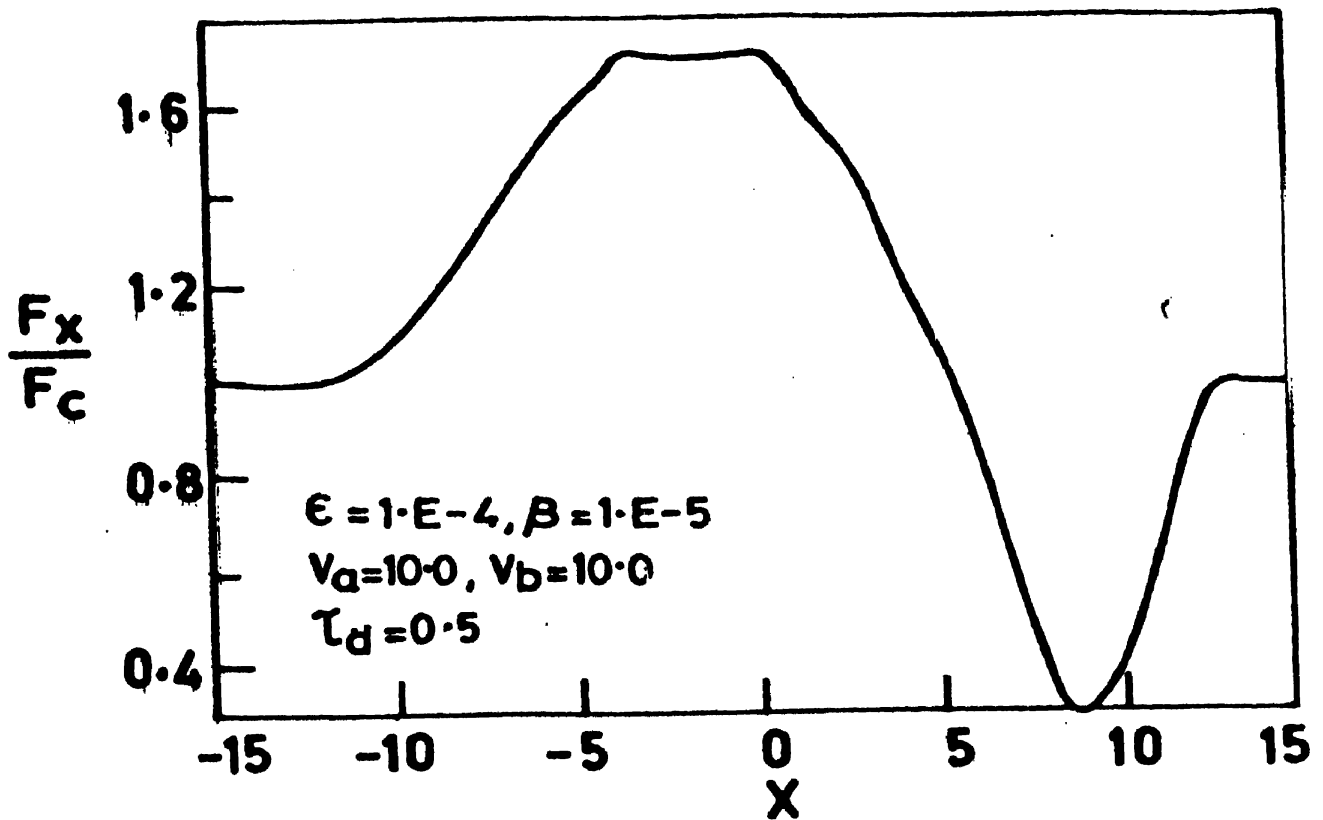
Figure 6.2.23   Same as in Figure 6.2.21 but $\tau_d = 0.5$.
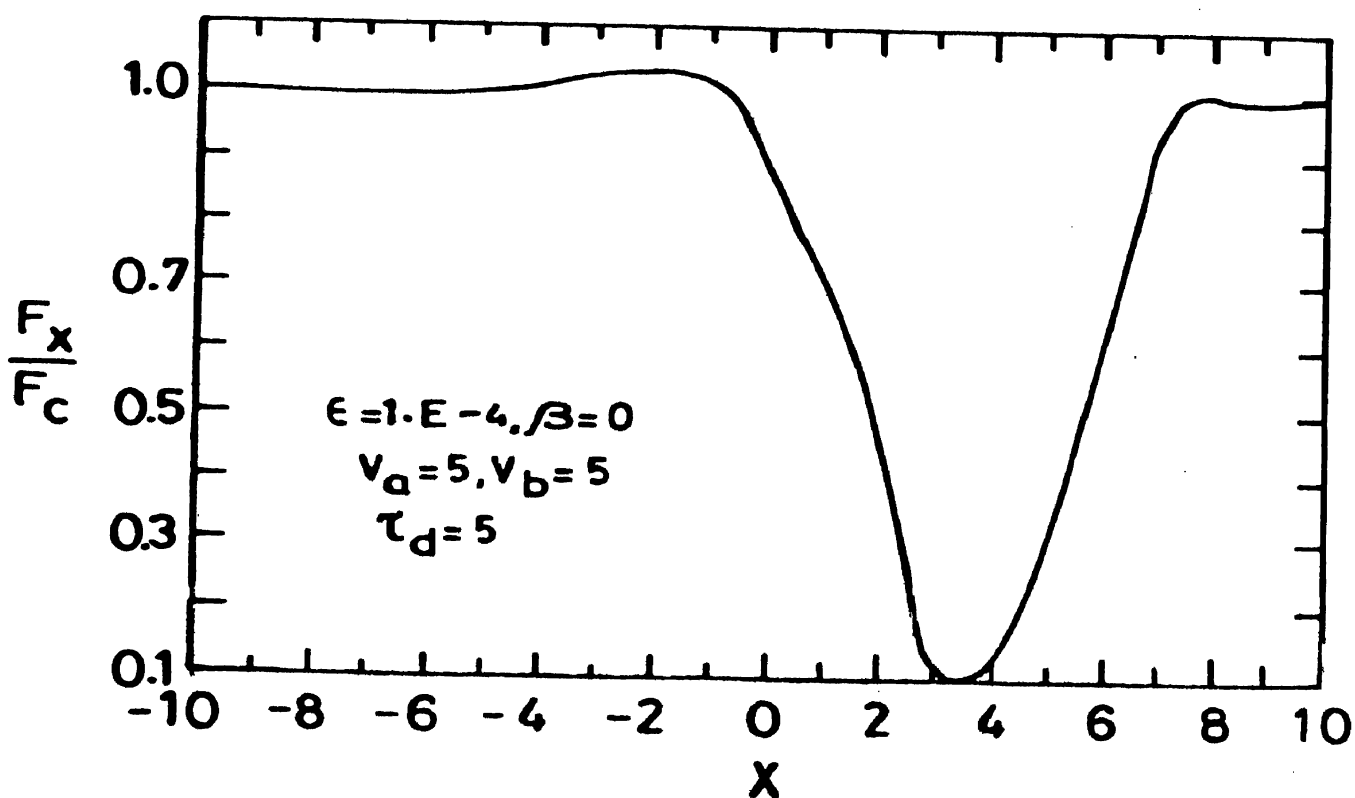
Figure 6.2.24   Same as in Figure 6.2.21 but $\tau_d = 5.0$.
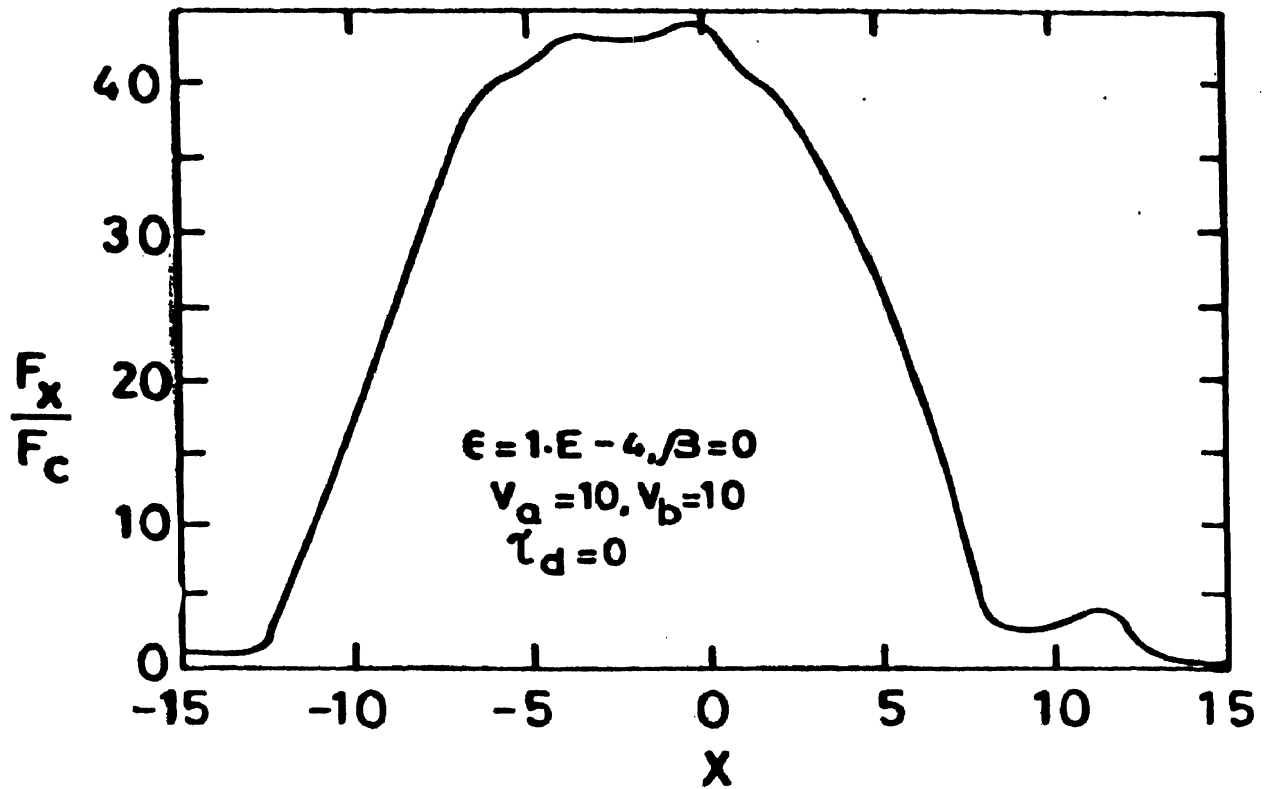
Figure 6.2.25   Same as those in Figure 6.2.21 with velocity of expansion V_b= 10 mtu without dust contents.
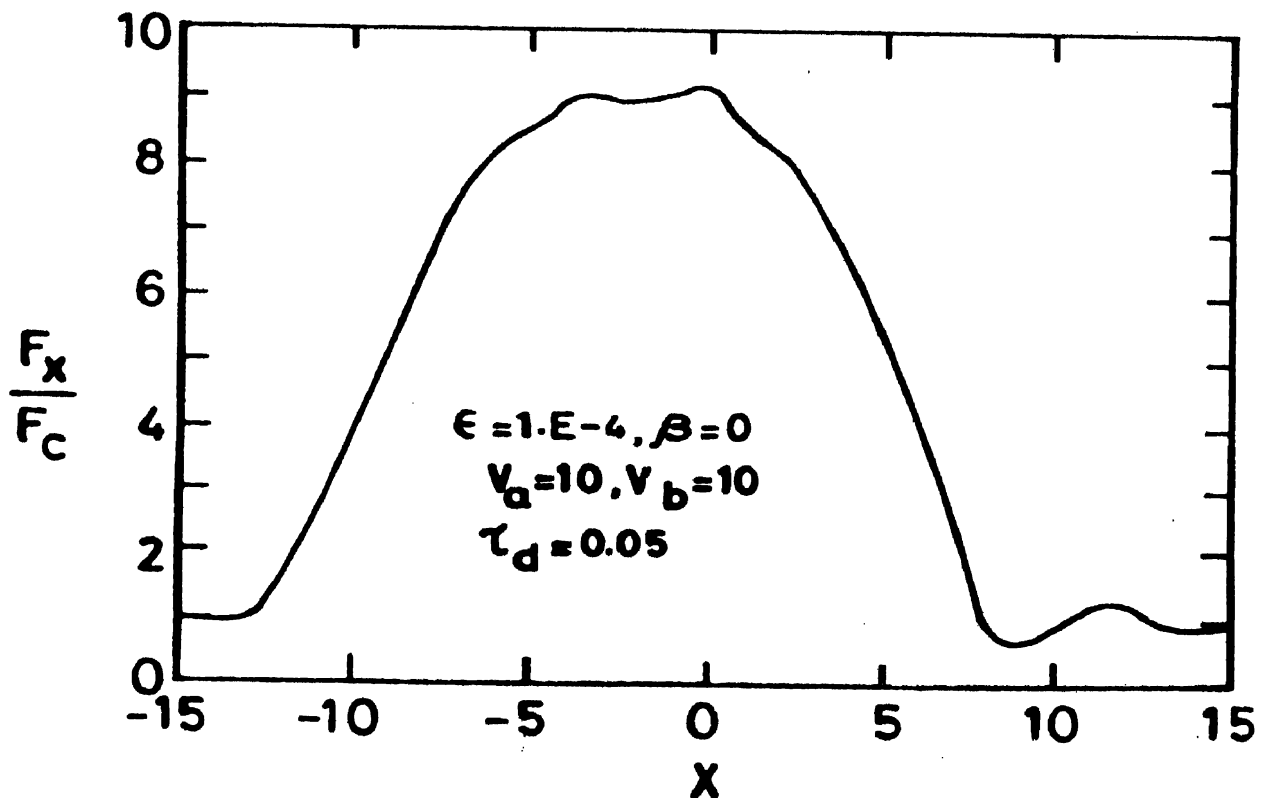
Figure 6.2.26   Same as in Figure 6.2.25 but uniform dust distributed offering an optical depth τ_d= 0.05.
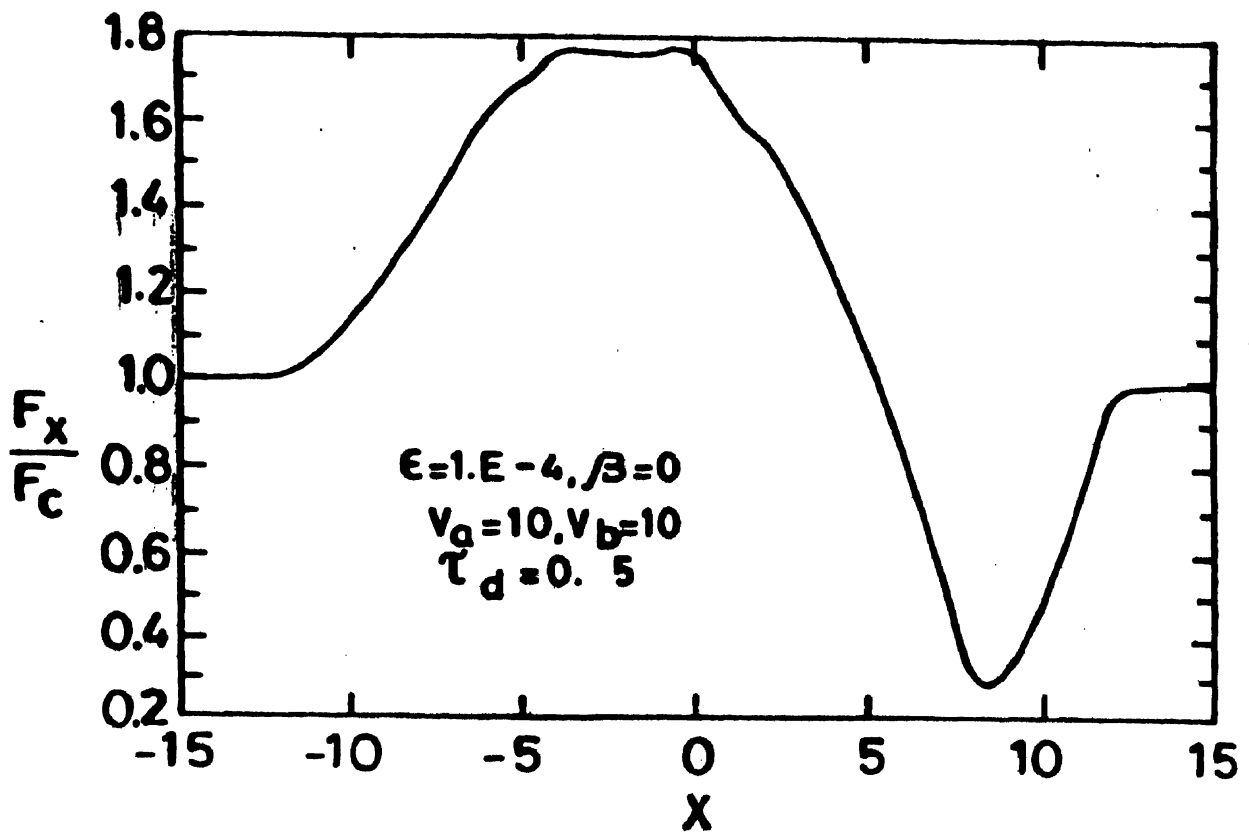
Figure 6.2.27   Same as in Figure 6.2.25 but dust is more τ_d= 0.5.
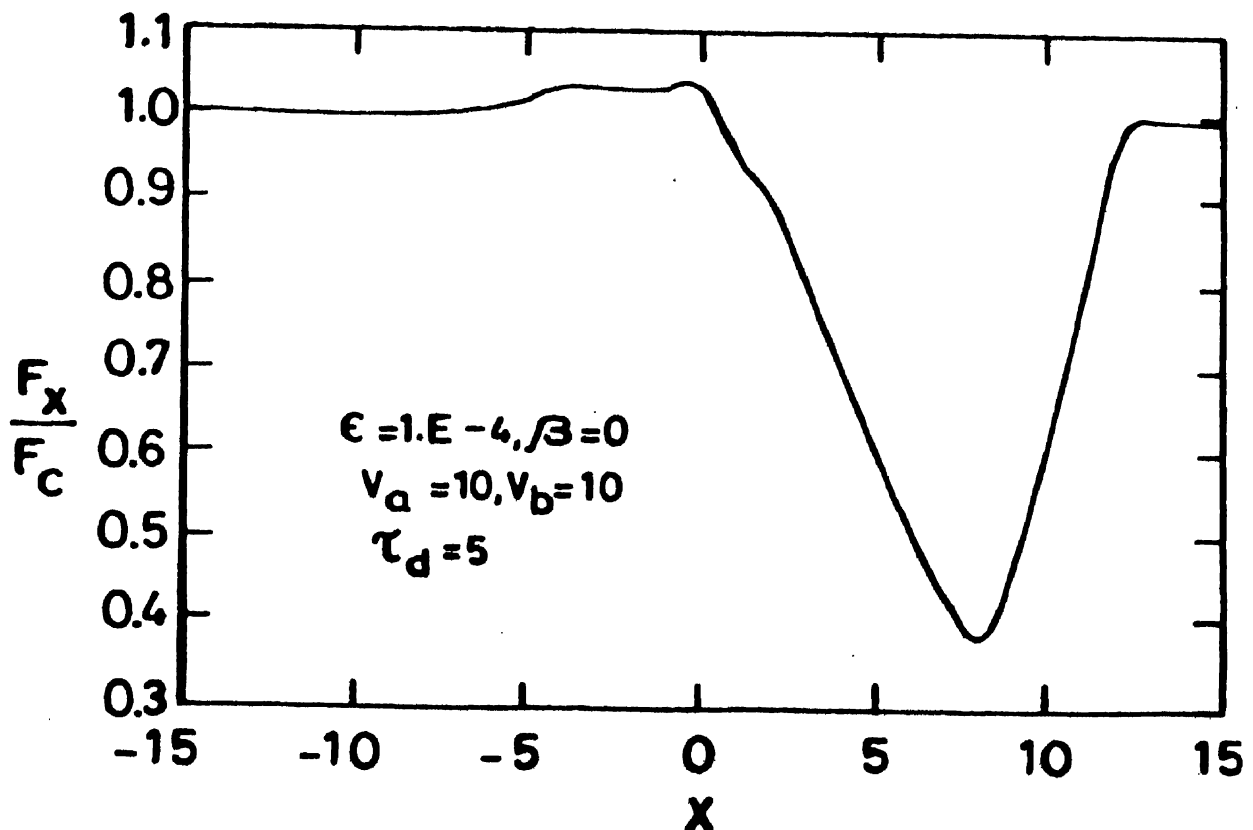
Figure 6.2.28   Same as in Figure 6.2.25 with τ_d= 5.0.
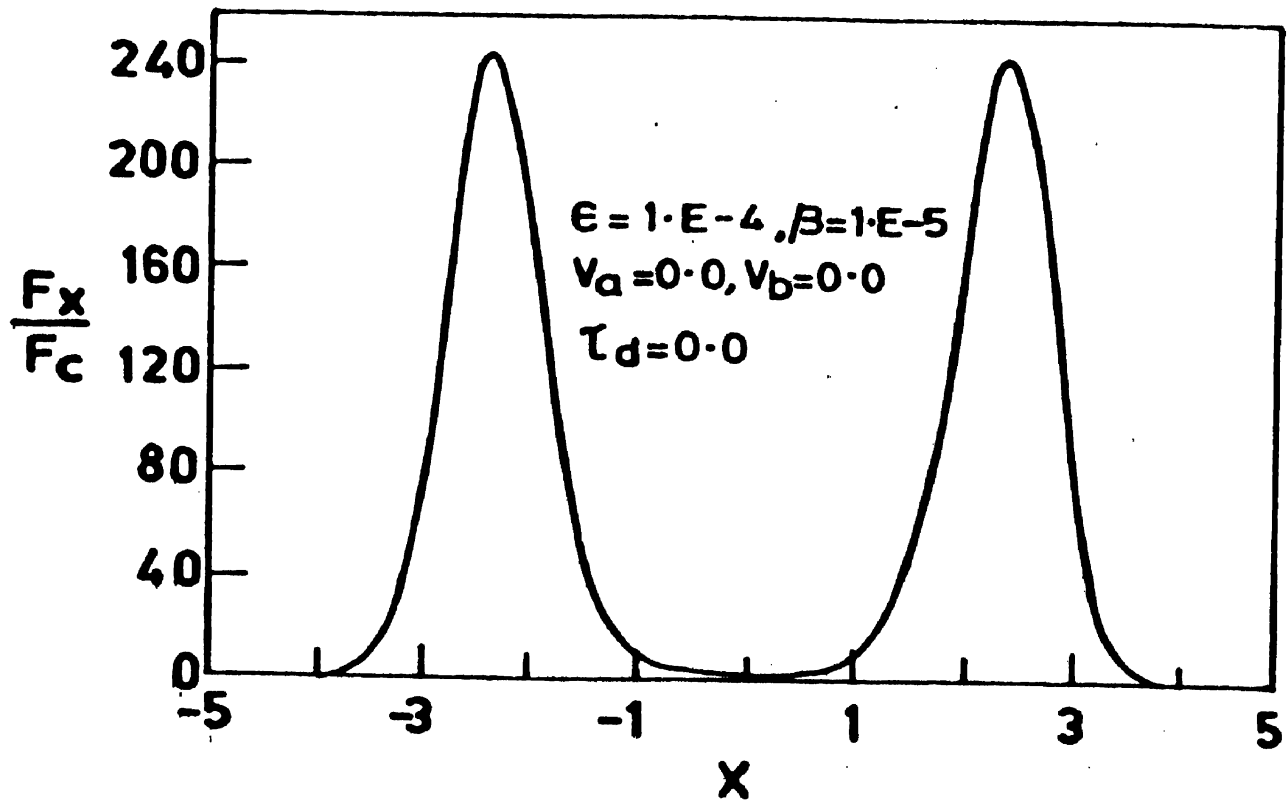
Figure 6.2.29   Line profiles in a static medium without dust.
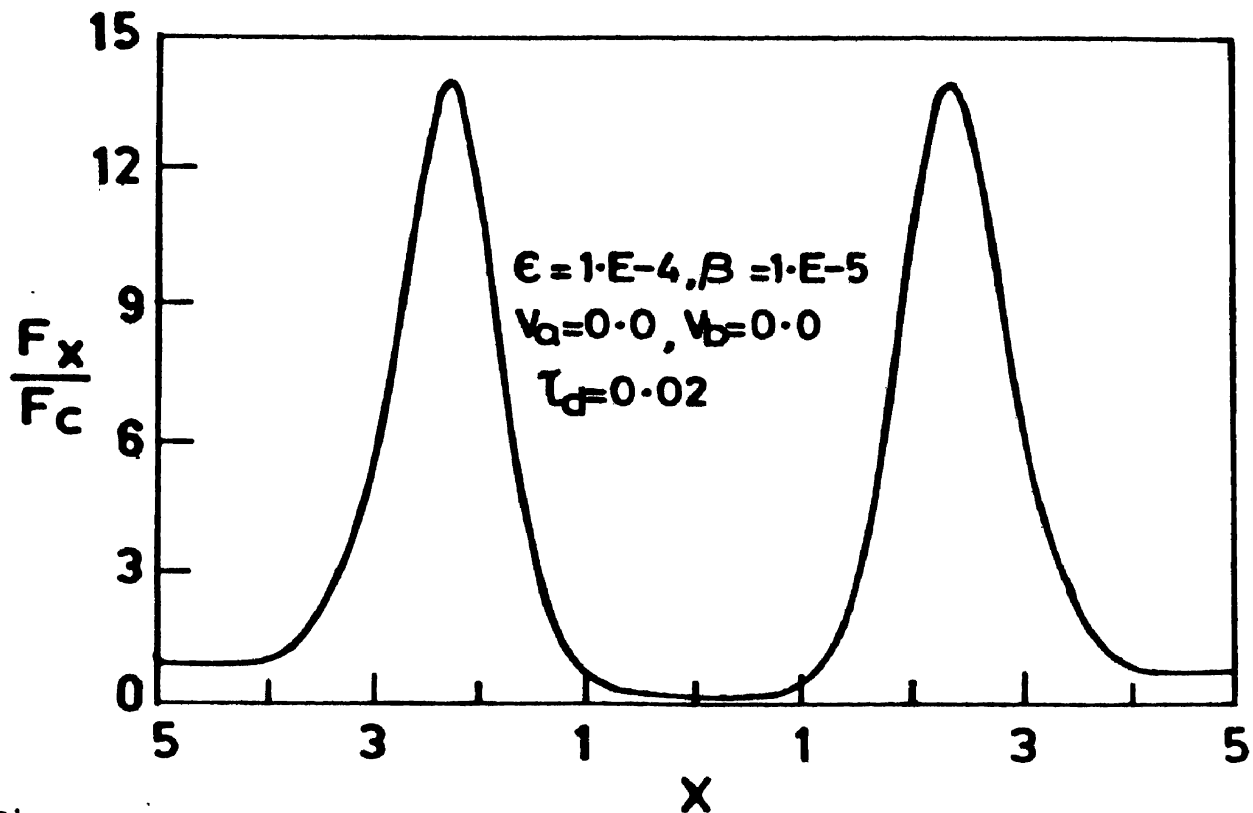
Figure 6.2.30   Line profiles formed in a static medium with dust,
$\tau_d = 0.02$.
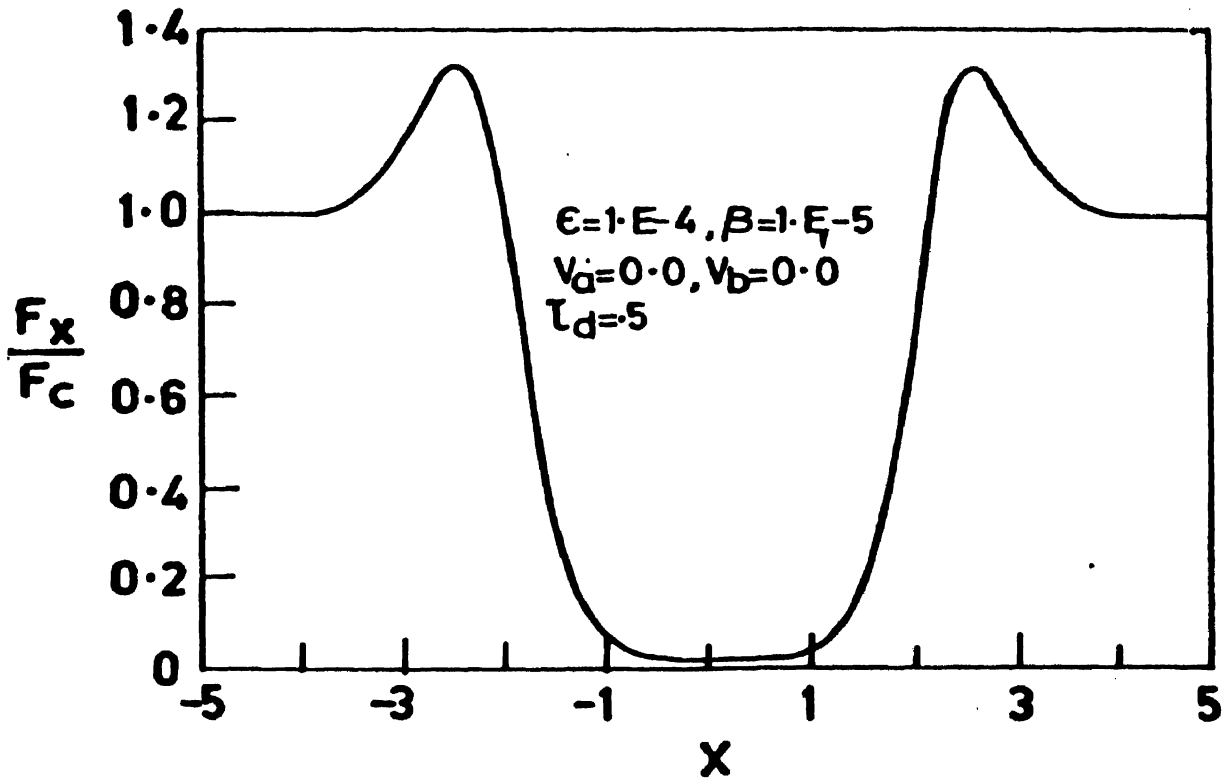
Figure 6.2.31   Line profiles formed in a static medium with dust,
$\tau_d = 0.5$.
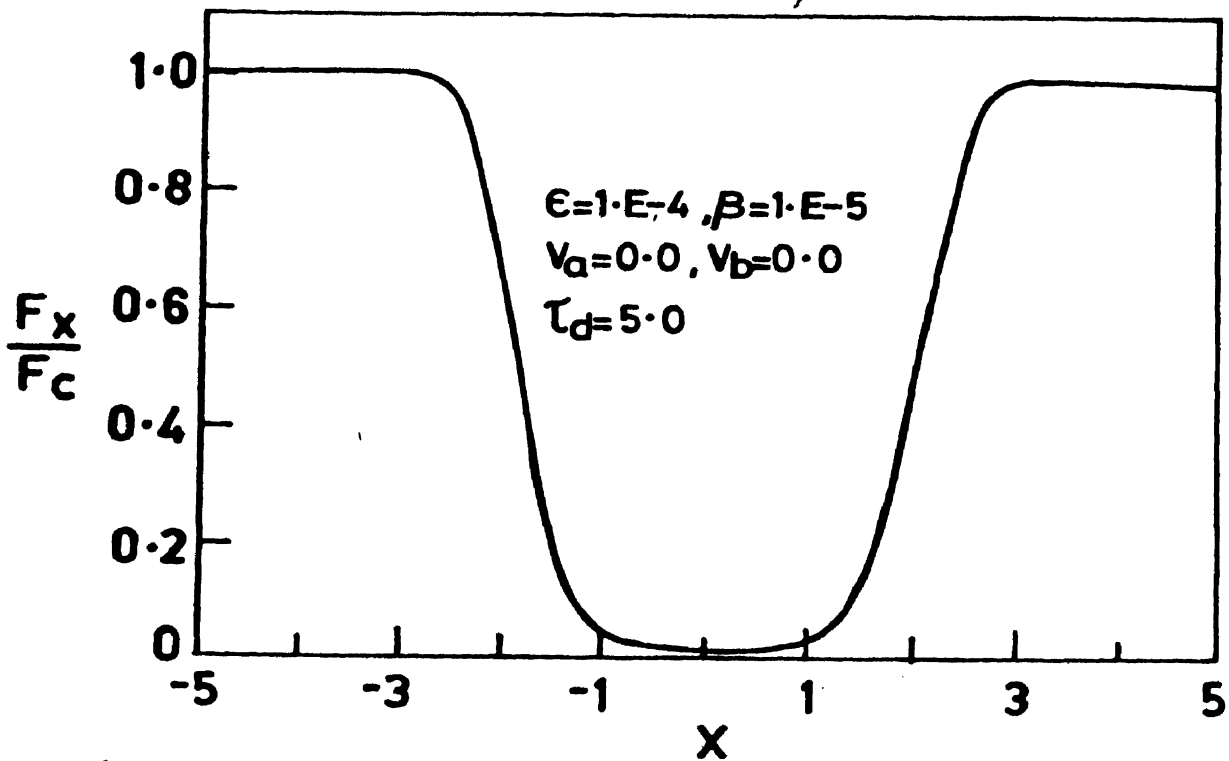
Figure 6.2.32   Line profiles formed in a static medium with du:
$\tau_d = 5.0$.

$\epsilon = 1 \cdot E - 4, \beta = 1 \cdot E - 5$
$V_a = 0 \cdot 0, V_b = 5 \cdot 0$
$\tau_d = 0 \cdot 0$

Figure 6.2.33   Line profiles formed in an expanding medium with velocity gradients and velocity of expansion $V_b = 5$ mtu.

$\epsilon = 1 \cdot E - 4, \beta = 1 \cdot E - 5$
$V_a = 0 \cdot 0, V_b = 5 \cdot 0$
$\tau_d = 0 \cdot 02$
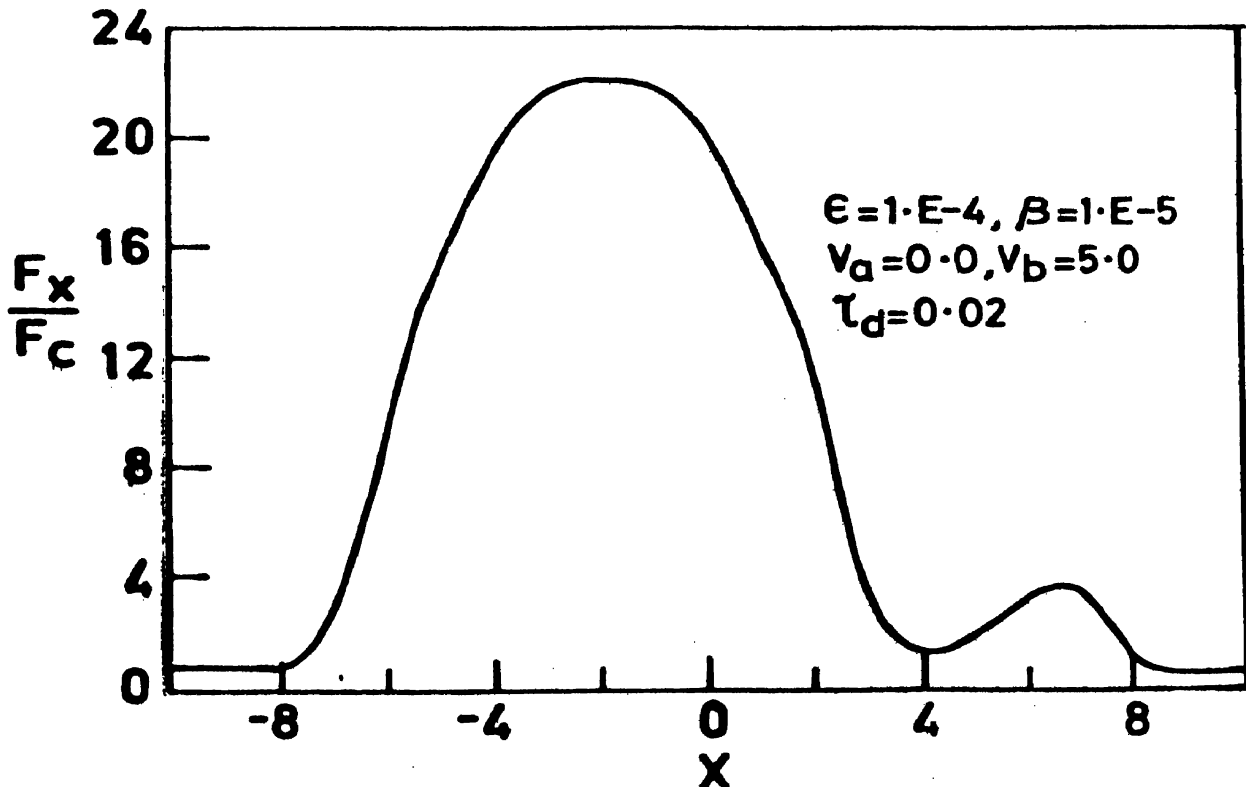
Figure 6.2.34   Same as in Figure 6.2.33, with dust contained in the medium $\tau_d = 0.02$.
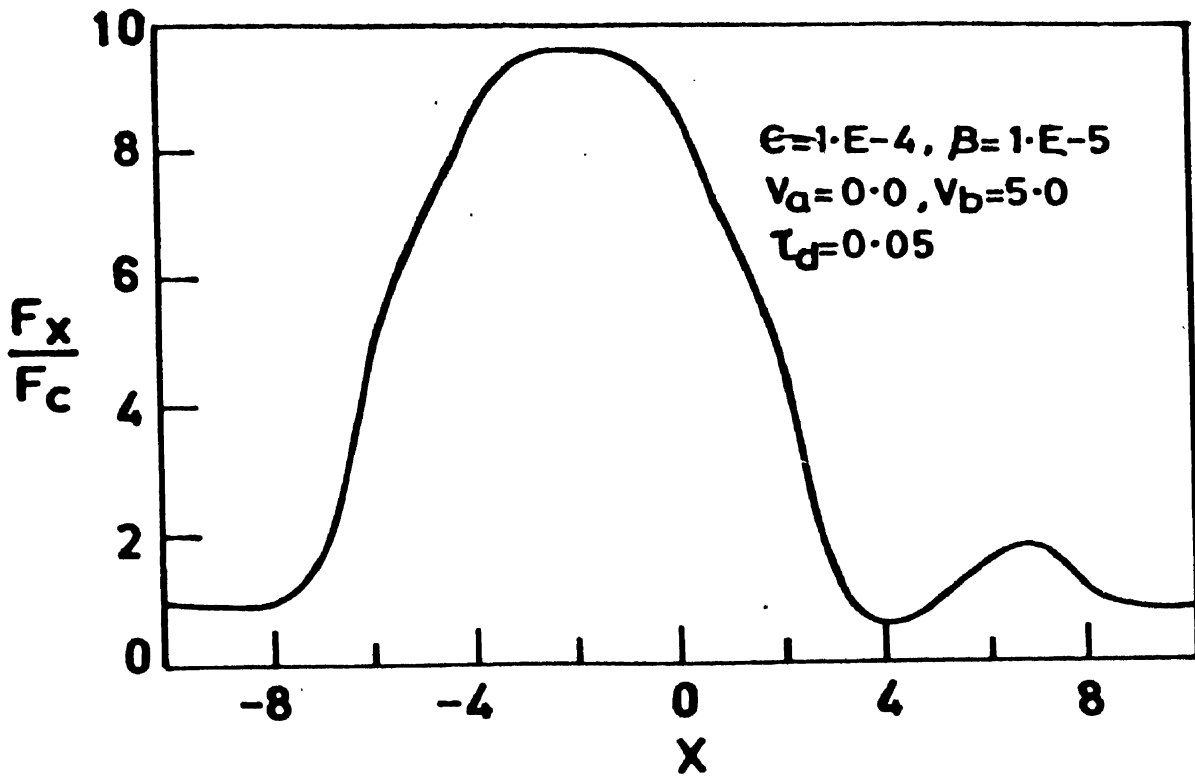
Figure 6.2.35   Same as in Figure 6.2.33, with dust contained in
the medium τ_d = 0.05.
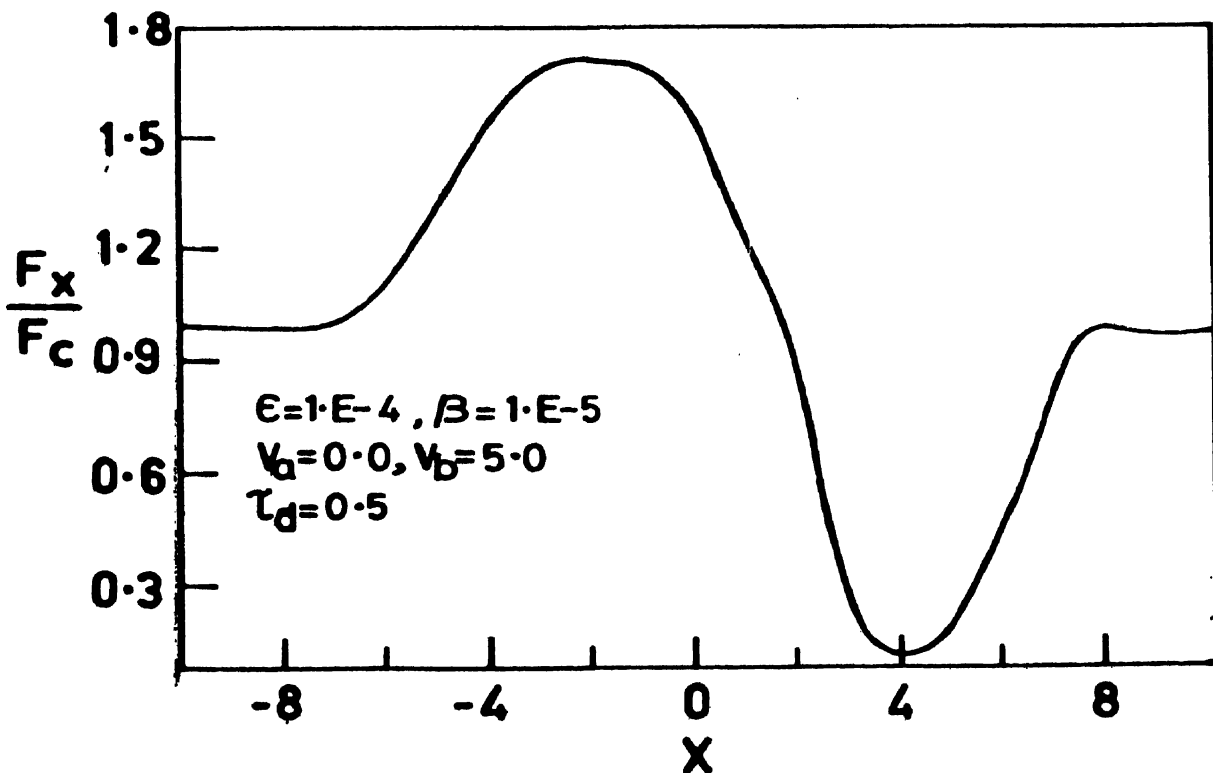
Figure 6.2.36   Same as in Figure 6.2.33, with dust contained in
the medium τ_d = 0.5.
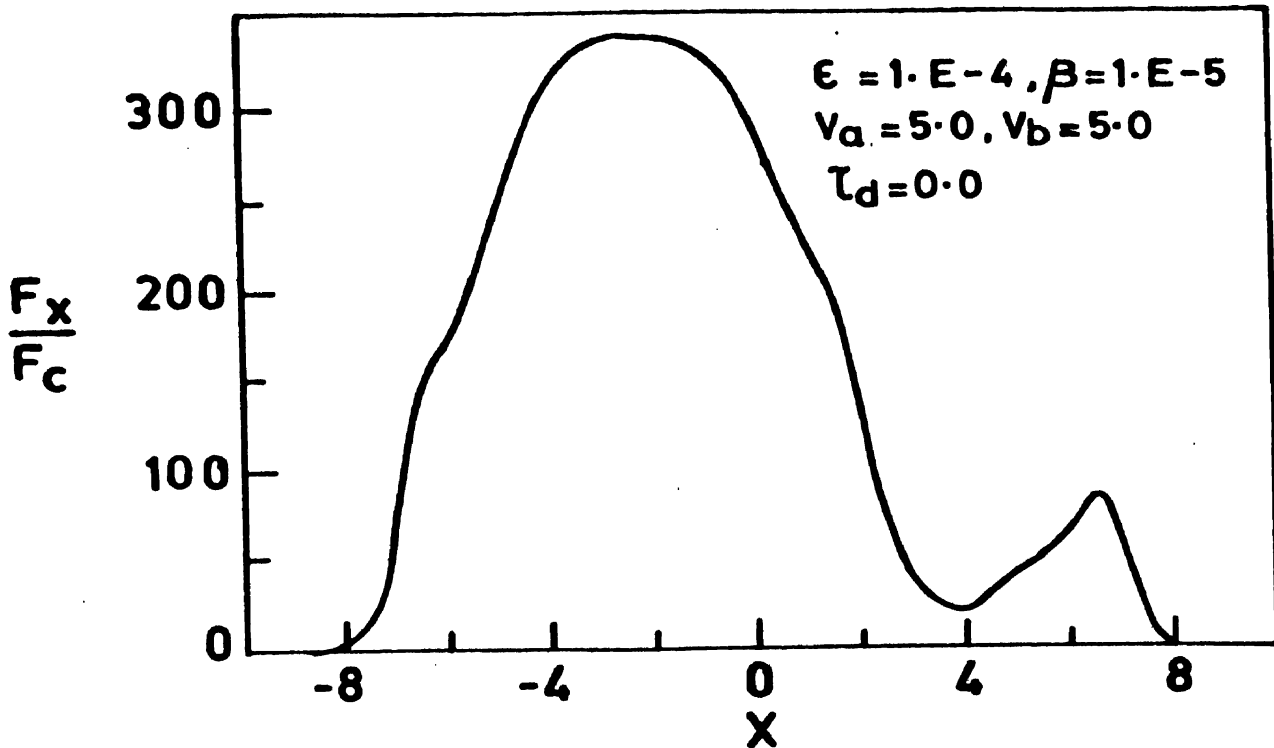
Figure 6.2.37   Line   profiles   formed   in   an   expanding   medium
without velocity gradients, velocity of expansion
is equal to 5 mtu.
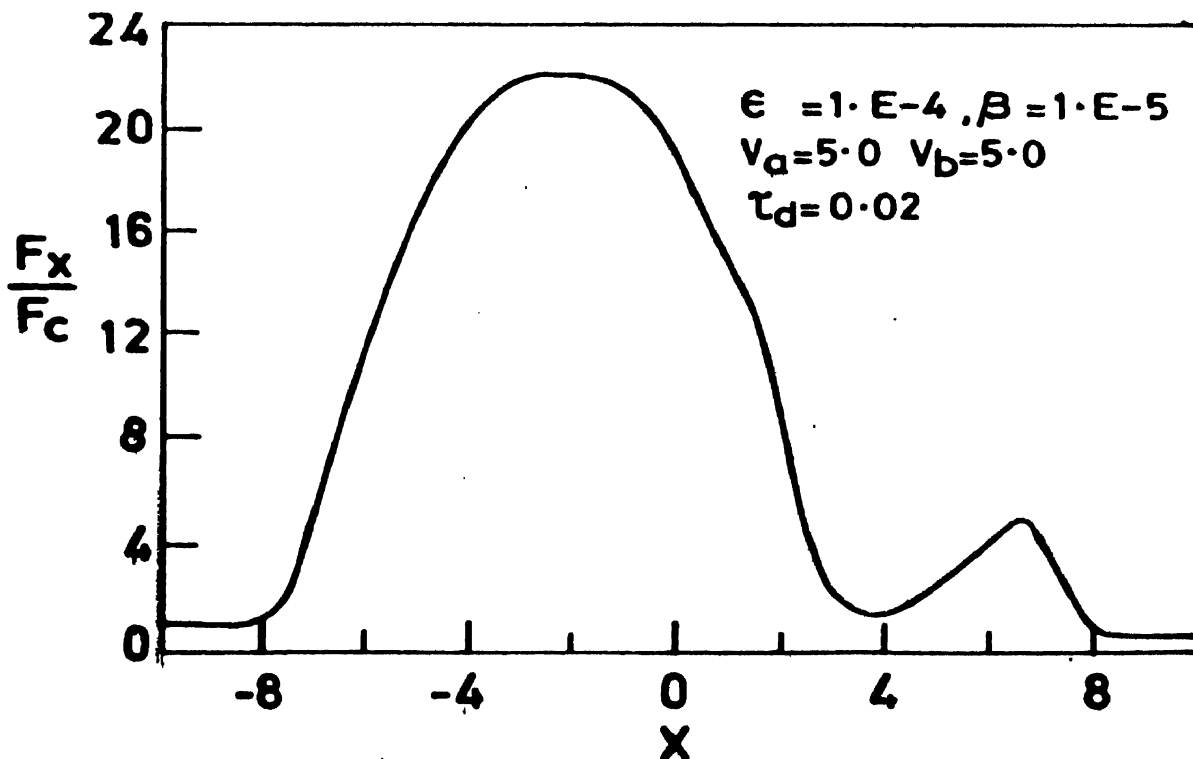
Figure 6.2.38   Same as those of Figure 6.2.37 but with dust
τ_d 0.02.
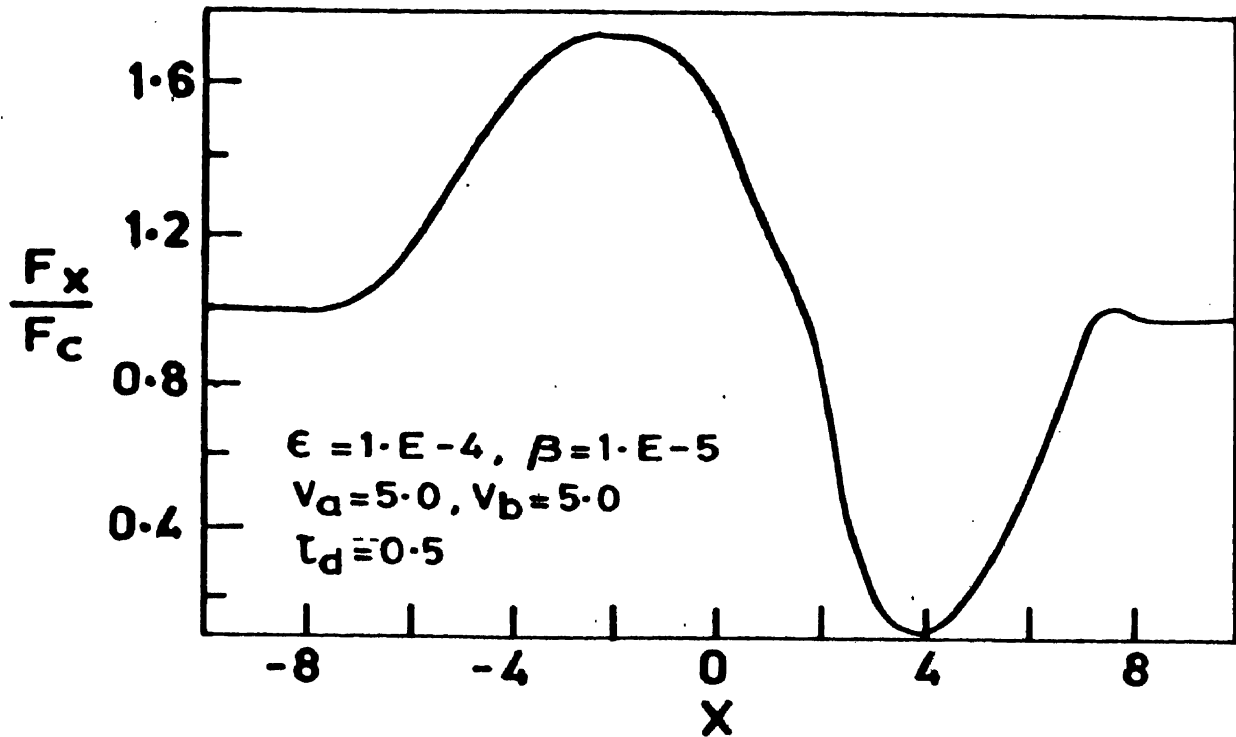
Figure 6.2.39   Same as those of Figure 6.2.37 but with dust

τ_d = 0.5.
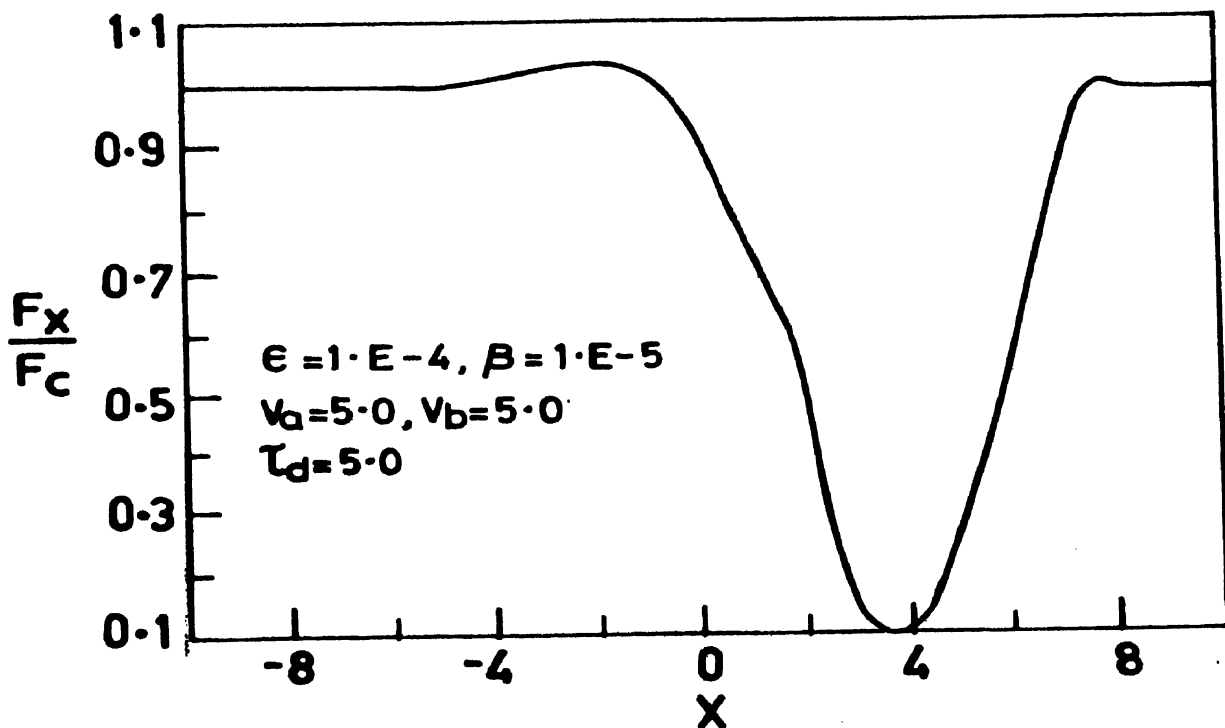
Figure 6.2.40   Same as those of Figure 6.2.37 but with dust

τ_d = 5.0.
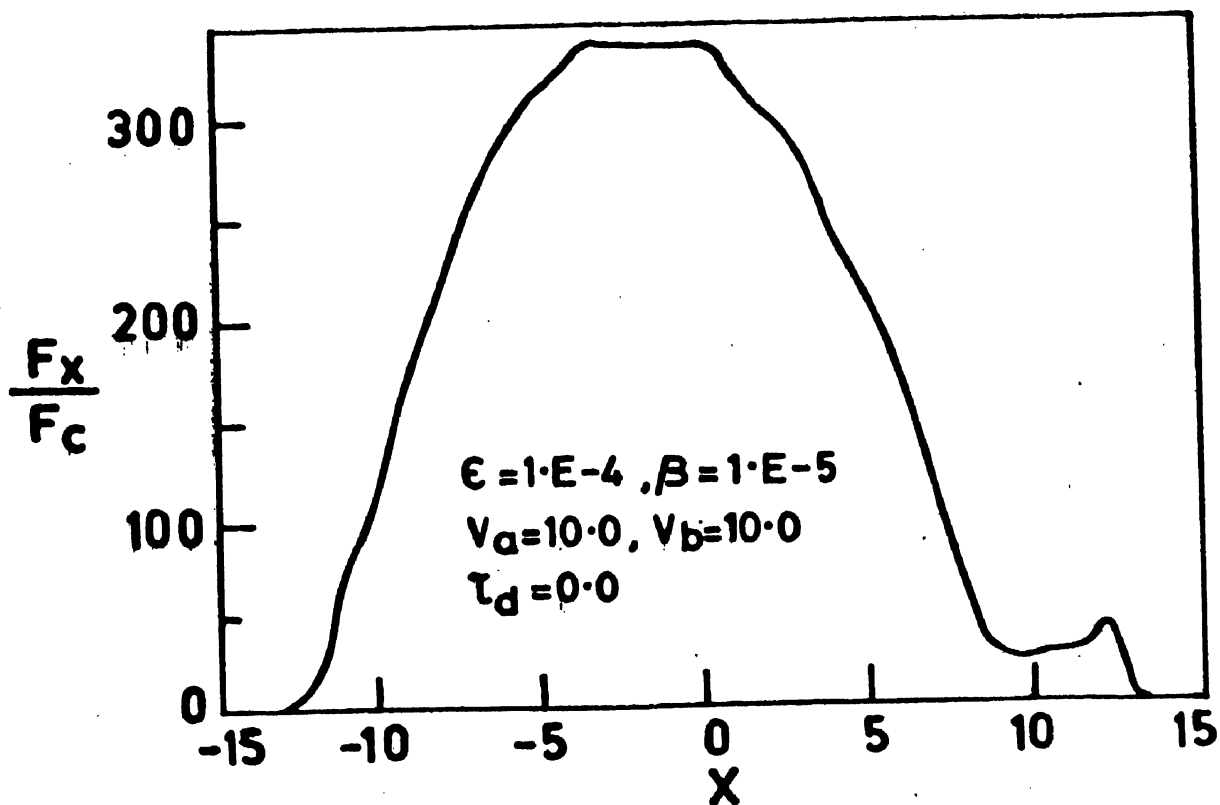
Figure 6.2.41   Line profiles formed in an expanding medium without velocity gradients, velocity of expansion of the medium V_b= 10 mtu.
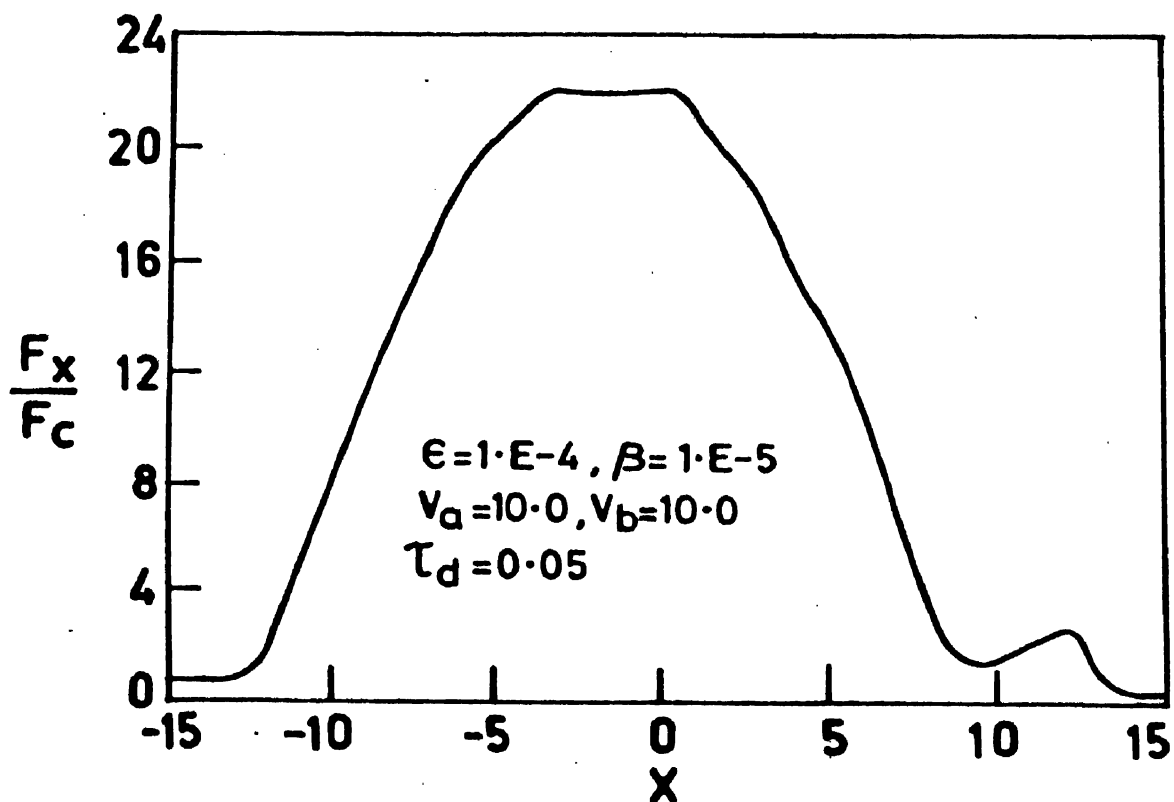
Figure 6.2.42   Same as in Figure 6.2.41 but with dust τ_d= 0.05.

Figure 6.2.43   Same as in Figure 6.2.41 but with dust $\tau_d = 0.5$.
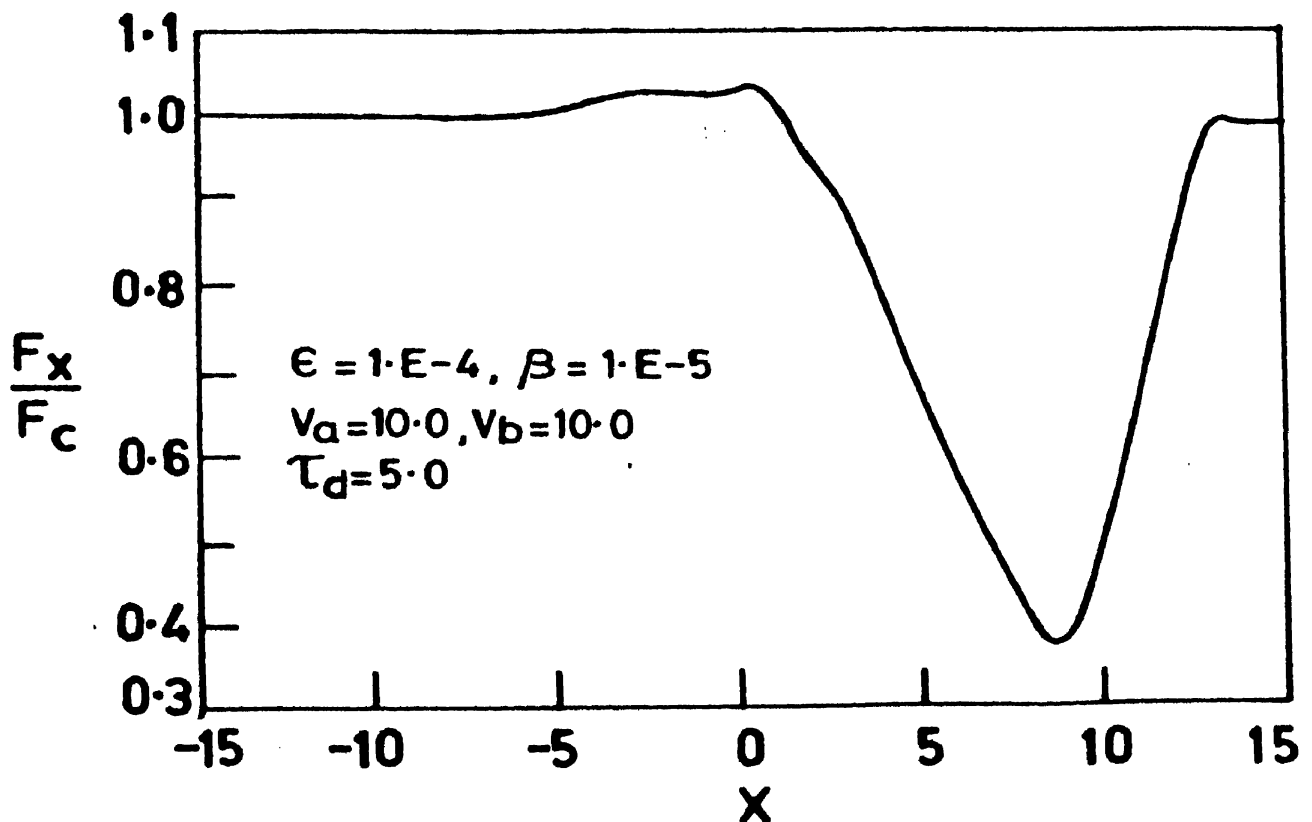
Figure 6.2.44   Same as in Figure 6.2.41 but with dust $\tau_d = 5.0$.
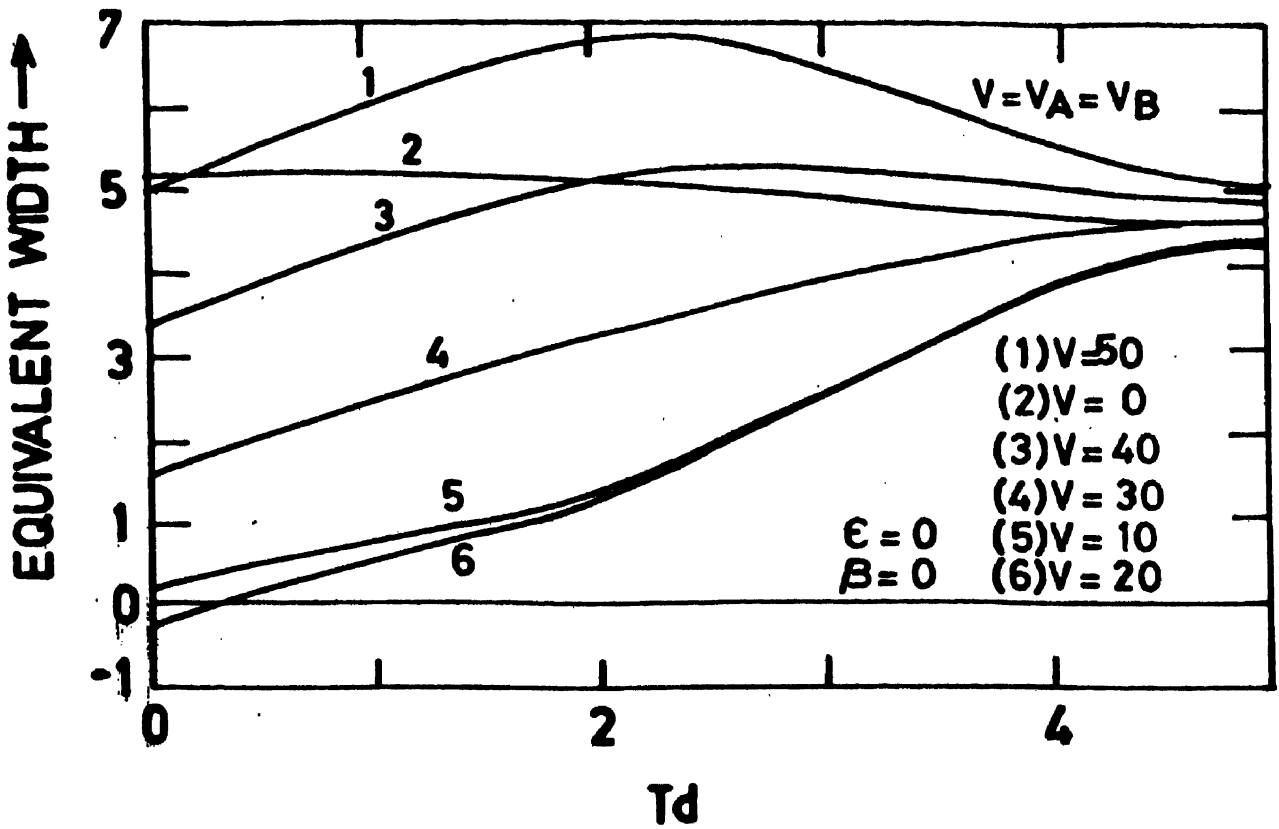
Figure 6.2.45   Variation of equivalent width with dust optical
depth (τ_d) for various velocities of expansion
(without velocity gradients).
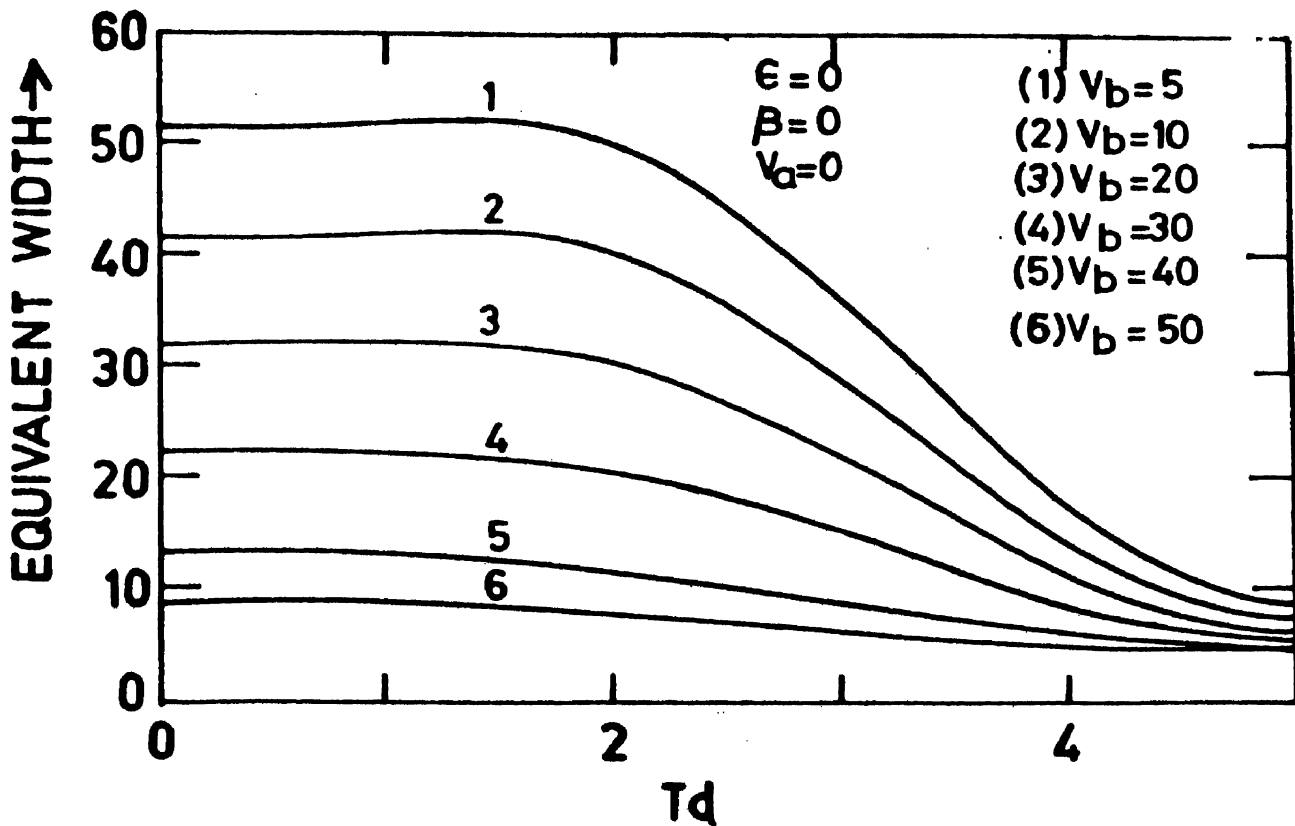
Figure 6.2.46   Same as in Figure 6.2.45 but with velocity gradients
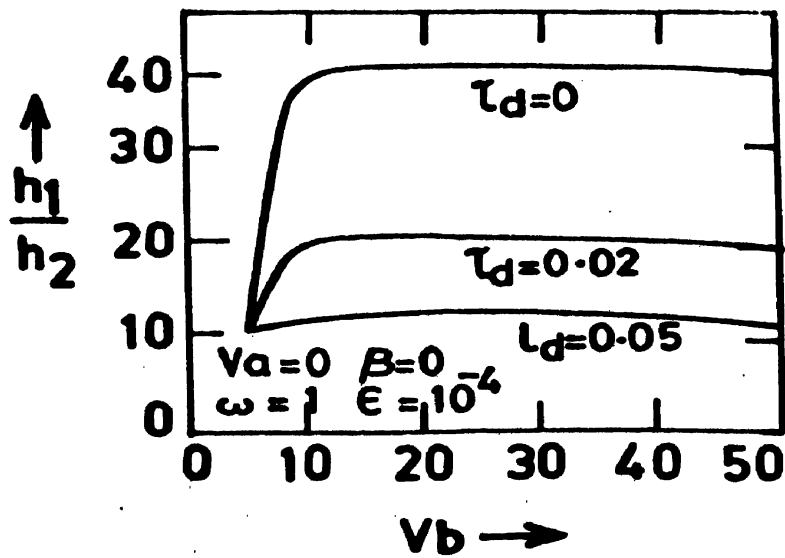
Figure 6.2.47   Variation of the ratio of two emission peak heights ($\frac{h_1}{h_2}$) in an expanding medium with velocity (V_b) (with velocity gradients).
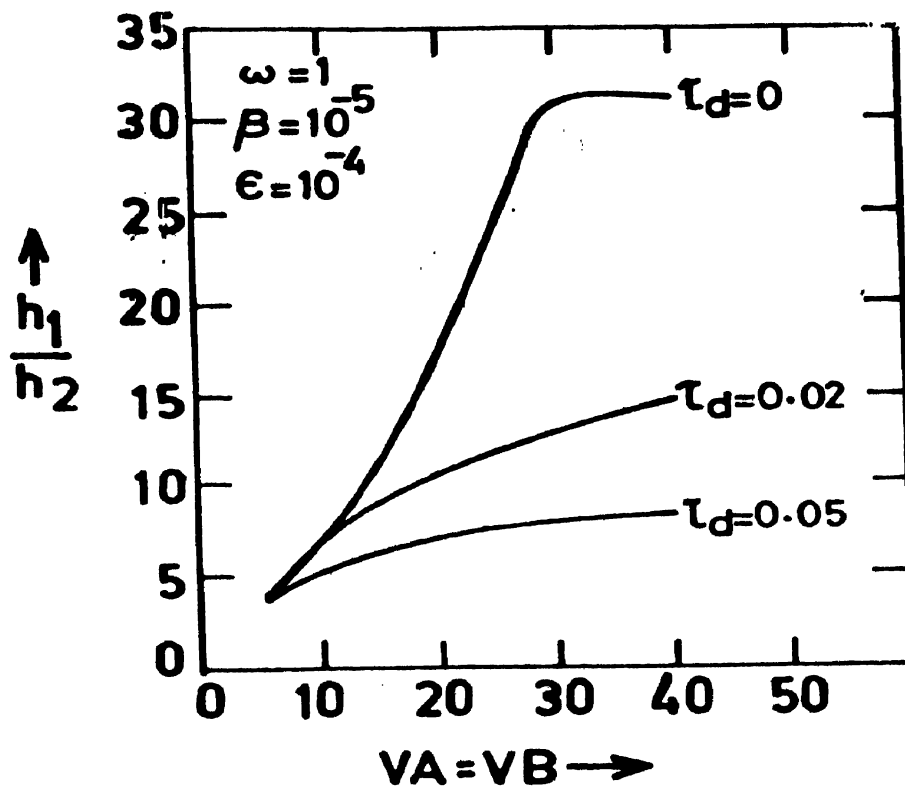
Figure 6.2.48   Same as those of Figure 6.2.47 but without velocity gradients.
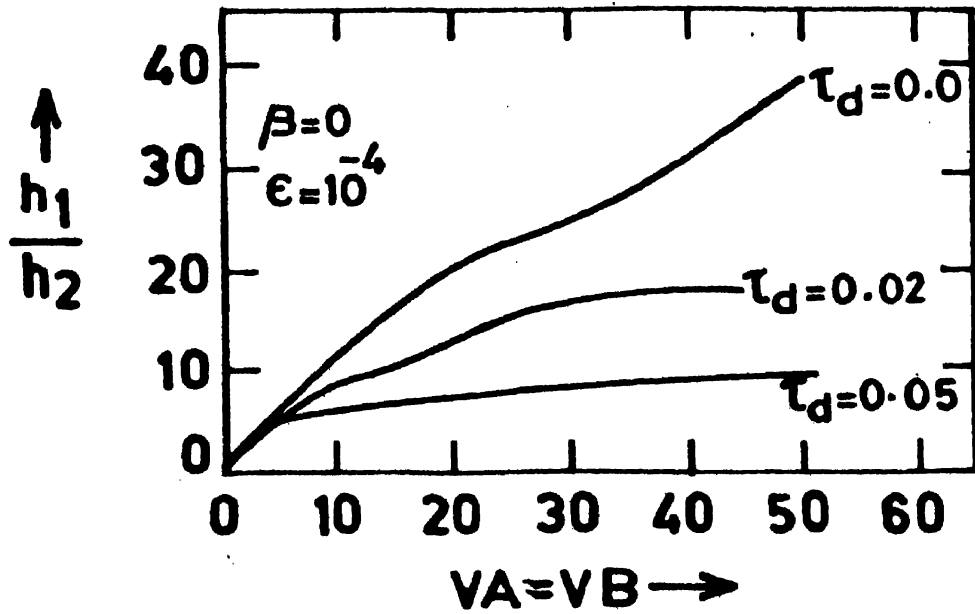
Figure 6.2.49   Same as in Figure 6.2.48 for $\beta = 10^{-5}$
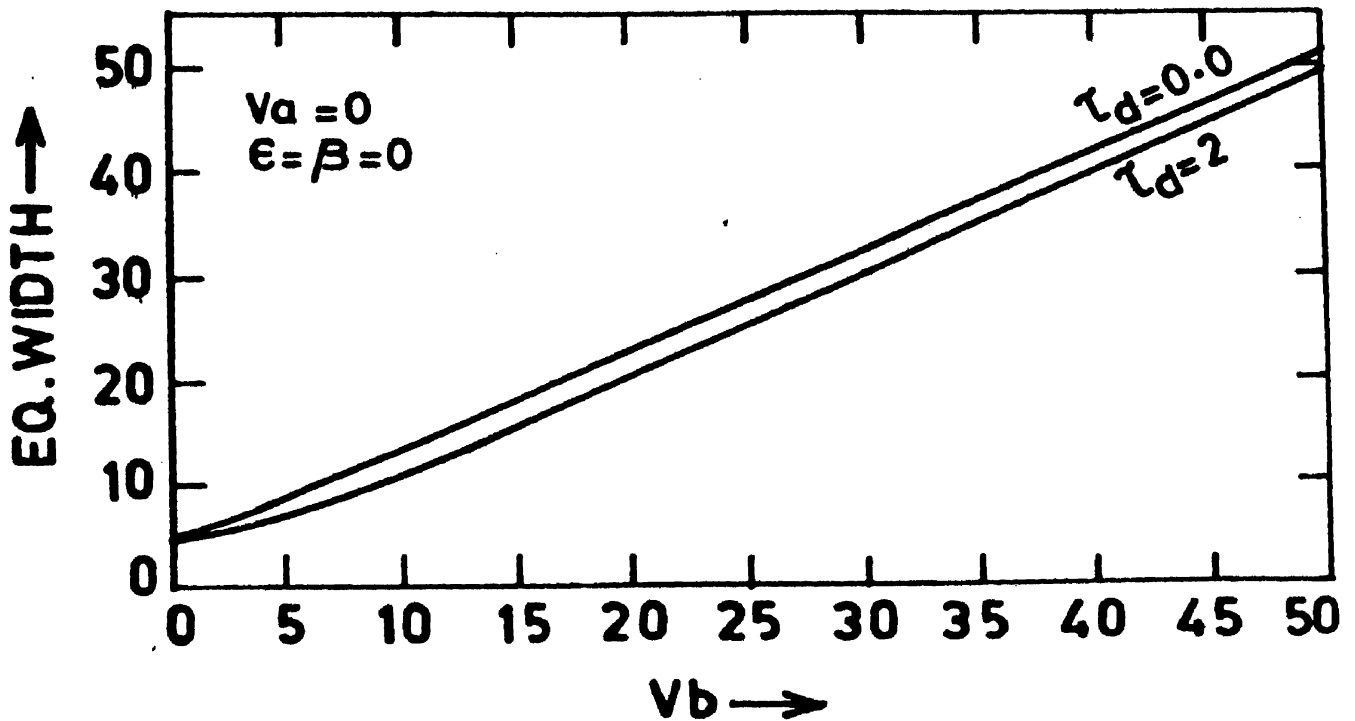
Figure 6.2.50   Variation of equivalent width of lines with velocity of expansion (with velocity gradients).
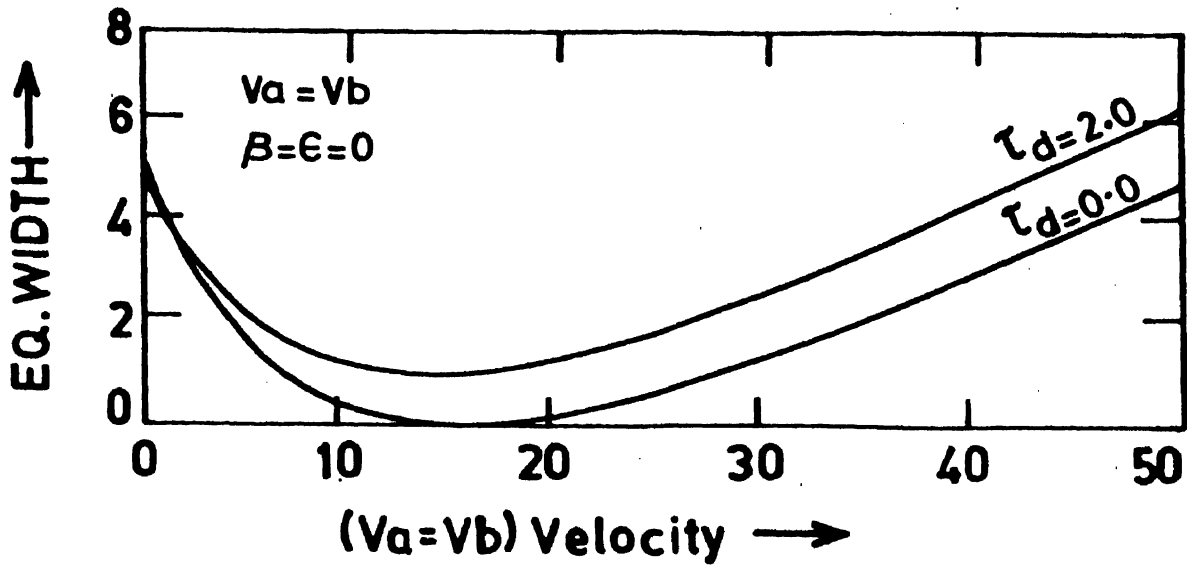
Figure 6.2.51   Same as those in Figure 6.2. 50 (without velocity gradients).
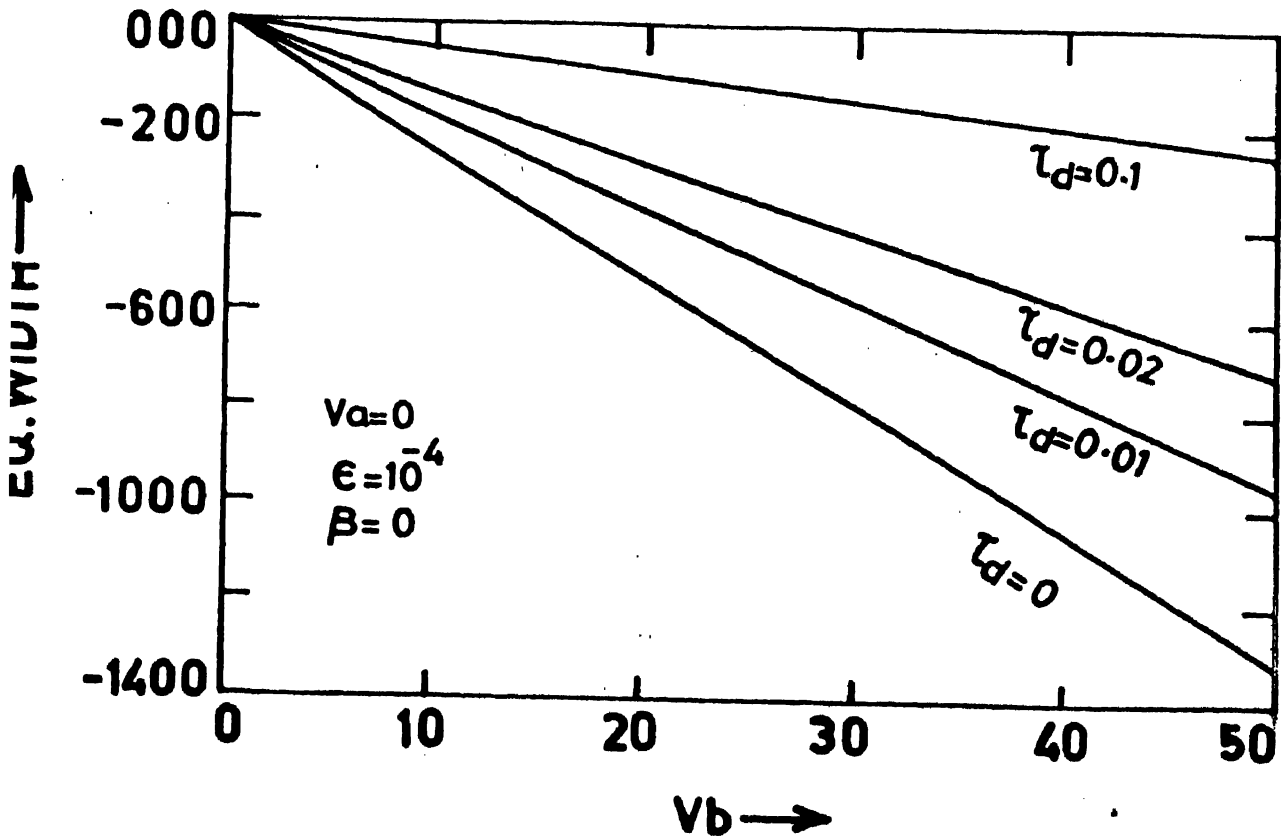
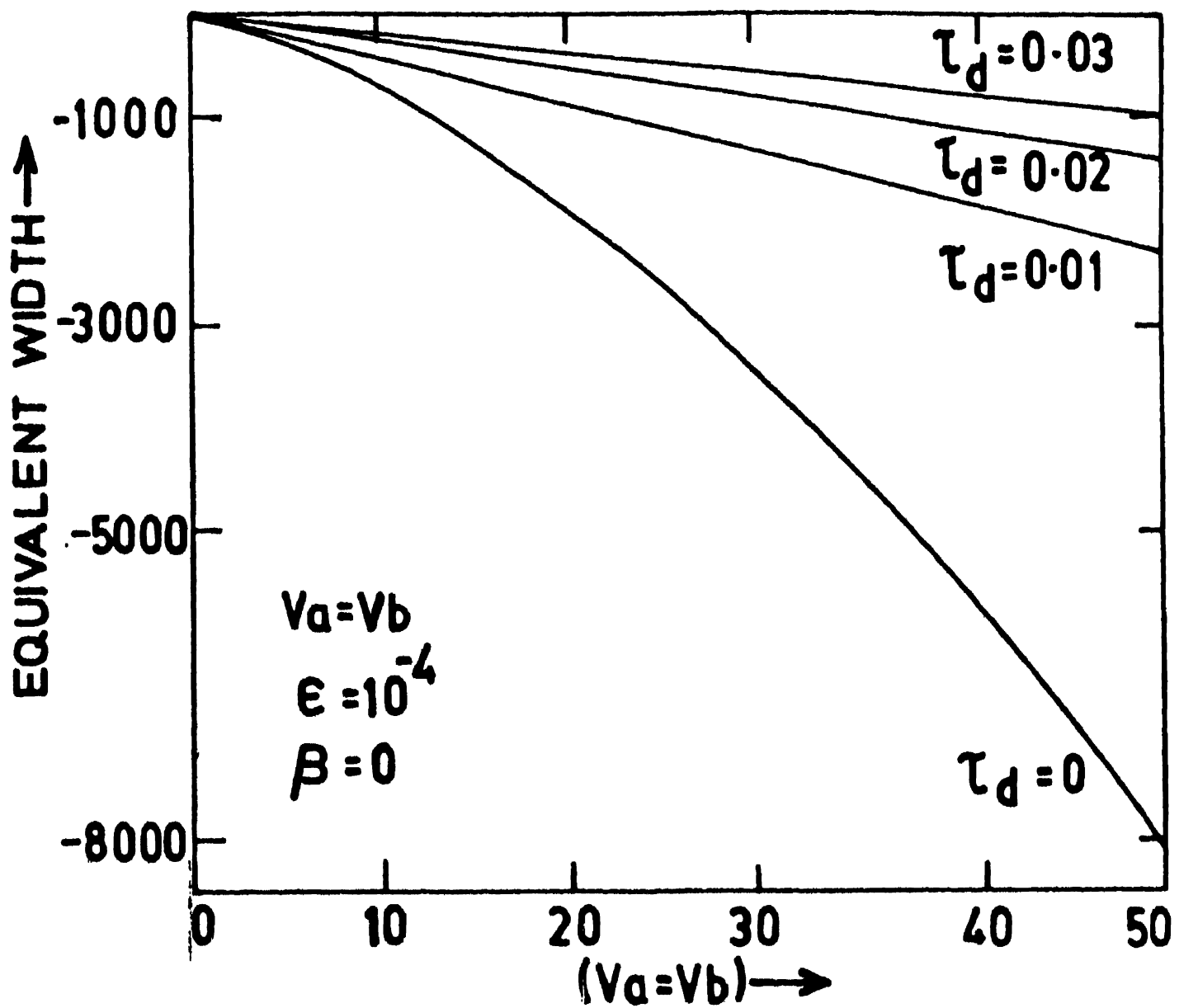Figure 6.2.52   Same as those of Figure 6.2.50 but for $\varepsilon = 10^{-4}$.
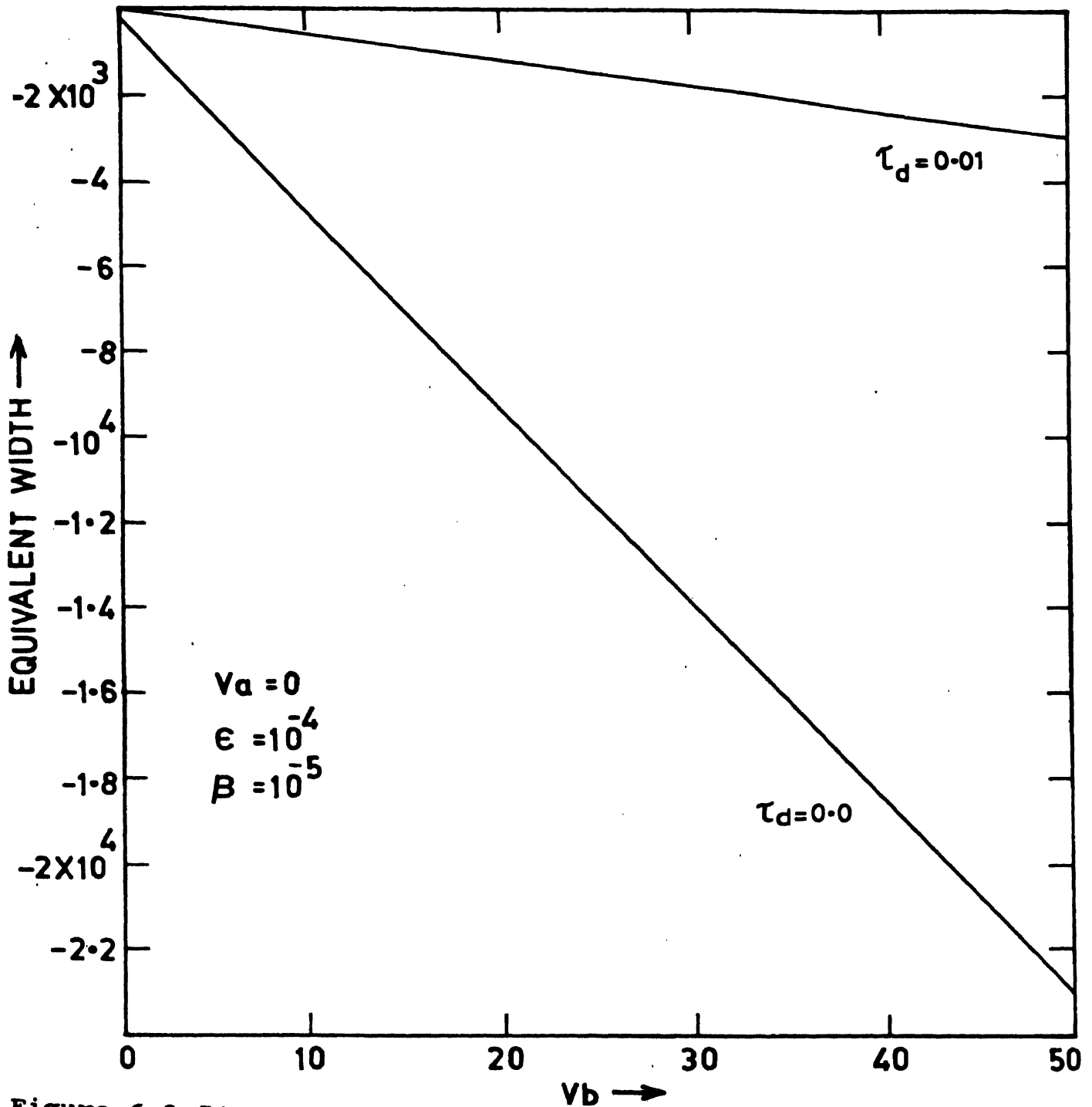
Figure 6.2.54   Same as those in Figure 6.2.50 but with $\varepsilon = 10^{-4}$ and $\beta = 10^{-5}$.
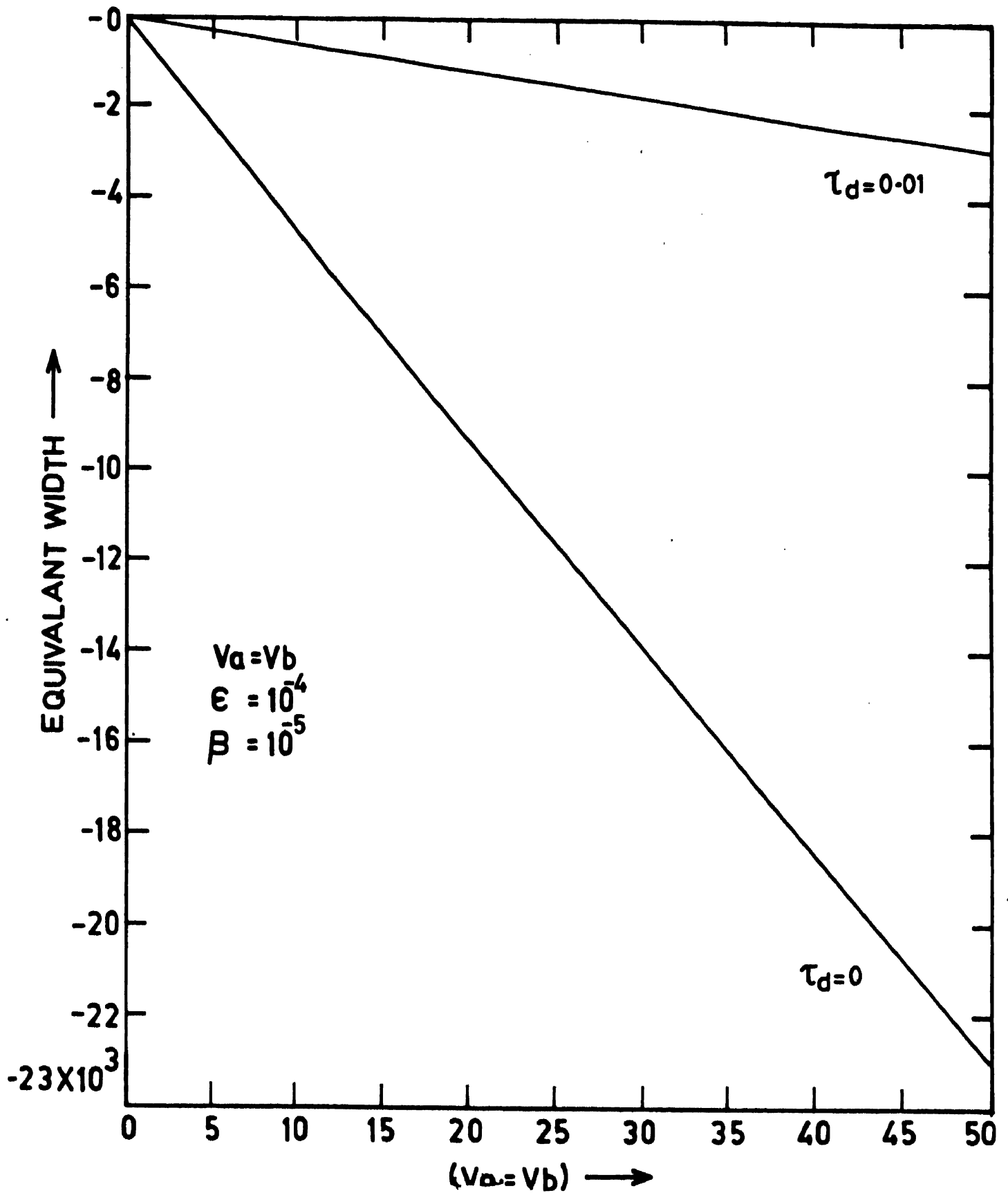
Figure 6.2.55   Same as those in Figure 6.2.51 but with $\varepsilon = 10^{-4}$
and $\beta = 10^{-5}$.

CHAPTER 7

CONCLUSIONS

In this chapter we are stating the results of our study briefly. The results have been illustrated by figures and explained seperately in the previous. chapters.

We have calculated the profiles of hydrogen lyman-α line in an expanding spherical atmosphere containing both dust and gas. We have investigated the variation of equivalent widths with velocities of expansion together with the amount of dust present in the medium. It is found that substantial changes in the equivalent widths are caused by the presence of dust in an expanding medium. It is noticed that dust also may increase the equivalent widths and there may be a possibility of overestimation of absorbing neutral atoms if the presence of dust is ignored. We have drawn curves of growth for different expansion velocities and dust optical depths.

We have also studied spectral lines in general by parametrising. Profiles have shown sharp dependance on the parameters like $\beta, \varepsilon, \tau_d, V_A, V_B$, etc. We have noticed that the wings in the spectral lines are prominent in dust free atmosphere and when dust content is increased emission in the wings reduces drastically. Impact of dust is also noticed in the absorption core. Further, velocity of expansion is found to introduce asymmetry in the shape of lines leading to P-cygni type of profiles in many cases. By constructing models taking all the parameters mentioned above into considerations it may be possible to make reliable investigations regarding physical structure of the outer layers of stars.

REFERENCES

Abhyankar K.D., 1964a, Astrophys.J.<u>140</u>,1353.

Abhyankar,K.D., 1964b,Astrophys.J.<u>140</u>,1368.

Abhyankar,K.D., 1965, Astrophys.J.<u>141</u>,1056.

Allen, D.A. and Swings, J.P., 1972, Astrophys.Lett.<u>10</u>,83.

Allen, D.A., 1973, M.N.R.A.S. <u>161</u>, 145.

Aller, L.H., 1963, The Atmospheres of the Sun and Stars, Ronald Press Co., New York.

Ambartzumian, V.A., 1943, Dokl.Akad.Nauk.SSR,<u>38</u>,229.

Canfield, R.C., 1970, Solarphys.<u>12</u>,63.

Chandrasekhar, S., 1945, Rev.Mod.Phys.<u>17</u>,138.

Chandrasekhar S., 1950, Radiative Transfer (Oxford).

Chandrasekhar, S., 1960, Radiative Transfer, Dover , New York.

Ciurla, T., 1966, Acta Astr.<u>16</u>,249.

Duval, P., and Karp, A.H., 1978, Astrophys.J.<u>222</u>,220.

Ebbets, D., 1978, Astrophys.J.224, 185.

Felli, M., 1982, Mem.Soc.Acad.It.<u>53</u>,349.

Geisel, S.L., 1970, Astrophys.J.Lett.<u>161</u>,L105.

Grant,I.P.,and Hunt,G.E., 1968, M.N.R.A.S.<u>141</u>,27.

Grant,I.P and Hunt, G.E., 1969,Proc.Roy.Soc.Lond.A:<u>313</u>,183.

Grant,I.P., and Peraiah, A., 1972, M.N.R.A.S.,<u>160</u>,239.

Grasdalen,G.L., 1976, Astrophys.J.Lett.<u>205</u>,L83.

Gray, D.F., 1975,Astrophys.J.<u>202</u>,148.

Gray,D.F.,1976,The observation and Analysis of Stellar Photospheres, Wiley,N.Y.

Gray,D.F.,1978,Solar Phys.<u>59</u>,193.

Henkel,C.,Mathews,H.E.,and Morris,M.,193,Astrophys.J.<u>267</u>,184.

Huggins, P.J., Glassgold, Morris, M., 1984, Astrophys.J.279,284.

Hummer, D.G., and Kunasz, P.B., 1980, Astrophys.J.236,609.

Kalkofen, W., 1970, Spectrum Formation in Stars with Steady
    State Extended atmospheres. N.B.S.Spec.Publ.No.332,
    eds Groth, H.G. and Wellman, P., P.120, U.S.Dept.
    of Commerce, Washington.

Karp, A.H., 1973, Astrophys.J.180,895.

Karp, A.H., 1975, Astrophys.J.201,641.

Karp, A.H., 1978, Astrophys.J.222,578.

Kubikowski, J.and Ciurla, T., 1965, Acta Astro.15,177.

Kunasz, P.B., and Hummer, D.G., 1974, M.N.R.A.S.166,19.

Kunasz,P.,and Hummer,D.G.,1974,M.N.R.A.S.,166,57.

Kwan, J., and Hill,F.,1977,Astrophys.J.215,781.

Lathrop,K., and Carlson,D.G.,1967,J.Comp.Phys.2,173.

Mihalas,D.,Kunasz, P.B., and Hummer, D.G., 1975, Astrophys.
    J.,202, 465.

Mihalas,D., Kunasz, P.B., and Hummer, D.G., 1976, Astrophys.
    J. 203,647.

Mihalas, D., 1978, Stellar atmospheres II.ed.(Freeman, San
    Franscisco).

Noerdlinger, P.D., and Rybicki, G.B., 1974, Astrophys.193
    651.

Panagia,N. and Ranieri, M., 1973, Astron.Astrophys.24,219.

Pecker, J.C., and Thomas, R.N., 1961, IAU.Symposium No.12.

Peraiah,A., and Grant,I.P.1971 (Sept 6-8) Proc.III.Colloquium
    held in Trieste.

Peraiah,A., and Grant, I.P. 1973,J.Inst.Maths.Applcs.12,75.

Peraiah, A., and Wehrse, R., 1977, Astron.Astrophys.61,719.

Peraiah, A. and Wehrse,R., 1978, Astron.Astrophys.70,213.

Peraiah, A., and Wehrse, R., 1978, Astron.Astrophys.71,289.

Peraiah,A.,1980,Acta. Astro.30,525.

Peraiah,A., 1980,J.Astrophys.Astron.1,3.

Peraiah,A.,1981,Astrophys.Space Sci.77,243.

Peraiah,A., 1984, Methods in Radiative Transfer, W.Kalkofen
        (Ed), (Cambridge) P.281.

Peraiah, A., Varghese B.A., and Srinivasa Rao,M., 1987,
        Astron.Astrophys.Supp.Series,69,345.

Persi,P.,Ferrari-Tonilolo,M.,Grasdalen G.L., 1983,Astrophys.
        J.269,265.

Perisendorfer,R.W., 1965,Radiative Transfer on Discrete Spaces,
        Oxford, Peragamon Press.

Redheffer, R.M., 1962, J.Maths.Phys.41,1.

Rybicki, G.B., 1970, Spectrum formation in stars with steady
        state extended atmospherere.No.332, Eds.Growth,
        H.G., and Wellman,P., P.87, U.S.Dept.of Commerce
        Washington.

Schwartz, P.R., Thronson, J.R., 1983, Astrophys.J.271,625.

Simon,M.,Rignini-Cohen,G.,Felli,M.,Fischer,J.,1981,Astrophys.
        J.244,552.

Simon,M.,Felli,M.,Cassar,L.,Fischer,J.,Massi,M.,1983,Astro-
        phys.J.266,623.

Simonneau,E.,1973,Astr.Astrophys.29,359.

Slettebak,A.,1956,Astrophys.J.124,173.

Smith,M.A.,and Gray,D.F.,1976,Publs.Astr.Soc.Pacif.88,809.

Stothers,R., and Chin, Chao-Wen,1977,Astrophys.J.211,189.

Underhill,A.B.,1947,Astrophys.J.106,128.

Van-de Hulst,H.C.,1965,New look at Multiple scattering.
New York, NASA Institute for Space Studies.

Van Hoff,A., and Deurnick, R., 1952, Astrophys.J.115,166.

Vemury,S.K.,and Stothers,R., 1977, Astrophys.J.214,809.

Wehrse,R. and Peraiah,A.,1978,Astron.Astrophys.71,289.

Wehrse,R. and Peraiah, A., 1979, Astron.Astrophys.71,289.

Wehrse,R., Kalkofen W., 1985, Astron.Astrophys.147,71.

Worrall,G., 1969, Solar Phys.8,18.